AN INVESTIGATION OF THE BEHAVIOUR OF POLYSTYRENE BEAD FOAM UNDER COMBINED IMPACT LOADING

by

John H.F. Woodrooffe

Submitted to the Faculty of Science and Engineering of
the University of Ottawa in partial fulfillment
of the requirements for the degree of
Master of Applied Science in
Mechanical Engineering

ABSTRACT

An experiment has been performed to determine the behaviour of Polystyrene Bead (PSB) foam under combined impact loading.

It has been found that the impact stress-strain characteristics of PSB foam under combined loading conditions are similar to that of normal impact loading of PSB foam. It has also been found that a predictive normal impact equation could be successfully used to determine the stress-strain behaviour of PSB foam under combined loading.

ACKNOWLEDGEMENTS

The author is indebted to many people whose assistance in this project were vital to its completion.

In particular, thanks go to:

Dr. J.A. Newman, the author's supervisor, for his dedicated support and interest in this project.

Mr. F.C. Meunier who's input and advice was most helpful during the course of the research.

Much appreciation is directed to Mr. G. Toth and his staff for the excellent workmanship in the fabrication of the test apparatus.

Finally, the author wishes to acknowledge Bell Helmets Inc., Long Beach, California for their financial assistance during this work.

TABLE OF CONTENTS

LIST OF FIGURES

PAGE

I INTRODUCTION

I.1 General Discussion of Foams

Polymeric foams are now widely used in the field of impact protection. They exhibit characteristics which lower the impact forces and absorb a large amount of impact energy. The most popular use for the material is in the packaging industry. "Foams serve to cushion the packaged items by damping out vibration and mitigating shock so that the items will reach their final destination without damage" (1).

Polymeric foams are also used in protective head gear and in automobile dashboards to shield passengers from head injury during a collision (2,3).

"Foams designed for impact applications must exhibit a specific stress-strain behaviour as well as the ability to dissipate energy. It is important for an impacting object to undergo a constant deceleration, for maximum force could be destructive to the object. A foam which exhibits a plateau region in its stress-strain curve, resembling yielding, will absorb impact energy at a relatively constant deceleration. Since the force is the product of mass and acceleration, a constant stress during compression will give a constant deceleration during impact" (4).

Expanded polystyrene bead (PSB) foam is a common polymeric foam used for the purpose of impact protection. (It also serves as an insulation and flotation material.) Low cost and simple moulding procedures make it an attractive choice. PSB foam stock is produced in the form of foam beads about 2-3mm in size, which are shipped in bulk to moulding plants. The beads are placed in moulds which are injected with steam thus bonding the beads together thereby producing the desired part.

To date, investigative work has concentrated on the dynamic behaviour of normally loaded PSB foam. Meunier (5) conducted experiments with PSB foam and arrived at a predictive equation for the behaviour of foam during normal impacts. In reality, however, there are very few items that are loaded this simply. Combined loading during impact is the norm rather than the exception. Such protective items as helmets, dashboards, instrument packaging and even egg cartons frequently experience combined loading when under stress. To properly predict the performance of such protective items, it is clear that one must know more than simply the normal loading characteristic of the foam.

The purpose of the present study, therefore, is to investigate the performance of PSB foam under combined shear and normal loading, and to determine if the equation developed by Meunier can be applied to such impact conditions.

I.2 Experimental Studies

To the author's knowledge, there has been no work to determine the behaviour of PSB foam resulting from combined impact loads. For that matter, very few papers have been published relating to shear loading behaviours of rigid foams.

Zaslawsky (6) in 1973 stated "... much effort has been expanded in uniaxial tests on foam; much yet remains to be done. However, the behaviour of foam under multiaxial states of stress has had little attention". This generalized statement holds true today.

Zaslawsky studied multiaxial stress behaviour of rigid polyurethane foam by subjecting standard tubular specimens to interior pressure and axial load with a maximum axial stress rate of 20 psi/min. A high speed motion picture camera was employed to study the fracture propagation. He found that fracture, distinct from excessive yielding, occurred at the conclusion of every test which was both "catastrophic" and "instantaneous". He also concluded that decreasing density weakened the material significantly in compression and in the hoop direction yet it has no observed effect on axial tension. His reasoning for this is that the decrease in density increases the sensitivity to buckling and cell wall collapse. However, the tensile bonding of the beads is not affected by density thus tensile strength remains relatively constant.

Patel and Finne (7) also used thin tubes of plastic foam under tension, internal pressure and axial compression in their tests. They conducted experiments on rigid, CO_2 blown polyester based polyurethane foams. For low density foam, they found that the compressive strength is greatly affected by the stress-strain characteristics of the solid phase while the tensile fracture is not. With respect to biaxial loading they conclude that the geometric configurations of foam are such that the loading of foam in one direction would not affect its strength in the orthogonal directions.

The shear properties of flexible silicones were investigated by Aspey and Hodge (8). Using a function generator to drive an electromagnetic shaker, the motion of the shaker was transferred through a flexible coupling to an input bell crank which applied a sinusoidal torque to the cylindrical specimen. The tangential displacement was measured by linear displacement transducers. It was found that a reduction in cell size reduced the compressive modulus only very slightly while the sheer modulus decreased some 20%.

Meier and Rudd (9) studied the shear response of phenolic foam by bonding foam samples to a fixture as shown in Figure 1. The small blocks of foam used were either 1 in^3 or 1 in^2 x 0.5 inches thick. Shear stress values were measured at shear rates of 2 in/min. both parallel and perpendicular to the rise direction.* They determined the shear strength of 2 lb/ft^3 phenolic foam material to be approximately 5.5 psi. This was applied to the design of a mechanical shock absorber used on the vent doors of a nuclear reactor containment vessel.

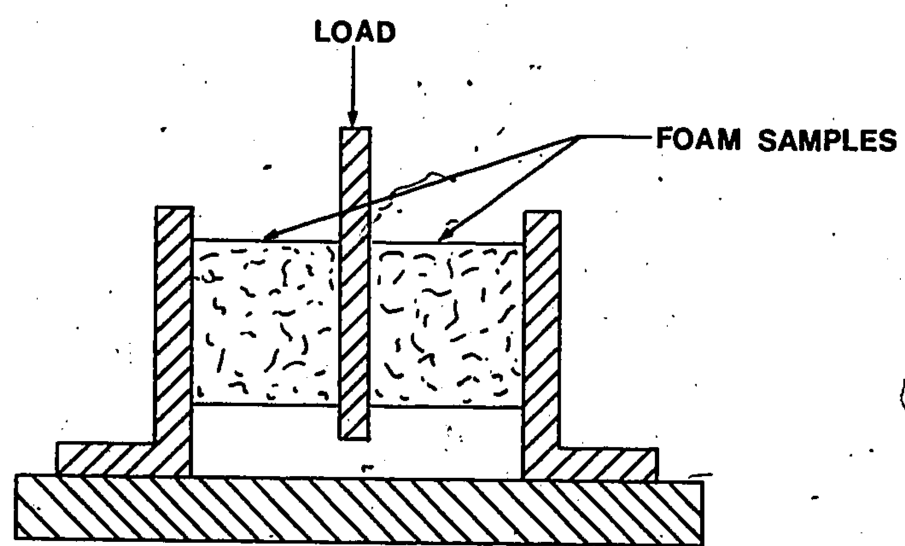

Fixture used by Meier and Rudd for Shear Response Studies

Figure 1

*Rise is the general direction in which the expanding foam travels during the foaming process.

Rind and Hoge (10) used cylindrical PSB foam specimens on a torsional oscillating machine to study the shear properties of the foam. Values obtained by Rind and Hoge for the yield stress density dependence of PSB foam in shear were in the form $\sigma_y = A\rho^{1.475}$. Patel and Finnie (11) who studied the density dependence of PSB foam in compression, obtained a similar form of equation $\sigma_y = A\rho^{1.46}$.

I.3 The Testing Concept

Since the present study was concerned with the application of Meunier's equation under the new conditions of biaxial loading, it was advantageous to adopt a similar type of impact test using similar equipment. To achieve this similarity for the biaxial impacts, it was necessary to design and build a conceptually unique test apparatus as seen in Appendix A.

When using this apparatus the approach adopted was to initially impact a series of samples normally so as to establish agreement with Meunier's equation. The second aspect required impacts of increasing degrees of biaxial loading. This was achieved using a drop frame with a series of removable impactors of different degrees of inclination which drop onto anvils of similar angles as shown in figure 2. Data generatred from these tests were then compared to data generated by Meunier's equation.

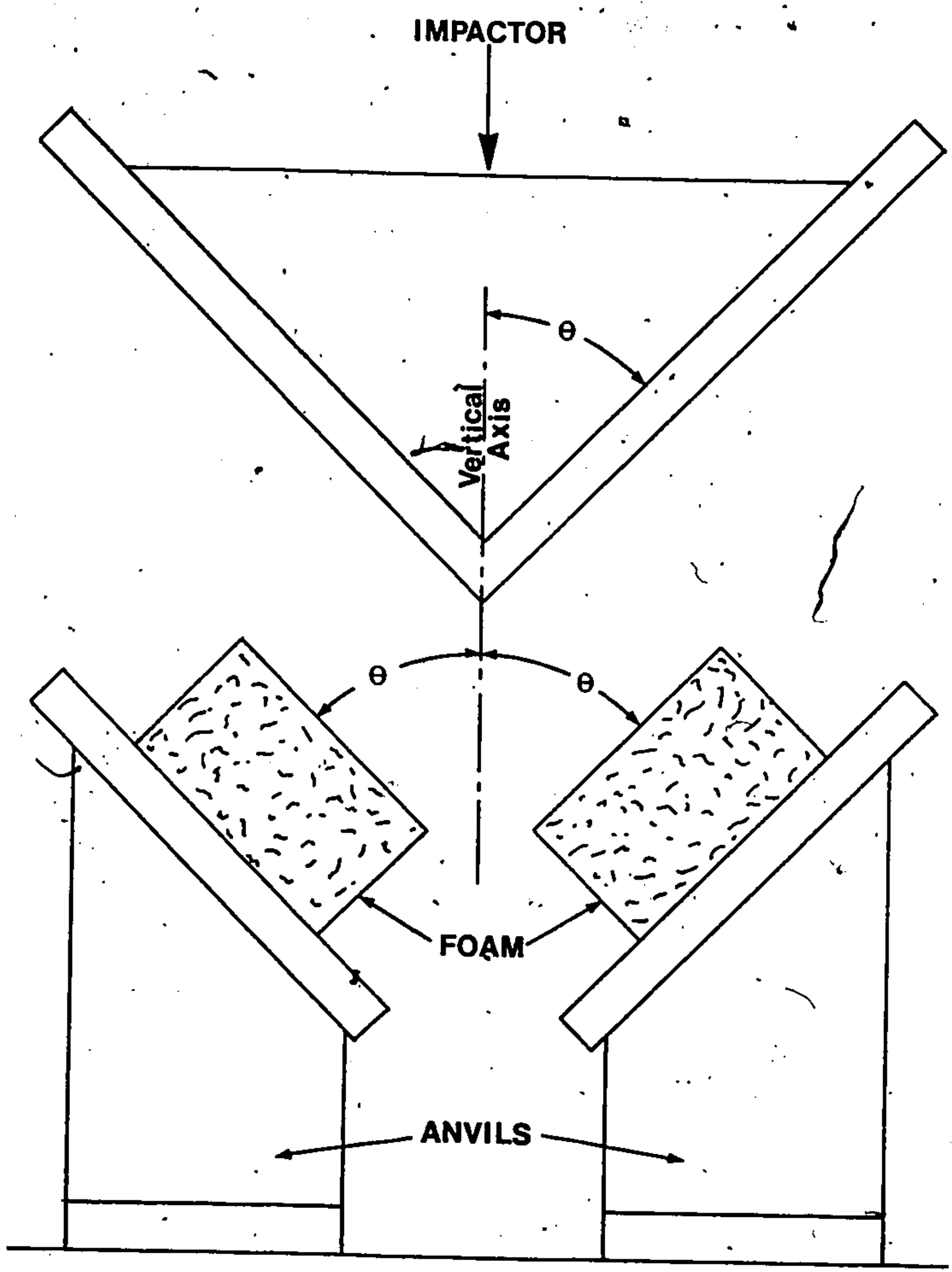

A Schematic of the Combined
Loading Apparatus

Figure 2

II FOAM SAMPLES

The polystyrene bead foam used for both Meunier's and the present study was manufactured from Dow Chemical Pelspan Bead Stock by Morval Durofoam of Kitchener, Ontario. In a typical moulding cycle, pre-expanded beads are loaded into a steam injected mould. The steam expands the beads a little further and sets them in place in approximately two minutes. Immediately after production the foam is very soft and supple. An estimated time lapse of three weeks is necessary before full strength is approached.

A variety of densities were acquired from which three nominal densities were selected; 0.030 gm/cm^3 (1.9 lb/ft^3), 0.037 gm/cm^3 (2.3 lb/ft^3), and 0.058 gm/cm^3 (3.6 lb/ft^3). All samples used for the test were 7 cm by 7 cm by 4 cm thick. Uniformity of the sample size was achieved using a jig designed for the purpose. The samples were cut using a band saw with a blade speed of 100 ft/min to prevent overheating of the cutting zone. This overheating would melt the styrene and coat the finished edge with solid polystyrene. This would affect the density and the strength of the sample wall.

The samples were individually numbered, weighed and their dimensions measured. These data were processed by computer (see Appendix D for details of the program) to select sample groups which were within specific density and height limits of ±0.002 gm/cm^3 and ±0.2 cm respectively. Because of the need to counterbalance the angled impactor, two samples were used, orientated at equal angles either side of the vertical axis of travel of the impactor as illustrated in Figure 2. This required the consideration of common densities and heights when choosing sample couples for each run.

A selected number of samples were sandwiched between aluminum plates using epoxy as a bonding agent. The aluminum plates were designed to engage into corresponding ridges on the anvil and impactor to ensure that there would be no slippage between the foam samples and the impacting surfaces as shown in Figure 3. Preliminary tests showed that the aluminum plates did not have any significant effect on the behaviour of the foam, but the signal noise was greatly increased by the vibration of the plates as seen in Figure 4. Because of this, the use of the plates was discontinued.

To aid in the evaluation of the deformation history of the foam samples a grid was printed on the side of the samples. A silk screen technique was developed to print the uniform square grid which is shown in Figure 5. The grid was clearly visible on the high speed film clips of the impact event as seen in Figure 6(A-C). It also served well in the analysis of the permanent deformation of the sample as shown in Figure 7.

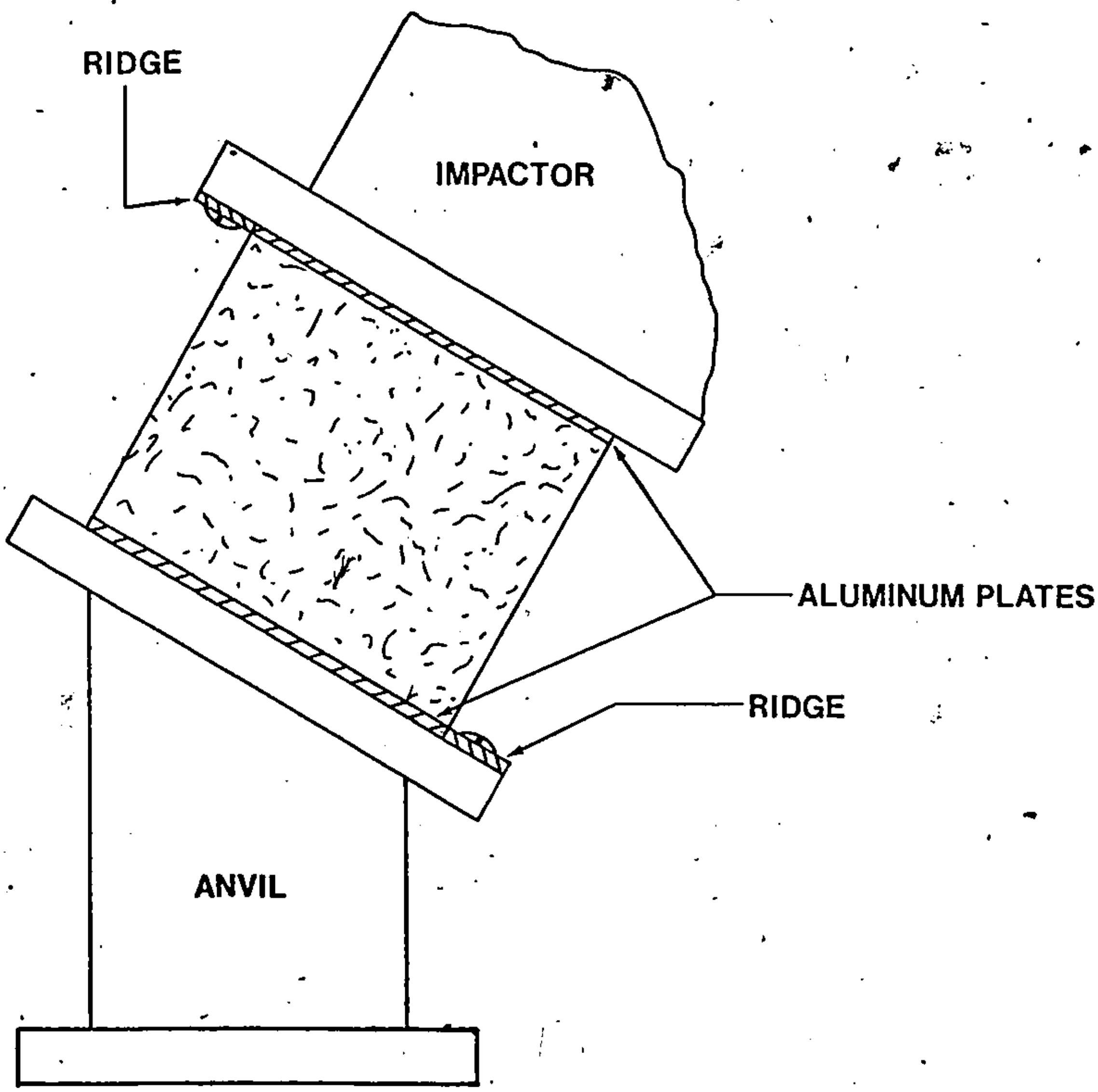

Aluminum Plate and Steel Ridge System used
in Preliminary Experiments
Figure 3

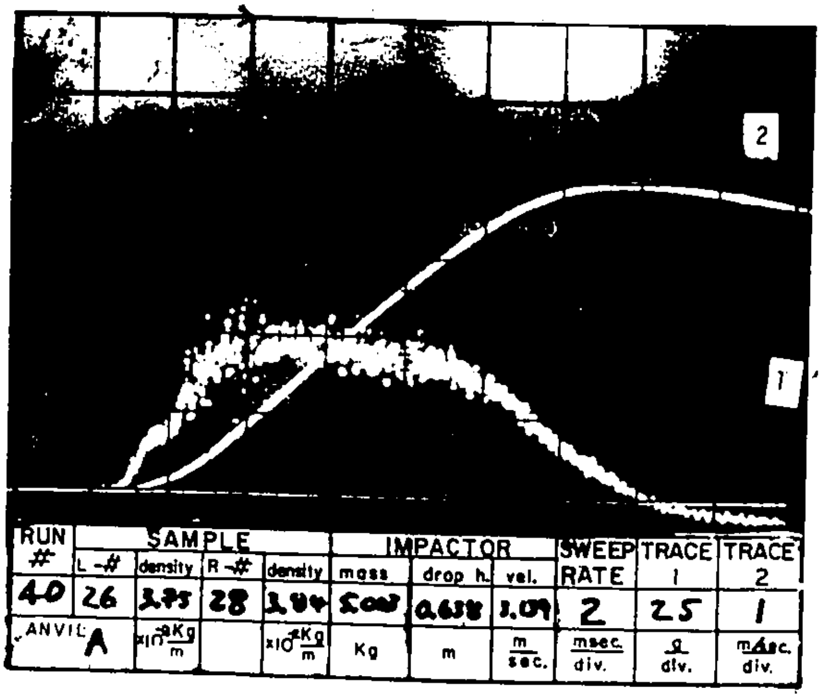

Accelerometer and Velocity Traces of Impacts with Aluminum Plates

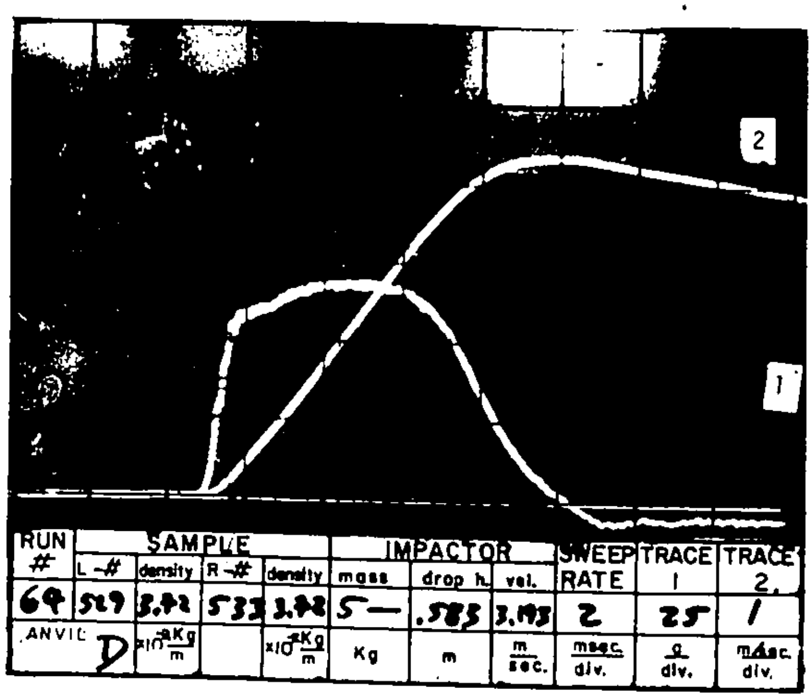

Accelerometer and Velocity Traces of Impacts Without Aluminum Plates.

Figure 4

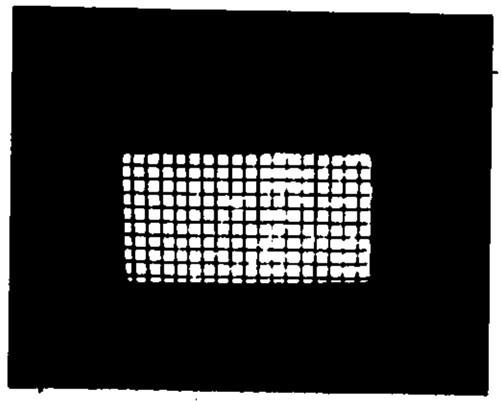

Grid Printed on the Sample by Means of a Silk Screen Technique.

Figure 5

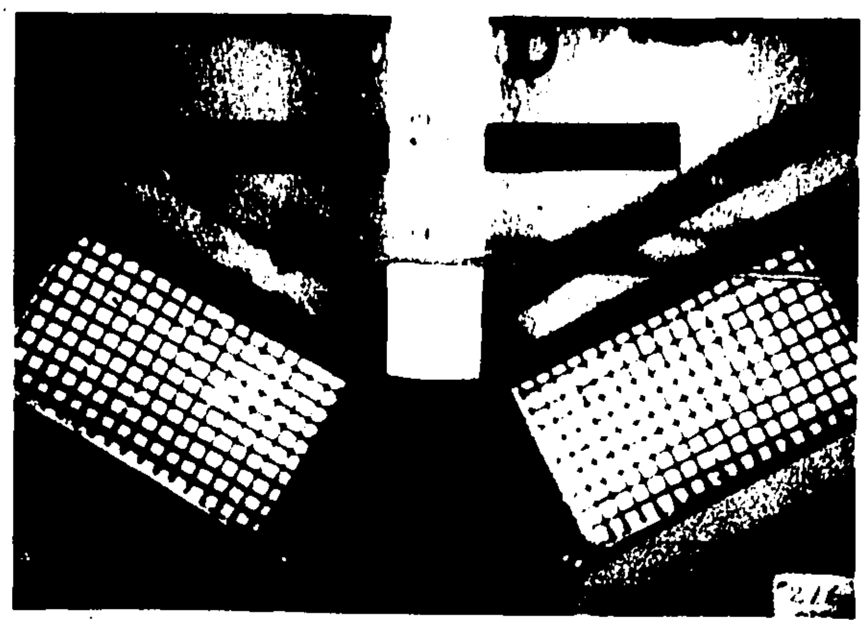

Film Clips of the Deformation Sequence Illustrating the Clarity of the Printed Grid.

Figure 6A

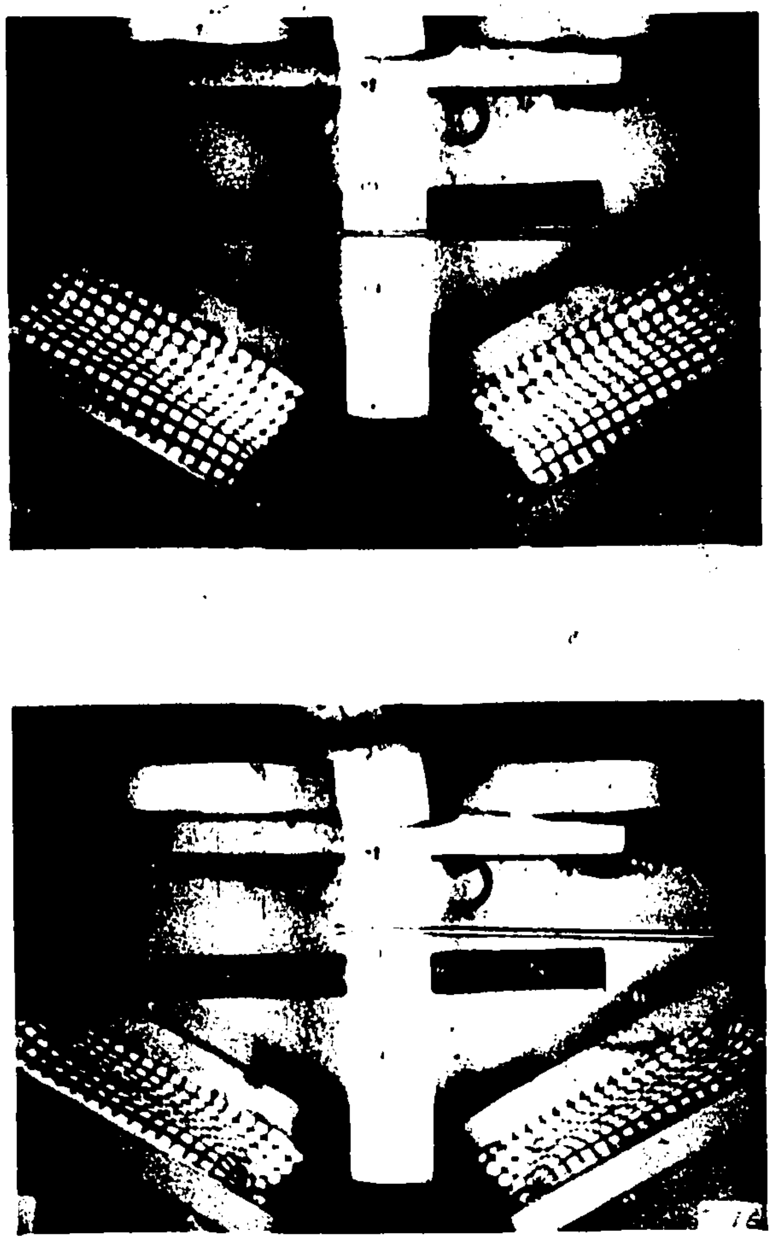

Figure 6B

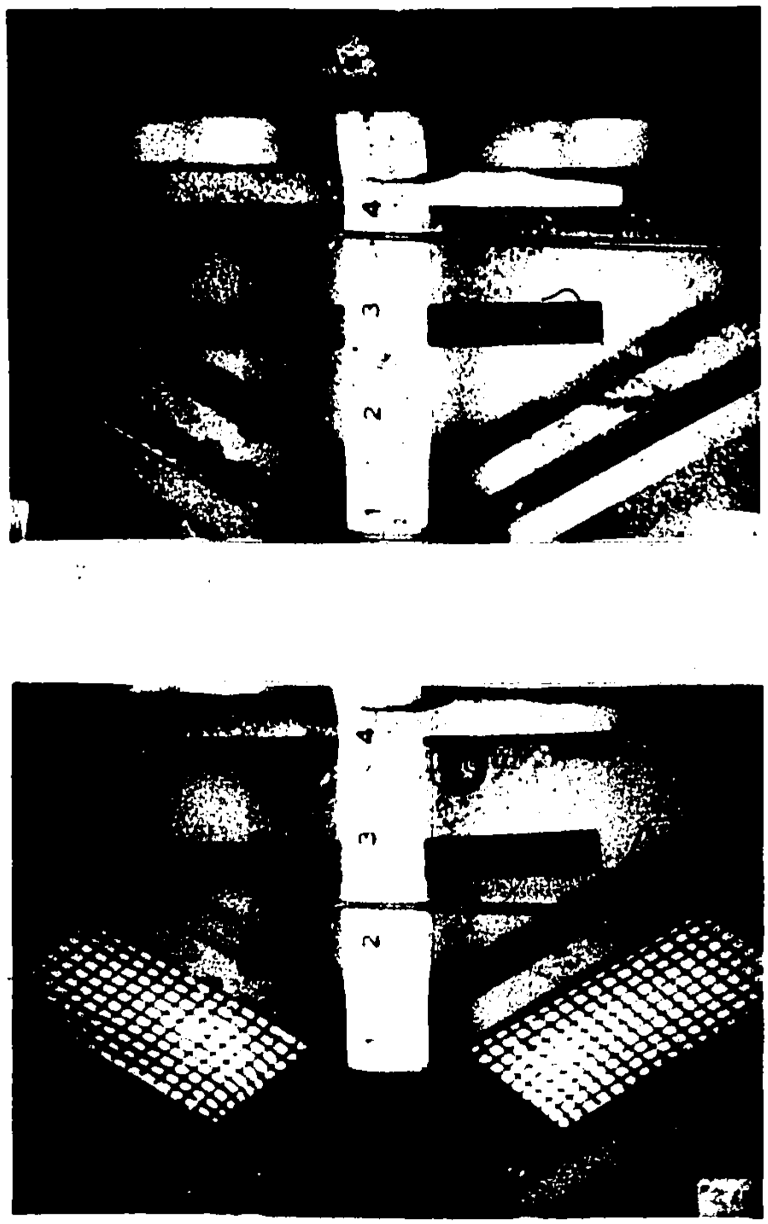

Figure 6C

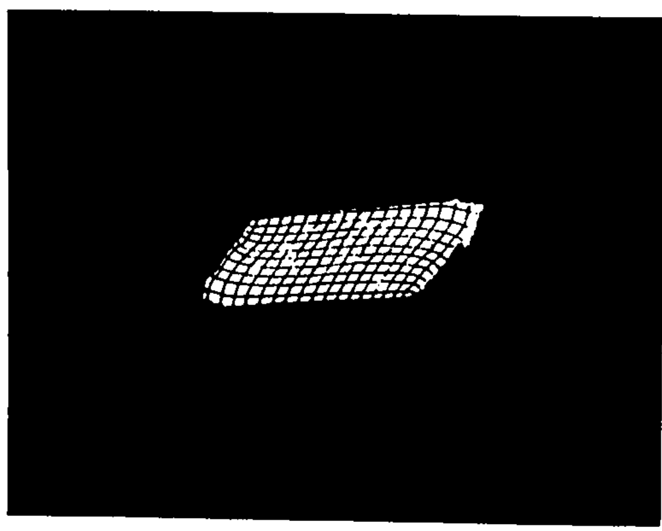

Grid Pattern Illustrating the Permanent Deformation of the Sample.

Figure 7

III DEVELOPMENT OF TEST APPARATUS

In an effort to become familiar with the general behaviour of PSB foam, a number of preliminary experiments were conducted (Appendix B). In addition, these experiments helped to determine the effects that different testing concepts previously developed for other engineering materials had on PSB foam.

The shear box, used in soils testing for example, proved to be inadequate because under shear, the foam would fail by extrusion well below the intended shear plane. (See Appendix B): This produced large pockets of irregular shapes making it very difficult to determine the shear area and to differentiate between sheared and normally loaded material.

It was at this point that the concept of using an angular impactor was introduced. By employing an angular mass and anvil, different biaxial loadings were obtainable by jointly varying the angle of impactor and anvil.

The five impactor angles selected for this experimental program were 0^{o}, 15^{o}, 30^{o}, 45^{o} and 60^{o}. The 0^{o} angle acted as the reference test for the conventional normal impact loading. For each angle an impacting mass of 5 kg at energy levels of 25, 50, 75, 100 Joules and a mass of 10 kg at every levels of 50, 100, 150 and 200 Joules were used. The various impactors were bolted to a steel frame which was guided vertically by two steel rods which has been installed for a previous study(13). A photograph of the apparatus set-up is seen in Figure 8.

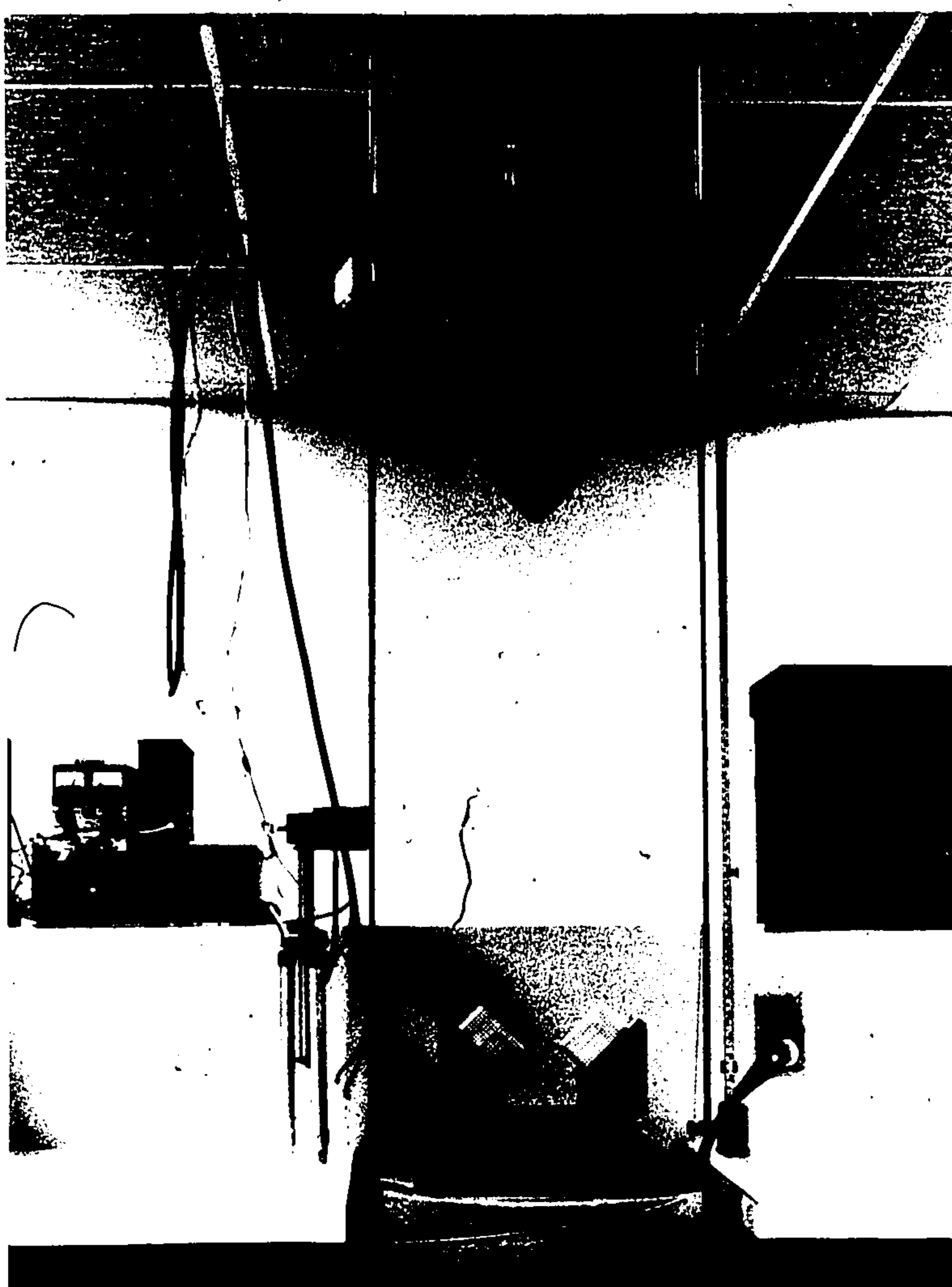

The Test Apparatus Set Up

Figure 8

The five impactors were constructed from 3/8" cold-rolled 1020 steel. All joints were welded and the impacting and mounting surfaces were milled flat. Two steel strips were screwed to the impacting surfaces to act as positioning stops for the foam samples prior to impact as seen in Figure 9.

The impactor which was screwed to the drop frame also supported the weights which were bolted symmetrically to the impactor. An Endevco Accelerometer model 2271AM20 was secured to the impactor through the vertical center of the impactor. The drop frame assembly was guided by two stainless steel rods on 16" centers with a free fall capacity of approximately 3 meters.

The anvils were constructed from 3/8" cold rolled 1020 steel. They were welded and then machined and also included steel stop strips for the alignment of the foam samples. Each pair of anvils consisted of inclined surfaces mounted on support blocks. The two anvil components were bolted through slotted holes to a plate that was keyed parallel with the slotted holes of the anvils. The plate was in turn bolted to a permanently fixed base plate through slotted holes running perpendicular to the anvil slots. This gave the anvils linear freedom on the horizontal plane which was needed for proper alignment of the samples before impact. An illustration of the impactor and anvils is seen in Figure 9.

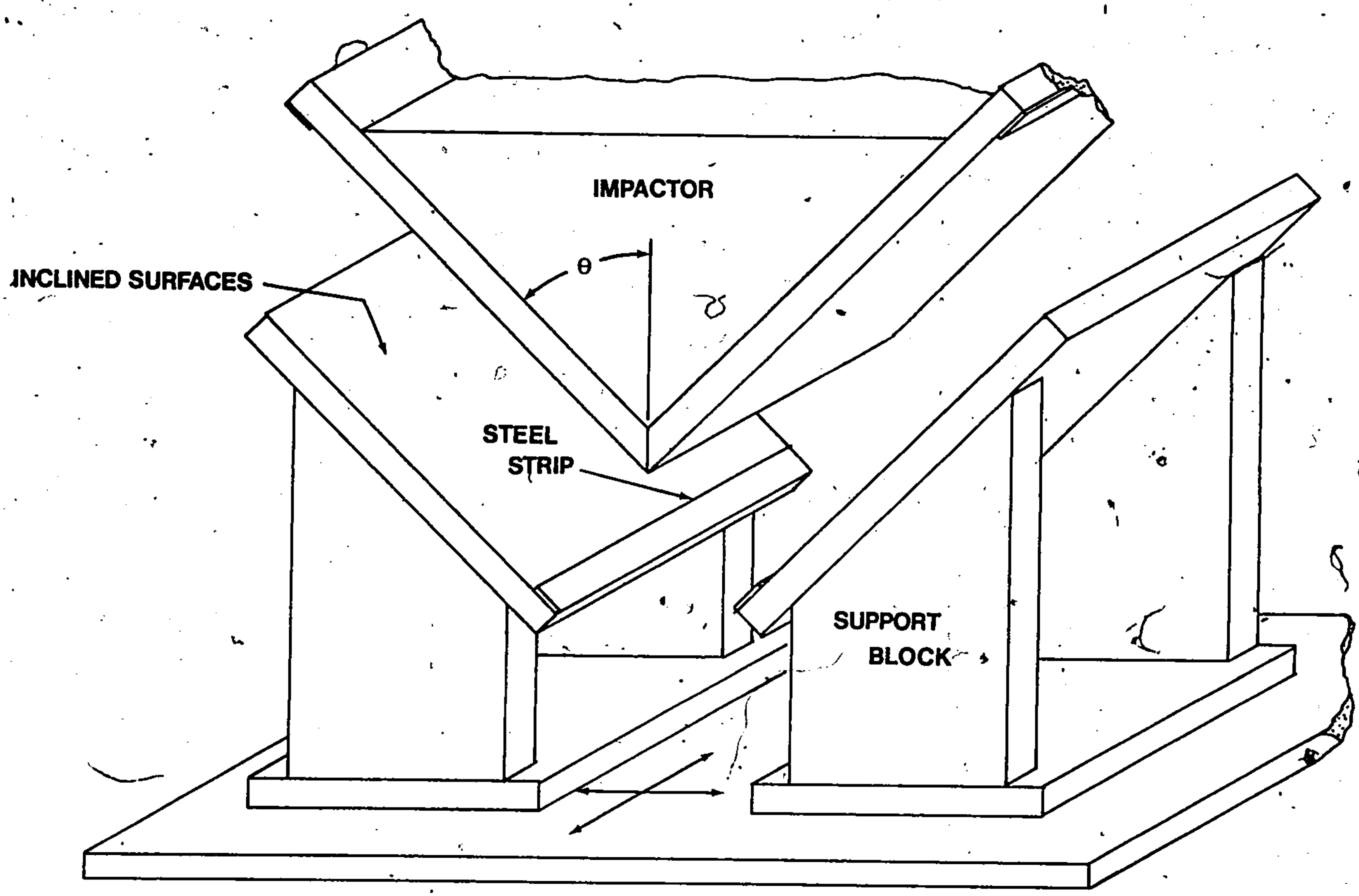

Main Components of the Impactor and Anvils
(Cross arrows refer to the positional adjustment of the Anvils)

Figure 9

IV INSTRUMENTATION

The sensing elements used for this study were an Endevco Accelerometer Model 2271AM20 and the velocity gate which had been designed for a previous study conducted at the University of Ottawa by Webster (13). The signal from the accelerometer was amplified by a Brüel and Kjaer Model 2625 charge amplifier. The output signal from the charge amplifier was split with one output going to an oscilloscope channel and the other output signal going to an electronic integrator. The integrated signal, velocity, was then fed to a second channel in the oscilloscope and both signals were stored on the oscilloscope screen. The stored signals were labeled and then photographed using Eastman Kodak #5369 35mm film at an exposure setting of 15sec at f 5 in normal working light.

The velocity gate was used to determine the velocity of the impactor just prior to impact and also to trigger the oscilloscope.

For some of the tests, high speed filming of the impact event was conducted. The "Locam" high speed camera with a framing rate of 500 frames/sec was used.* Light was provided by four 1000 watt quartz iodine spot lamps which were so arranged to minimize shadows and to produce an E.V. reading of approximately 4.5 at a distance of 1 foot from the surface of the foam. Kodak Tri-X, 16mm reversal double perforated film #7278 was used at an exposure setting of f 4 at 500 frames/sec with a shutter angle of 30^0.

* Problems with the camera speed control developed resulting in some of the impacts being filmed at 250 frames/sec rather than the expected 500 frames/sec. This made an analysis using the film very difficult as the time lapse between each frame became to great.

V TEST PROGRAM

The test program consisted of 131 tests of which 11 were void due to trigger failure and 6 were discarded because of other problems. As previously mentioned in section III the test program variables consisted of two masses, 5 and 10 kg, 3 densities 0.031, 0.038, 0.058 g/cc, 5 impactor angles 0^o, 15^o, 30^o, 45^o, 60^o and 4 energy levels per impact mass 25, 50, 75, 100J for the 5 kg load and 50, 100, 150, 200J for the 10 kg load.

Impactor angles were chosen in the following order so as to discourage biasing of the data; 45^o, 30^o, 60^o, 0^o, 15^o. For each angle 3 different density groups were used under the same impact energy. The impacting energies were also arranged randomly at 25, 75, 50, 100 Joules. The same general format was followed for the 10 kg impact masses.

A typical series of runs commenced with the installation of the pre-weighed impactor and its corresponding anvil. The calibration of the test equipment was checked by impacting a plastic calibration pad* which possesses repeatable response characteristics and comparing the results with pre-recorded calibration data.

Two foam specimens were selected and placed on the two anvils and then the two anvils were adjusted to insure that a proper simultaneous impactor contact was made with each specimen. The impactor was raised to a predetermined height to produce a chosen impact energy.

* Details of the calibration pad are presented in Appendix A.

The oscilloscope trigger and the velocity transducer zero were set. At this point the high speed cameras (when used) were started and the drop frame released. The accelerometer and the electronically integrated velocity traces were stored by the oscilloscope and a 35mm camera was employed to record the traces. An example of a data record is seen in Figure 10.

In addition, the tests were conducted at room temperature over a short period of time.

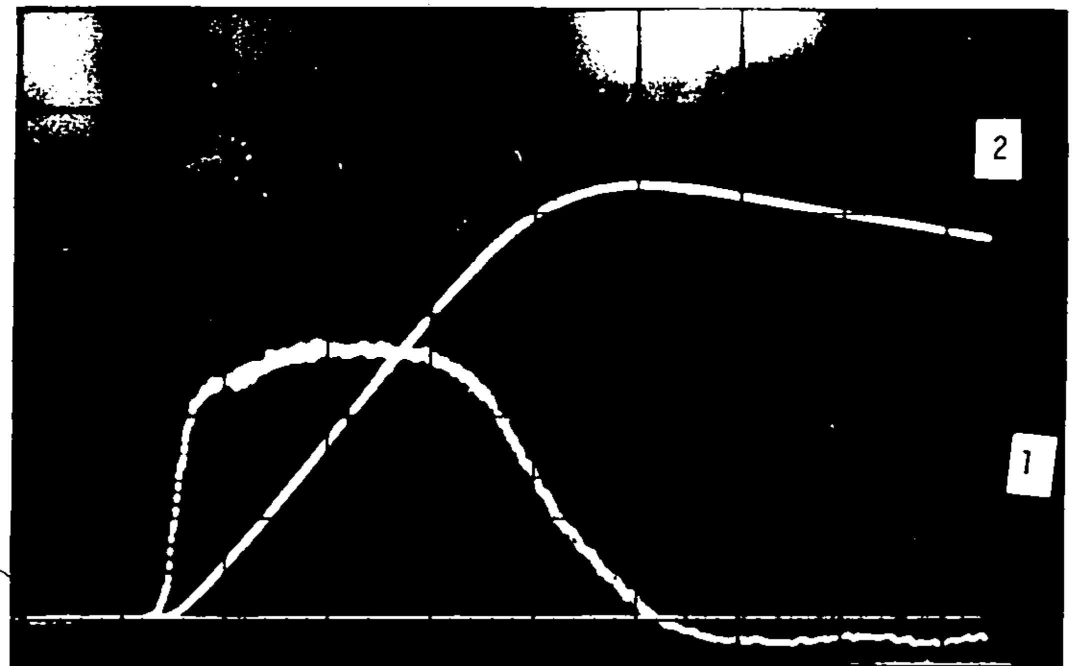

RUN #	SAMPLE				IMPACTOR			SWEEP RATE	TRACE 1	TRACE 2
	L-#	density	R-#	density	mass	drop h.	vel.			
26	492	2.77	523	2.77	5.006	.594	2.13[illegible]	2	25	1
ANVIL C		$\times10^{-2}\frac{Kg}{m}$		$\times10^{-2}\frac{Kg}{m}$	Kg	m	$\frac{m}{sec.}$	$\frac{msec.}{div.}$	$\frac{g}{div.}$	$\frac{msec.}{div.}$

An Example of the Data Record

Figure 10

VI OBSERVATION AND DATA

VI.1 Initial Discussion

As previously mentioned, test data were arranged in groups of common impact mass, energy and density with the variable in any given group being impact angle.

Plots were constructed to help illustrate the different performance characteristics of PSB foam with respect to changes of impact angle. The maximum acceleration values were plotted against impact angle with density and impact energy remaining constant. An example of which is shown in Figure 11.

An initial examination of the data with respect to the maximum acceleration versus the angle of inclination revealed a decrease in "g" forces with an increase in shear angle. The apparent conclusion was that an increased shear angle will provide increased shock attenuation. Upon closer examination of this observation through normalization of the data, it became clear that this initial conclusion was questionable.

VI.2 Normalization of Data

The normalization of the data involved an accounting for the change in sample orientation for biaxial impacts. This was achieved by plotting the product of maximum acceleration and $(\cos\theta)^{-1}$ against the impactor angle as seen in Figure 12. The resulting curve suggests that the initial conclusion that increased shear angle will provide increased shock attenuation is invalid. Because of this exercise it became apparent that special geometric considerations had to be made to account for the change in sample orientation. These would

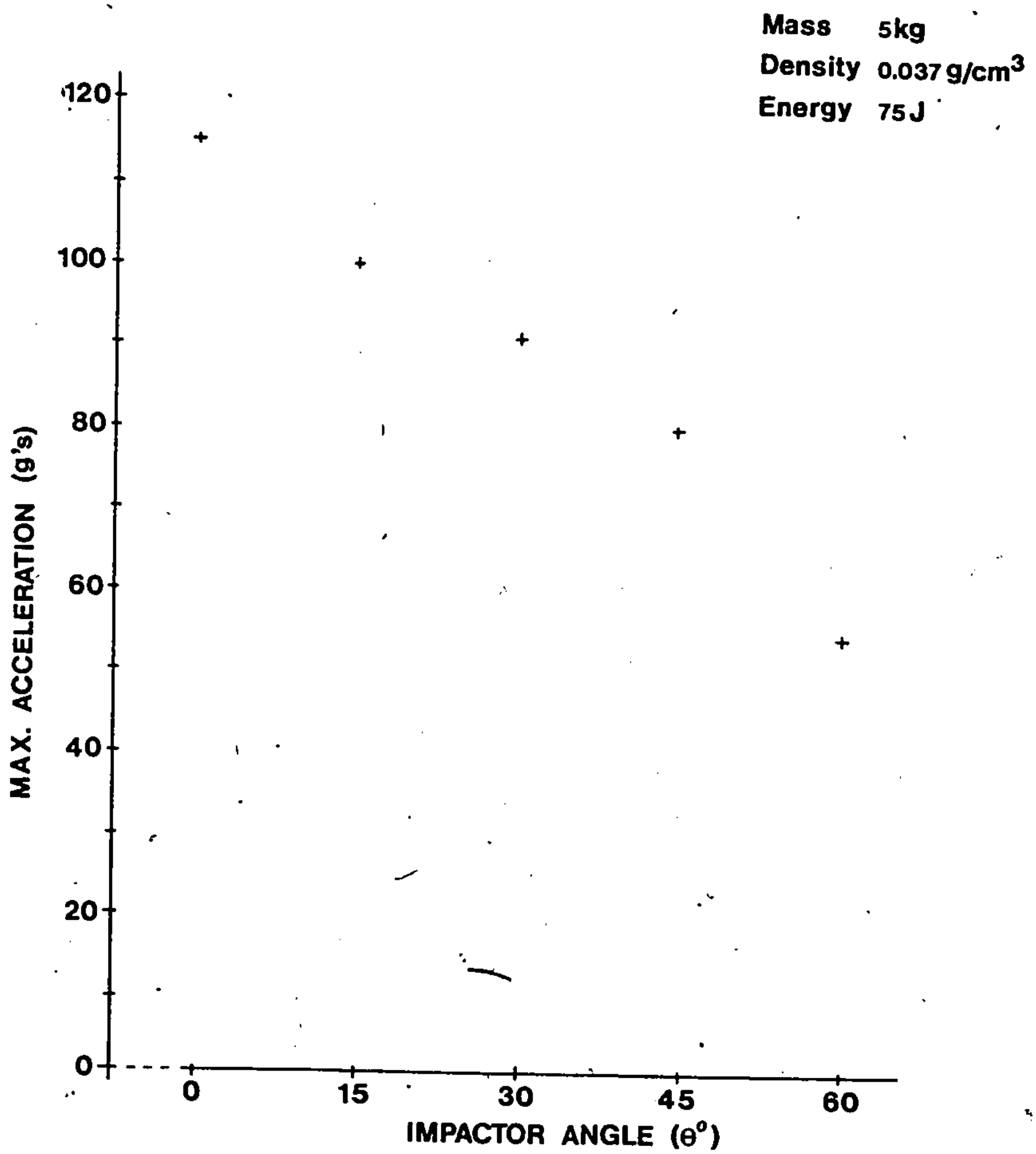

Maximum Acceleration Versus
Impactor Angle with Constant Impactor
Mass and Energy and Sample Density
(Experimental Data)

Figure 11

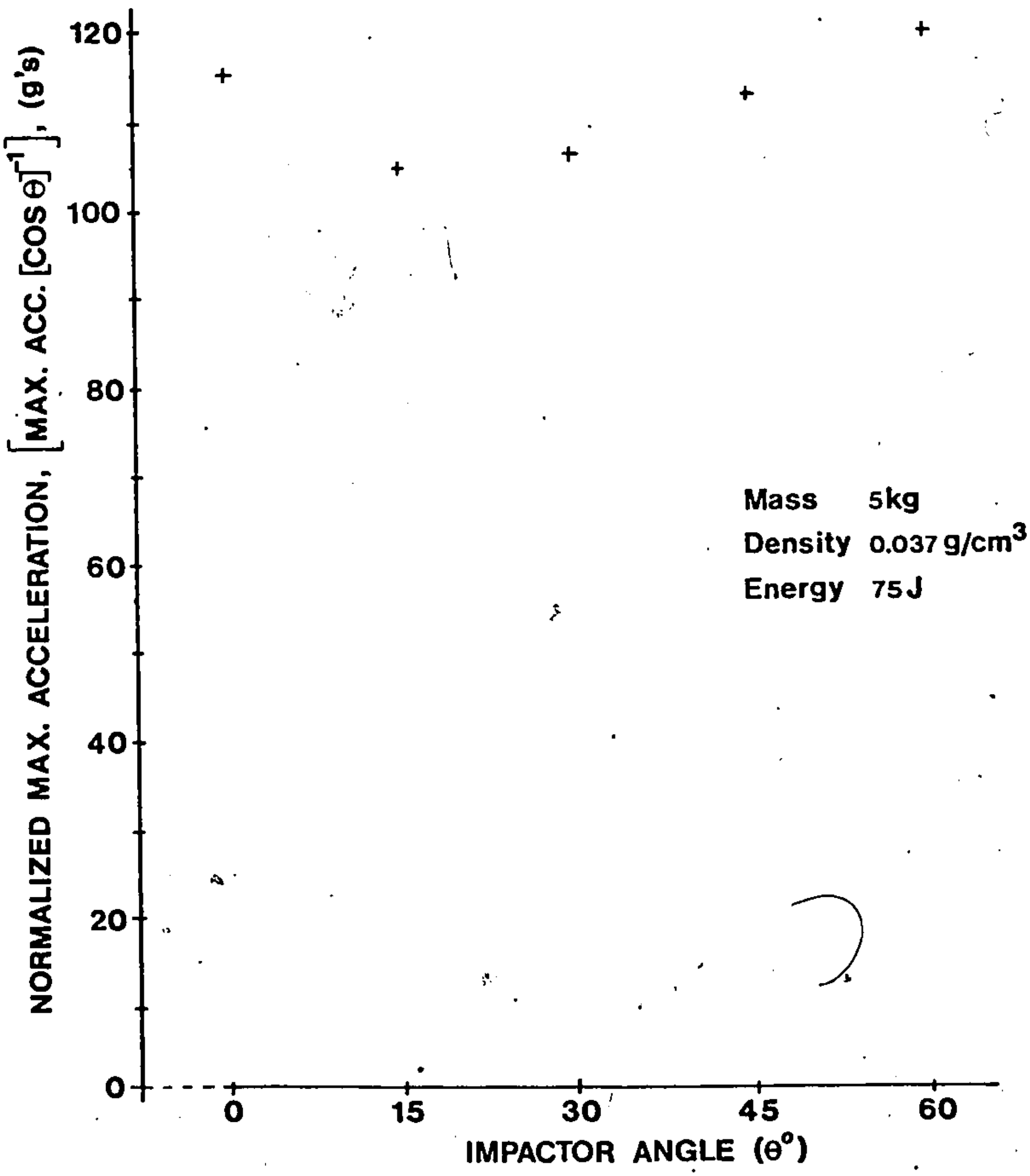

Normalized Peak Acceleration Versus
Impactor Angle with Constant Impactor
Mass and Energy and Sample Density
(Experimental Data)

Figure 12

be applied when working with equation A.

VI.3 Equation A

Meunier (5), using similar instrumentation arrived at the following predictive equation to describe PSB foam under high variable strain rates for normal impact conditions.

EQUATION A

$$\sigma = f(\varepsilon) \cdot f(\rho) \cdot f(\dot{\varepsilon}_o) \cdot f(v)$$

where

σ = stress in megapascals

$f(\varepsilon) = 415.72 \exp(0.88\varepsilon) + 0.01343 \exp(13.9\varepsilon) + 1.25 \times 10^{-13} \exp(42.0\varepsilon)$ (megapascals)

$f(\rho) = C_1 \rho^{1.5}$

$f(\dot{\varepsilon}_o) = C_3 \sinh^{-1} (C_4 \dot{\varepsilon}_o)$

$f(v) = 0.796 + 0.204 \dfrac{v}{v_o}$

ε = strain

$\dot{\varepsilon}_o$ = initial strain rate = v_o/T_o

ρ = density (g/cm^3)

v = instantaneous velocity (cm/min)

v_o = initial velocity (cm/min)

T_o = initial thickness of the foam (cm)

$C_1 = 0.098$, $C_3 = 0.03057$, $C_4 = 3.75 \times 10^{13}$ when ρ, v, v_o and T_o are given in units shown above.

By using this equation in conjunction with the data from the normal or 0^0 impacts of the present study, a comparative base was established. Initially, however, there was disagreement between the normal impact data from the present study and the curves generated by equation A. It was necessary, therefore, to alter equation A by applying a 10% corrective factor to the velocity term which led to a satisfactory correlation with the normal impacts as illustrated in Figure 13. Possible reasons for this discrepancy are differences in the precision of data for impact velocity and/or a greater sample surface area to periphery ratio between this study and Meunier's study.

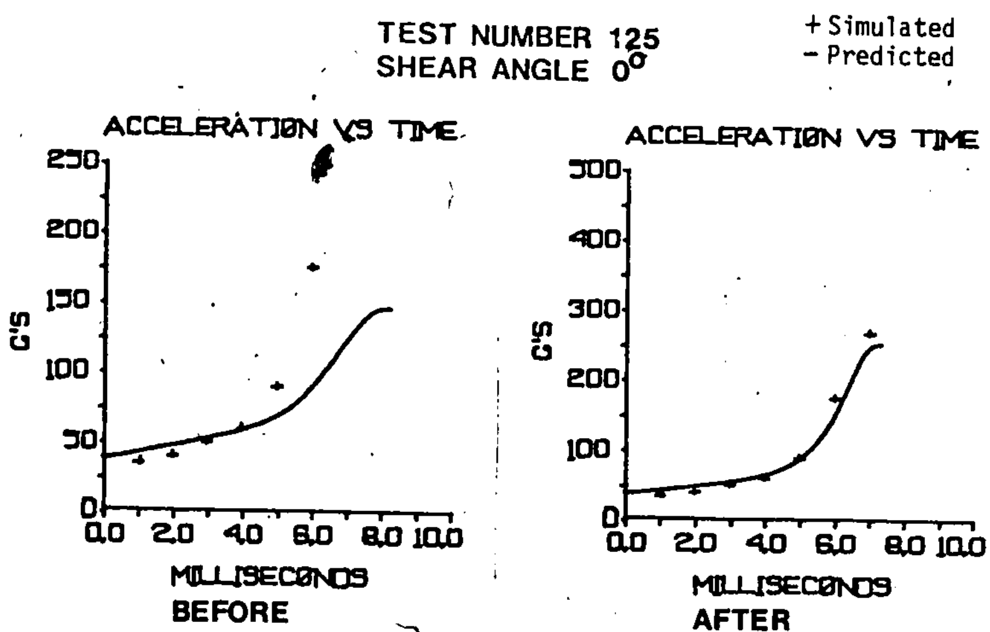

Comparison of Predicted Data with Simulated Results Before and After the Velocity Correction.

Figure 13

It was postulated that angled or biaxial impacts could be treated as normal impacts by applying certain geometric factors to Meunier's equation. If the resulting curves correlated well with curves produced by the predictive equation then it could be concluded that biaxial impact loading could be predicted using the normal impact equation.

VI.4 Geometric Analysis

As previously mentioned in section VI.2 special geometric consideration were needed when working with equation A. From a practical point of view, the change in sample orientation resulted in a change in surface area and thickness with respect to the axis of the impactor's travel.

For the normal impact condition we have the following geometric parameters as illustrated in Figure 14.

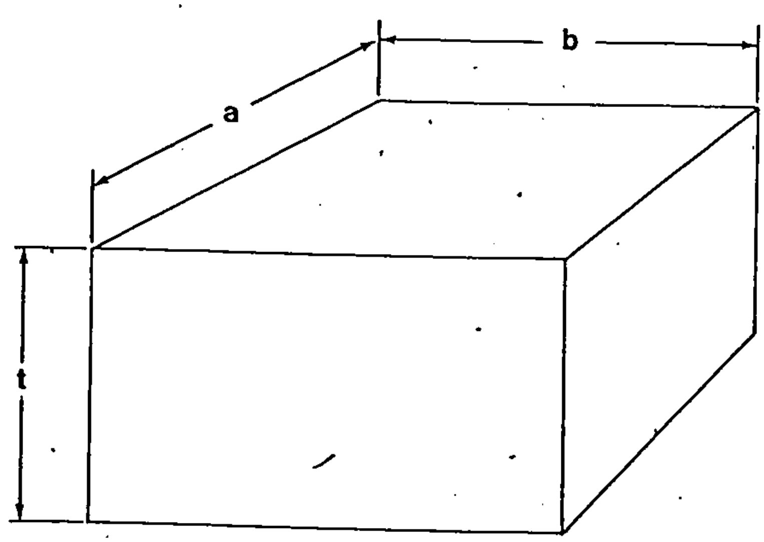

The Initial Geometric Parameters of the Sample.

Figure 14

Considering the biaxially loaded specimen in Figure 15 as normally loaded, the following geometric alterations are required.

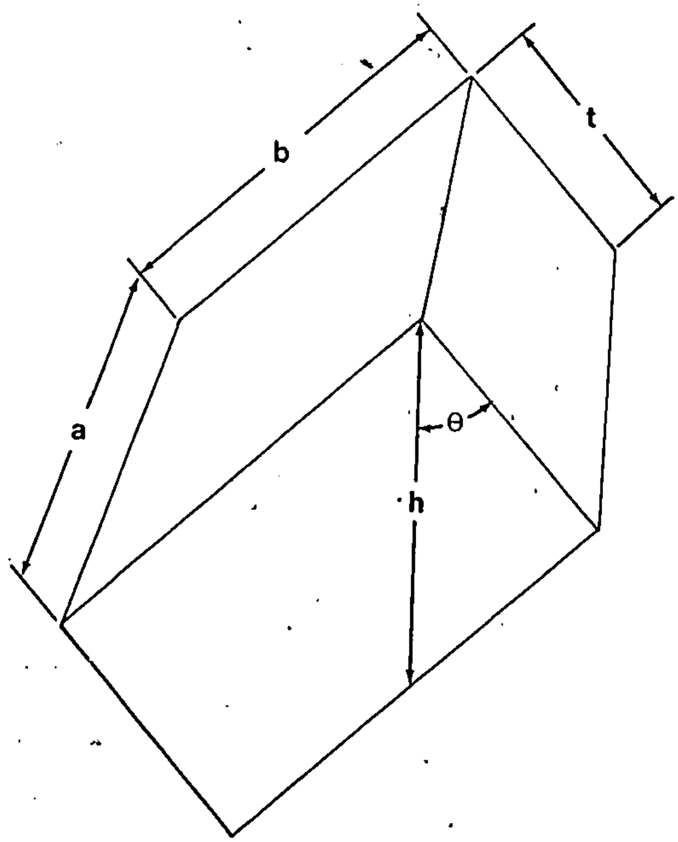

The Orientation of a Biaxially Loaded Specimen.

Figure 15

VI.4.1 Thickness

Thickness is regarded as the distance separating the surface of the impactor and anvil when the impactor makes initial contact with a non-deformed foam specimen. For the normal impact condition, thickness is represented by t. When biaxial loading occurs, the sample is tilted to angle θ. Thickness is no longer t but becomes t/cos θ represented by 'h' in figure 15.

VI.4.2 Impacting Area

During normal impacts, the impacting area A is taken as the plan projected area a x b, Figure 14, which is supported by a thickness t of foam. When the sample is tilted during biaxial testing, the projected area changes. The dimension 'a' remains the same while the dimension 'b' is altered resulting in a new area of A = ac seen in Figure 16.

Although ac is the true projected area, it is not totally supported by a constant thickness of foam at the extremities of the sample in the c dimension as shown in Figure 17.

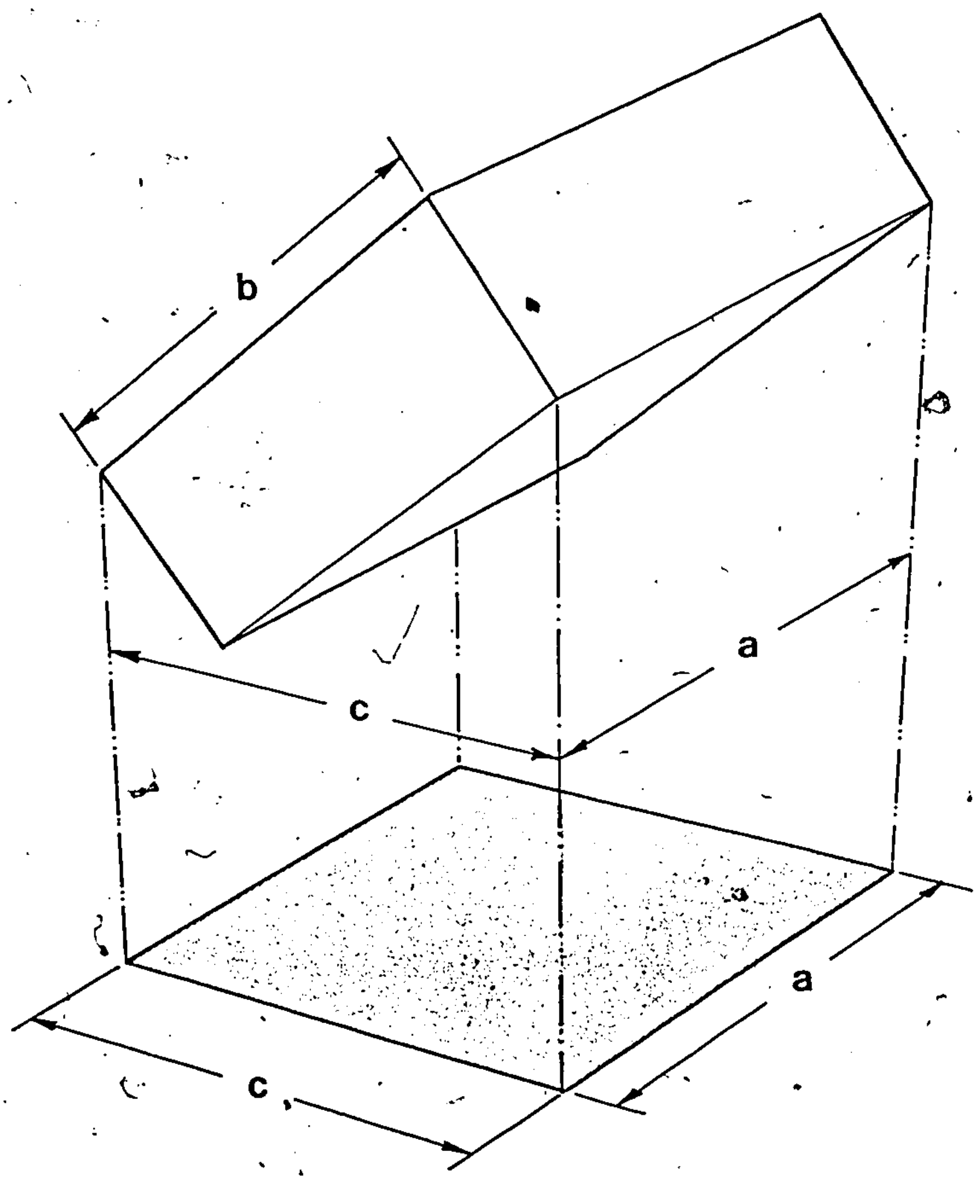

Projected Surface Area when
the Sample is Tilted

Figure 16

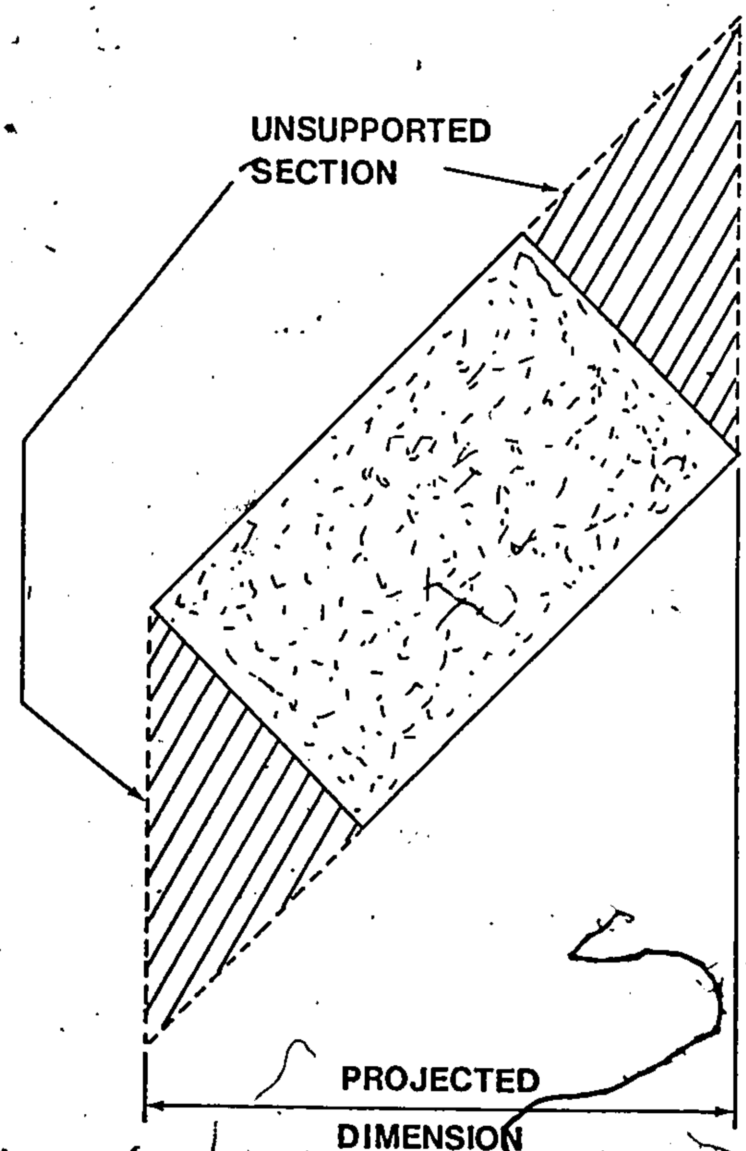

Sample Regions Not Supported by Foam

Figure 17

As a compromise, the corrected dimension chosen was the projected length of a line bisecting the sample at t/2 is illustrated in figure 18.

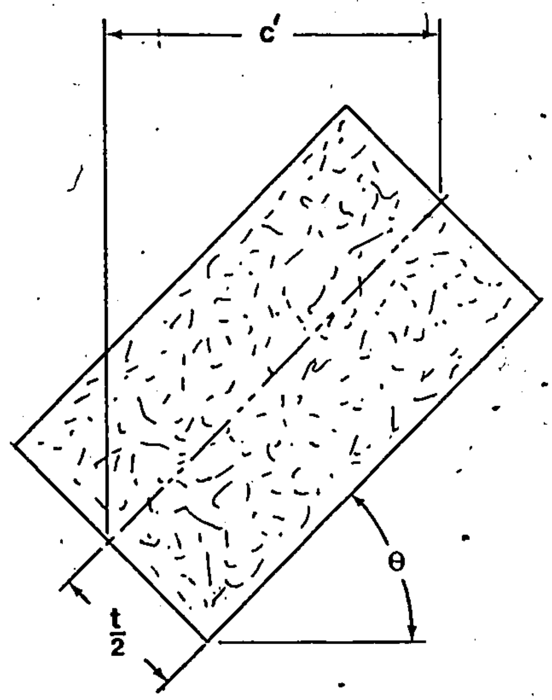

Corrected Dimension Chosen for Use in the Area Calculation.

Figure 18

The resulting projected dimension is $c' = b \cos \theta$. The corrected area term becomes $A_C = ab \cos \theta$.

In summary, the approach is to analytically alter the dimension of the biaxially loaded specimen to a normal impact condition and then to apply the results to the corrected equation "A" which follows.

VI.5 Equation "A" Revised

$$\sigma = f(\varepsilon) \cdot f(\rho) \cdot f(\dot{\varepsilon}_o) \cdot f(v)$$

where

$$f(\varepsilon) = 415.72 \exp(0.88\varepsilon) + 0.01343 \exp(13.9\varepsilon) + 1.25 \times 10^{-13} \exp(42.0\varepsilon)$$

$$f(\rho) = 0.098\rho^{1.5}$$

$$f(\dot{\varepsilon}) = 0.03057 \sinh^{-1}(4.125 \times 10^{13}\dot{\varepsilon}_o)$$

$$f(v) = 0.796 + 0.2244 \frac{v}{v_o}$$

$$\dot{\varepsilon}_o = \frac{v}{T_o}$$

ρ = density (g/cm^3)

v = instantaneous velocity (cm/min)

v_o = initial velocity (cm/min) (at point of impact)

T_o = initial thickness of the foam (cm)

ρ, v, v_o, and T_o are given in the units shown above.

The subsequent acceleration/time curves generated by this equation are compared with the experimental values of maximum "g" versus time from this current study. The maximum "g" values were determined manually from the photographed curves at intervals of 1 msec. If the curves correlate, then Meunier's normal-impact equation can be used to predict biaxial loading conditions provided a proper geometrical correction analysis is conducted.

From the accelerometer data one can generate through integration, the quantities of velocity and displacement of the impactor versus time. The acceleration value applied to Newton's Law of Force = Mass Acceleration yields force which, when divided by the impacting area, gives stress. Knowing the displacement and the stress over time it is possible to generate a stress-strain curve of the foam during impact. An example of this is shown in Figure 19.

TEST NUMBER 116
SHEAR ANGLE 0°

INITIAL DENSITY ØF SAMPLE = 0.0322 G/CU.CM
INITIAL THICKNESS ØF SAMPLE = 3.78 CM
INITIAL VELØCITY ØF IMPACTØR = 336.8 CM/SEC
MASS ØF IMPACTØR = 10.000 KG

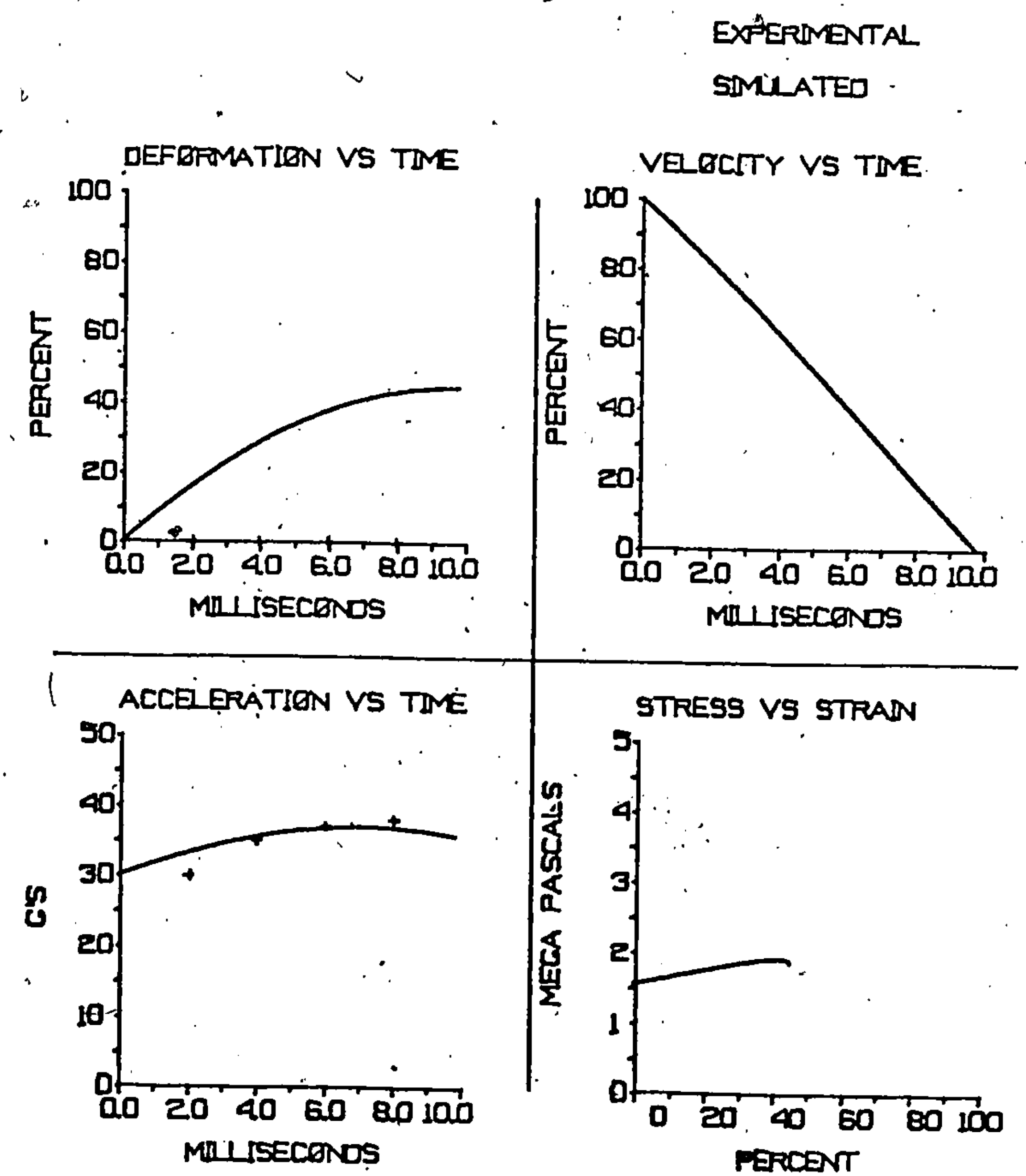

Different Curves Generated From the Results of Equation A

Figure 19

VII DISCUSSION OF RESULTS

VII.1 The Velocity Correction Factor:

As discussed in section VI.3, the 10% correction factor applied to the velocity term had the effect of minimizing the amount of disagreement between the experimental and calculated maximum acceleration values for normal impact conditions. The factor was arrived at through a rigorous iterative process whereby small incremental changes were made to the different variables and the resulting acceleration versus time curve compared with the experimental data. Through this exercise, velocity emerged as the variable which when altered, produced the best acceleration versus time agreement with the experimental results. This choice is reinforced through the following practical analysis of the velocity variable.

Velocity is the one factor that has the most profound effect on the calculated curve. A very small change in velocity, under certain conditions, will produce very large differences in peak acceleration. Velocity was also the most difficult variable for Meunier to evaluate. All of the other variables were direct measurements of weight and/or size.

The velocity term used by Meunier was arrived at through a complex exercise involving manual integration of the acceleration versus time curve using a time base derived from the displacement versus time trace. The time base used for the integration was determined by observing at what time the linear transducer indicated maximum compression. This, unfortunately, assumes that there is no lag difference between the linear transducer and the accelerometer and their respective interface networks.

An examination of Meunier's calibration trace of the linear transducer and the accelerometer (Figure 20) reveals an apparent time lag between the linear transducer and the accelerometer trace. The lag may be attributed to an inherent performance characteristic of the linear transducer coils whereby they act as a choke resulting in a detectable signal lag. In addition, the interpretation of the calibration trace requires a subjective judgement in determining the time of maximum displacement. This task is made especially difficult, as seen in Figure 21, where the point of maximum displacement is flanked on either side by asymptotically opposed slopes which make the choice of a definitive time of maximum displacement most difficult. Unfortunately, the linear transducer developed a short circuit before this present study was conducted, preventing a further investigation of this possible problem.

The impact velocity was determined in this current study using a calibrated velocity gate consisting of two infrared emitters and sensors. They were set a known vertical distance apart and were triggered by a knife edge on the falling impactor frame. When the beam from the first emitter was cut, a time clock was triggered. When the blade cut the second beam, the clock was stopped and a calculation produced the impact velocity. Because the velocity gate was positioned a few centimeters above the impact position, the ensuing calculation for velocity included a corrective function which accounted for the additional free fall of the impactor.

'ZERO POSITION' VOLTAGE

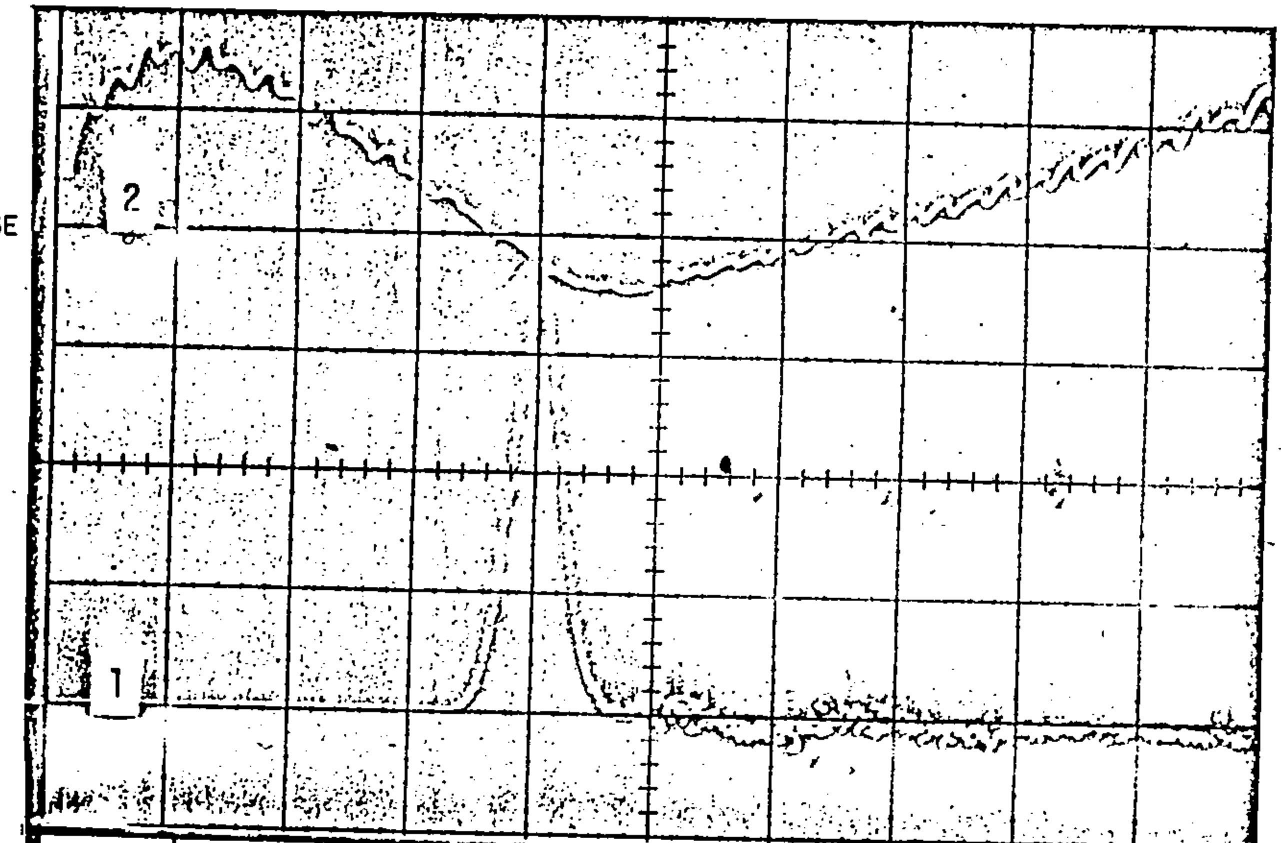

TEST	SAMPLE	SAMPLE T	SAMPLE ρ	IMPACTOR MASS	IMPACTOR VEL.	IMPACTOR DROP H	TRACE1	TRACE2
DGLTH	MEP	— cm	— $\frac{kg}{m^3}$	[illegible] kg	2.21 $\frac{m}{sec}$	2.0 m	[illegible]	LT [illegible]

LINEAR TRANSDUCER CALIBRATION TRACE. (From Meunier (5))

Figure 20

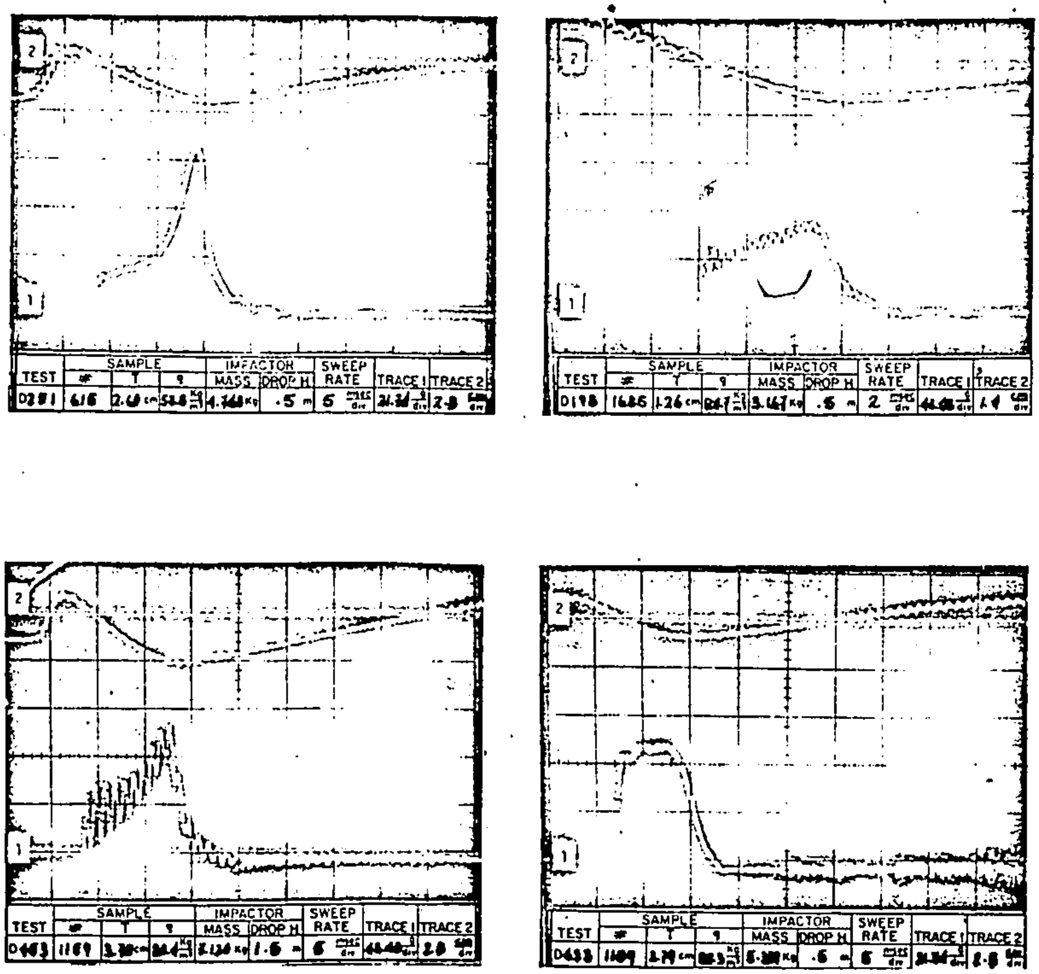

4 SAMPLE ACCELERATION RESPONSES. (From Meunier (5))

Figure 21

VII.2 The Relation of Predicted and Calculated Data for Acceleration versus Time Curves

VII.2.1 Initial Discussion

In figure 22 is displayed the results of test number 117, a normal (0^{0}) impact, which is a representative example of an acceptable agreement between predicted and experimental results.

The predicted or simulated values generated by equation A are represented by the solid curve. The experimental data points which are represented by the symbol +, were determined by individually analyzing each one of the photographed acceleration time curves. In total over 100 curves were analyzed, and the resulting data points stored on computer cards. The computer program used to display this data and the results of equation A was developed by Meunier (5).

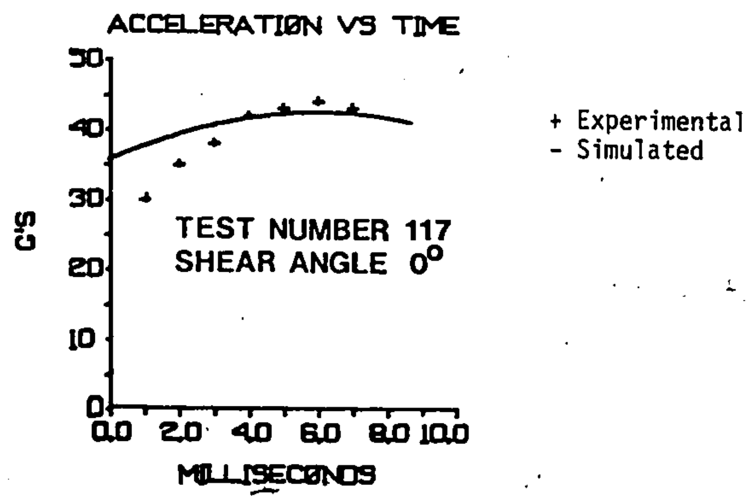

A Representative Example of
Acceptable Agreement Between
Predicted and Experimental Results

Figure 22

Typical of most curves from this study there is poor correlation during the first three msec. of impact. It is partially due to the nature of the predictive equation in that at time equal zero, calculated acceleration was not set equal to zero. All plotted data from this study were initialized to zero at time equals zero which resulted in an initial disagreement with the predicted results.

In addition, because Meunier obtained such remarkable correlation throughout the duration of the acceleration traces it became apparent that other factors apart from impact velocity may have influenced the results of this study. An examination of possible sources of disagreement follows.

VII.2.2 Thickness to side ratio:

Meunier's samples had a thickness to side ratio of 1:1.15 and 1:2.3. The samples thickness to side ratio used for this study was 1:1.75 per sample or 1:3.5 for each impact test, as there were two samples used simultaneously for each test. It is not likely, however, that this difference had a strong influence on the stress-strain performance of the foam. This is supported by Meunier (3) who, through preliminary experiments, concluded that large changes in the thickness to side ratio produced only small changes in the stress-strain performance. In addition, Rind (14) and Traeger (15) state that Poisson's ratio for polymeric foams is about 0.03. This low value suggests that a small change in area would not greatly affect the stress-strain performance.

VII.2.3 Surface Area

Meunier used sample surface areas ranging from 8.53 cm^2 to

76.74 cm^2. The range of surface area used during this study was 49cm^2 to 96cm^2. Surface area was not considered to be a questionable variable for two reasons. First, a change in surface area did not appropriately alter the acceleration-time performance so as to improve the correlation at 0^0 shear angle. Second, surface area is not a term contained within equation A. Instead, it is used in the force calculation from the stress term generated by equation A.

VII.2.4 Impacting Mass

The impacting masses of 5 kg and 10 kg used during this study were well within the limits of 2.374 kg and 19.984 kg used by Meunier. The impact energies of 25J to 200J were also with Meunier's range of 11.63 J to 418.6 J.

VII.2.5 Physical Properties of the Samples

Although the bead stock used in moulding of PSB foam slabs is of high quality and consistency, the quality of the finished product is less predictable. The chief reason for this is that the forming is done by hand and not on a regular production run, which results in variation of quality within any given batch. This is significant in that many samples must be discarded because of variations in density which makes experimental planning difficult. Also, the characteristics of the foam change with time. Meunier's foam aged one year before testing while samples used for this study aged approximately five months. Old samples are noticeably more brittle than fresh ones. Practically, this may lessen the energy absorption capabilities of the foam.

The variation of the density through the cross-section of a sample as displayed in Figure 23 is another contention point.

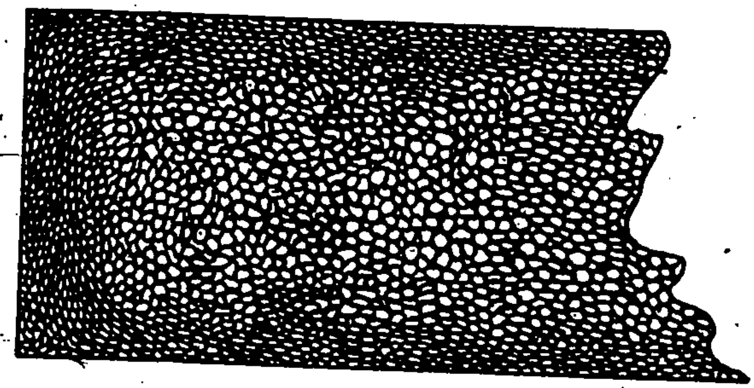

Density Distribution - Transverse Cut of a
Slab of PSB Foam. (From Meunier (5))
Figure 23

Homogeneous distribution of beads is rarely found in moulded PSB foam products. Rusch (16) indicates that such geometric variations of the cell size will affect the shape of the stress-strain curve. The large density gradient is likely the most important factor to consider when working with the performance predictability of PSB foams.

In the wake of the discussion it must be pointed out that the excellent correlation of experimental data to predicted results enjoyed in may areas of material science, can be expected only with large sample groups where statistical confidence can be achieved in the prediction of PSB foam.

VII.3 Comparison of Acceleration Versus Time Curves

When the plots of acceleration versus time for all impact angles from 0^0 to 60^0 were examined, two striking observations emerged.

1. when assembled into groups of similar specimen density, striker mass and impact energy, a comparison between the predicted and experimental curves showed good agreement. In cases where the predicted traces differed in shape from the experimental trend for the 0^{0} impact, the characteristic difference such as curve shape and often the points of intersection with the simulated curve carried through for the 15^{0}, 30^{0}, 45^{0}, and 60^{0}. See Figure 24, 25, 26, and 27.
2. the maximum values of acceleration from the data agreed very well with the predicted maximum acceleration for all impact angles except 60^{0}. The 60^{0} impact produced predicted maximum acceleration figures below the experimental values. See Figures 28, 29, 30, and 31.

Referring to the first observation, the good agreement achieved between predicted and experimental results clearly demonstrates that a reasonable prediction of the acceleration versus time response of PSB foam can be expected using an uniaxial compressive formula for a fiaxially loaded impact.

The conditions where a family of predicted curves (0^{0} to 60^{0} of common density impact mass and energy) consistantly differ in shape from the experimental trend must be considered further. Because the difference appears to be approximately the same for the 0^{0} as for the 15^{0}, 30^{0}, 45^{0} and 60^{0} one must conclude that if the equation could have better predicted the base condition, (0^{0}), it would have better predicted the other four angles 15^{0}, 30^{0}, 45^{0}, 60^{0} by the same order of magnitude.

The second observation suggests that greatest confidence can be placed in the value of predicted peak acceleration as opposed to any other point during the acceleration/time history.

Figures 24, 25, 26, 27 illustrate how the difference between predicted and experimental trends for 0^{o} impact carry through for the 15^{o}, 30^{o}, 45^{o}, and 60^{o} impacts.
(+ Experimental data
  - Simulated results)

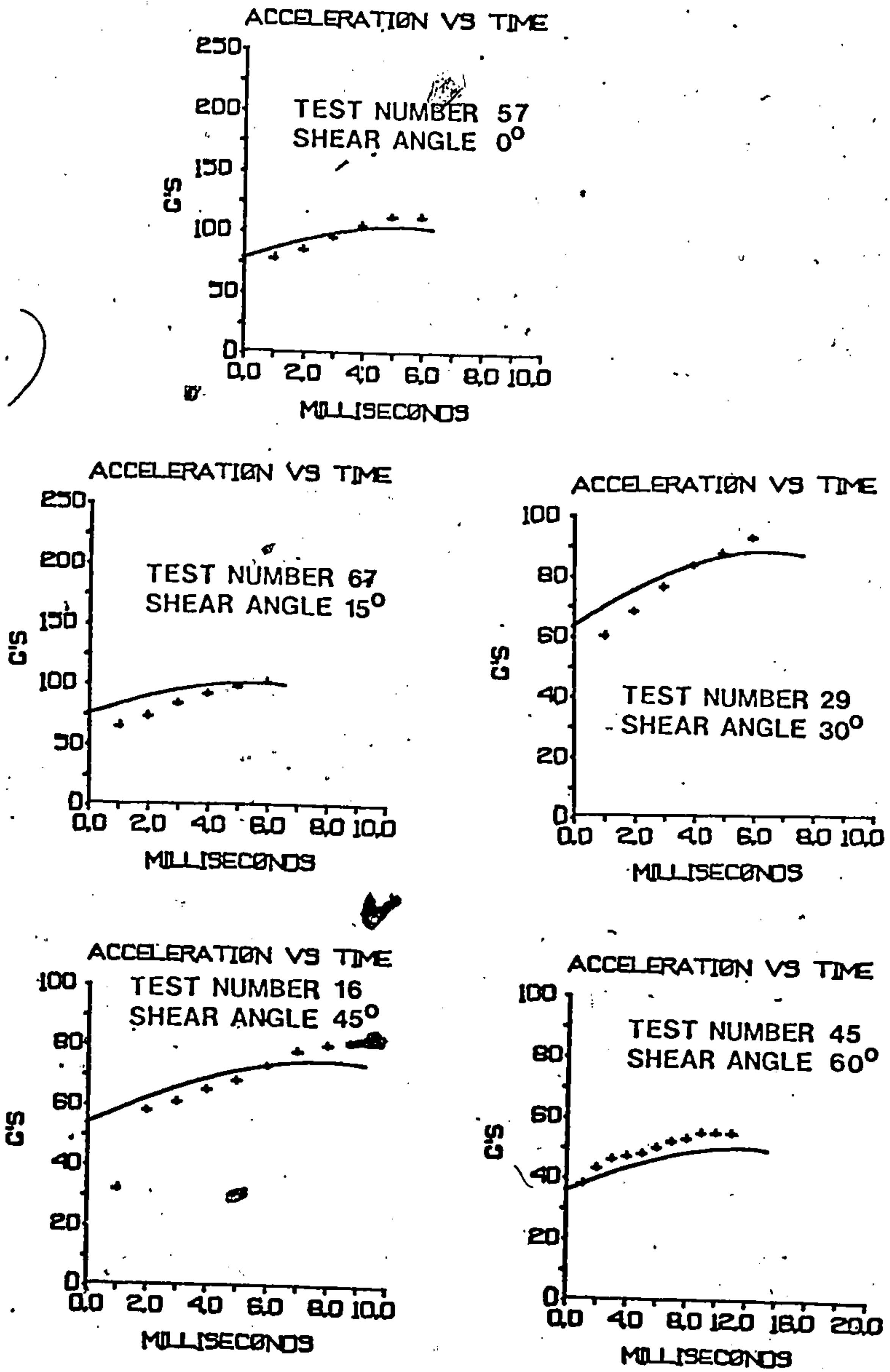
ACCELERATIØN VS TIME
TEST NUMBER 57
SHEAR ANGLE 0°
C'S
250
200
150
100
50
0
0.0 2.0 4.0 6.0 8.0 10.0
MILLISECØNDS
ACCELERATIØN VS TIME
TEST NUMBER 67
SHEAR ANGLE 15°
C'S
250
200
150
100
50
0
0.0 2.0 4.0 6.0 8.0 10.0
MILLISECØNDS
ACCELERATIØN VS TIME
TEST NUMBER 29
SHEAR ANGLE 30°
C'S
100
80
60
40
20
0
0.0 2.0 4.0 6.0 8.0 10.0
MILLISECØNDS
ACCELERATIØN VS TIME
TEST NUMBER 16
SHEAR ANGLE 45°
C'S
100
80
60
40
20
0
0.0 2.0 4.0 6.0 8.0 10.0
MILLISECØNDS
ACCELERATIØN VS TIME
TEST NUMBER 45
SHEAR ANGLE 60°
C'S
100
80
60
40
20
0
0.0 4.0 8.0 12.0 16.0 20.0
MILLISECØNDS

Figure 24

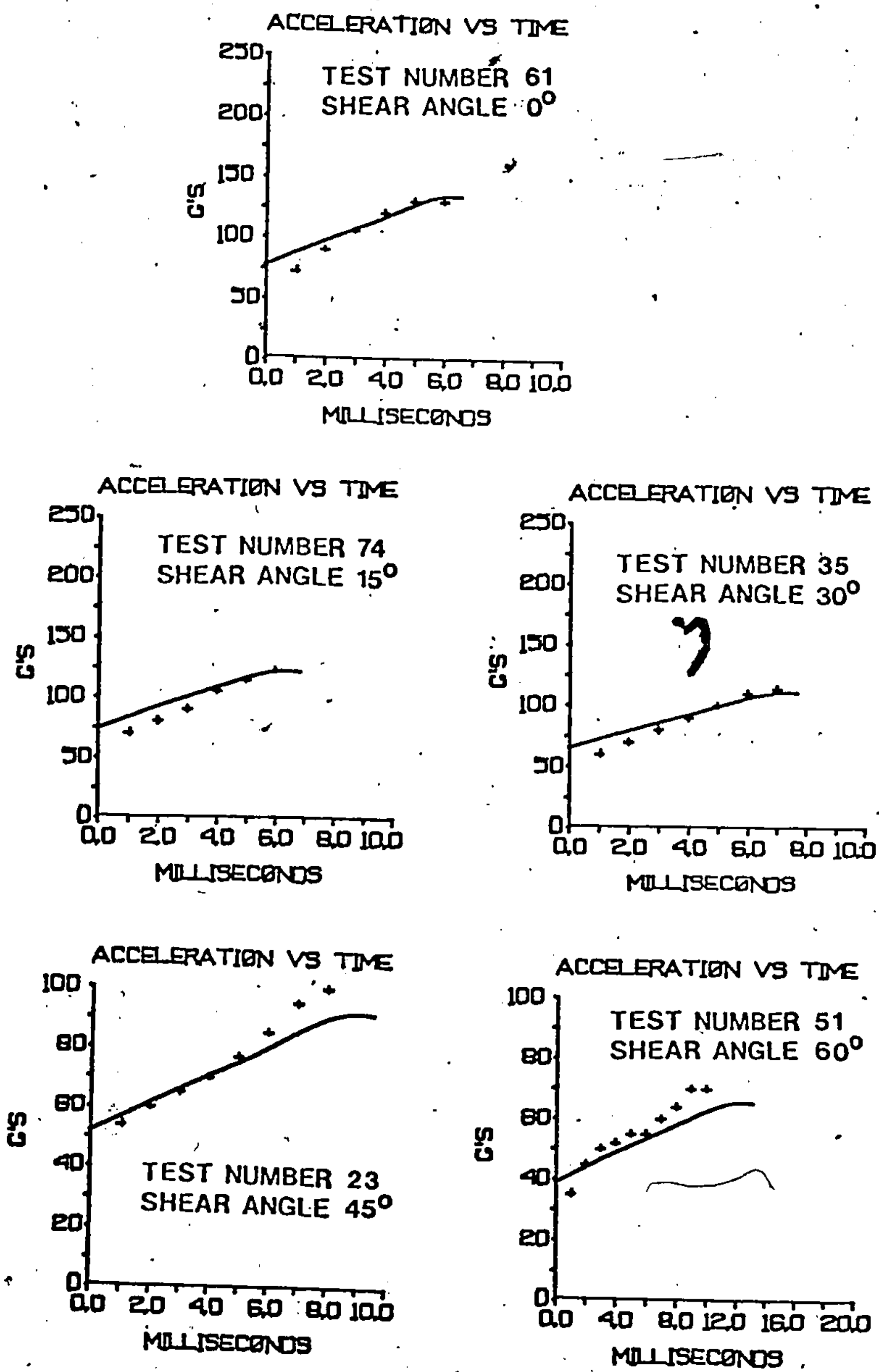
ACCELERATION VS TIME
TEST NUMBER 61
SHEAR ANGLE 0°
G'S
MILLISECONDS
ACCELERATION VS TIME
TEST NUMBER 74
SHEAR ANGLE 15°
G'S
MILLISECONDS
ACCELERATION VS TIME
TEST NUMBER 35
SHEAR ANGLE 30°
G'S
MILLISECONDS
ACCELERATION VS TIME
TEST NUMBER 23
SHEAR ANGLE 45°
G'S
MILLISECONDS
ACCELERATION VS TIME
TEST NUMBER 51
SHEAR ANGLE 60°
G'S
MILLISECONDS

Figure 25

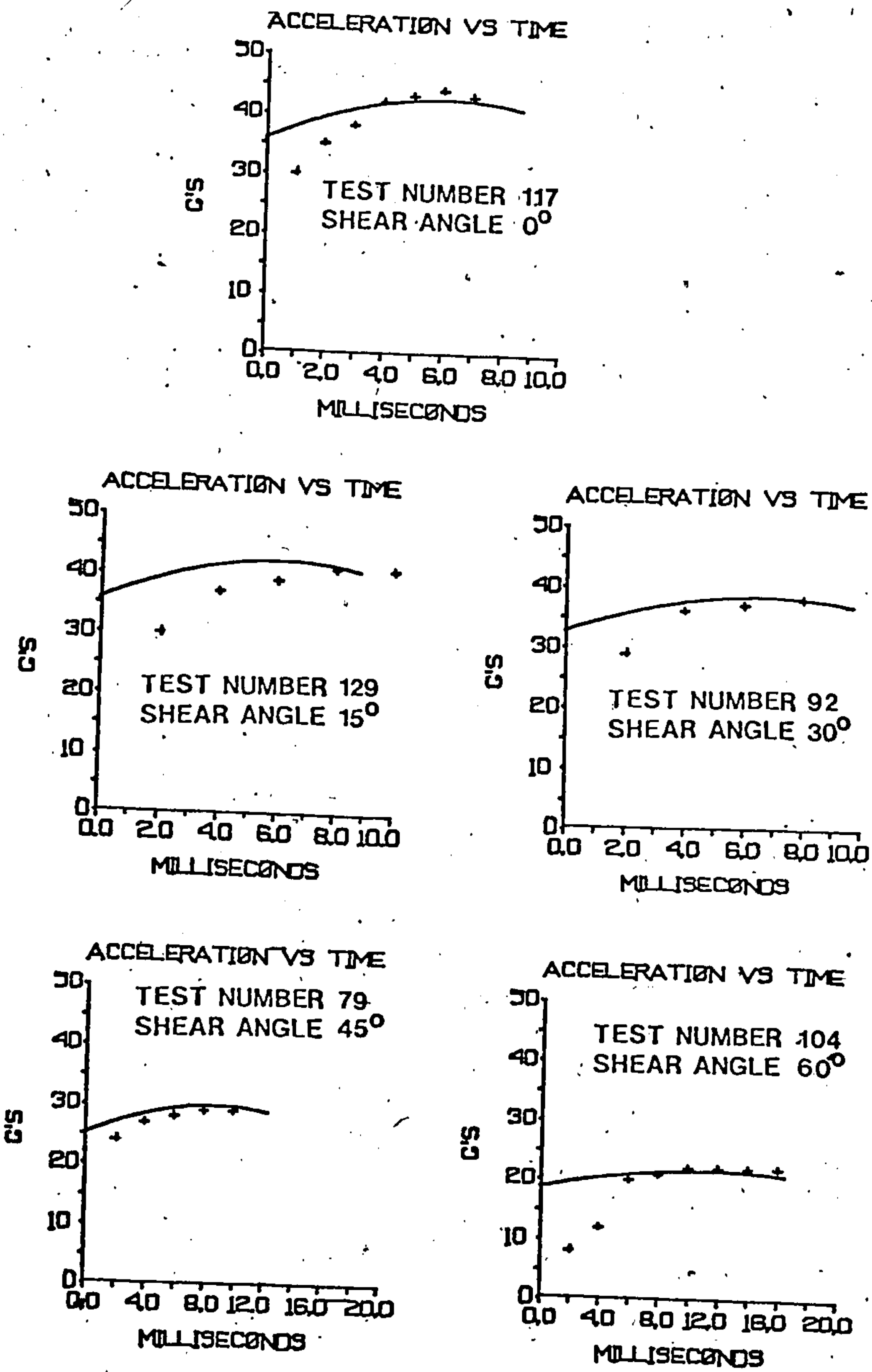
ACCELERATION VS TIME
TEST NUMBER 117
SHEAR ANGLE 0°
ACCELERATION VS TIME
TEST NUMBER 129
SHEAR ANGLE 15°
ACCELERATION VS TIME
TEST NUMBER 92
SHEAR ANGLE 30°
ACCELERATION VS TIME
TEST NUMBER 79
SHEAR ANGLE 45°
ACCELERATION VS TIME
TEST NUMBER 104
SHEAR ANGLE 60°
G'S
MILLISECONDS

Figure 26

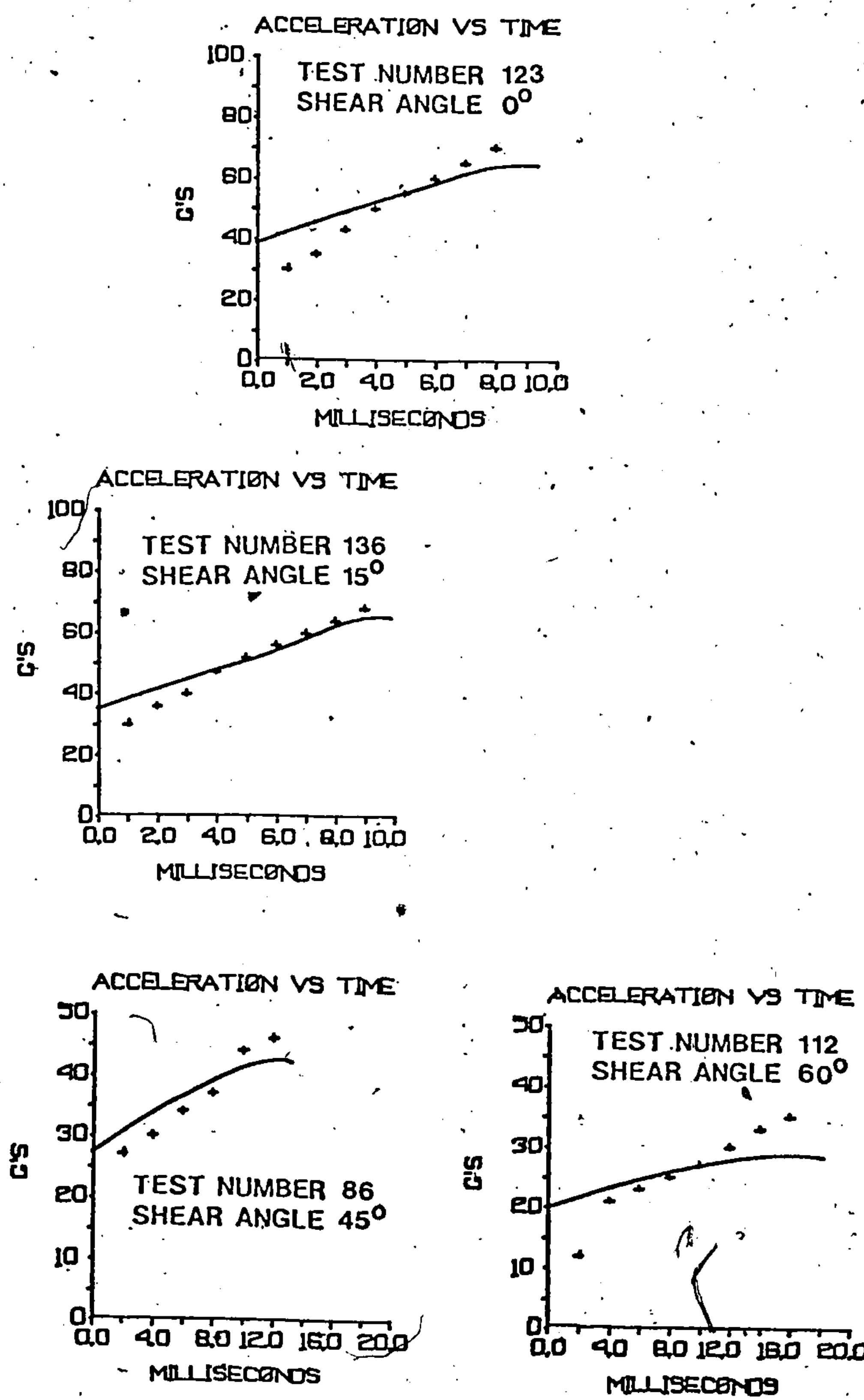
ACCELERATION VS TIME
TEST NUMBER 123
SHEAR ANGLE 0°
G'S
MILLISECONDS
ACCELERATION VS TIME
TEST NUMBER 136
SHEAR ANGLE 15°
G'S
MILLISECONDS
ACCELERATION VS TIME
TEST NUMBER 86
SHEAR ANGLE 45°
G'S
MILLISECONDS
ACCELERATION VS TIME
TEST NUMBER 112
SHEAR ANGLE 60°
G'S
MILLISECONDS

Figure 27

Figures 28, 29, 30 and 31 illustrate good agreement between predicted and experimental peak accelerations for impact angle of 0°, 15°, 30°, and 45°. The 60° impact, in most cases, produced predicted maximum acceleration curves below the experimental values.

(+ Experimental data
 - Simulated results)

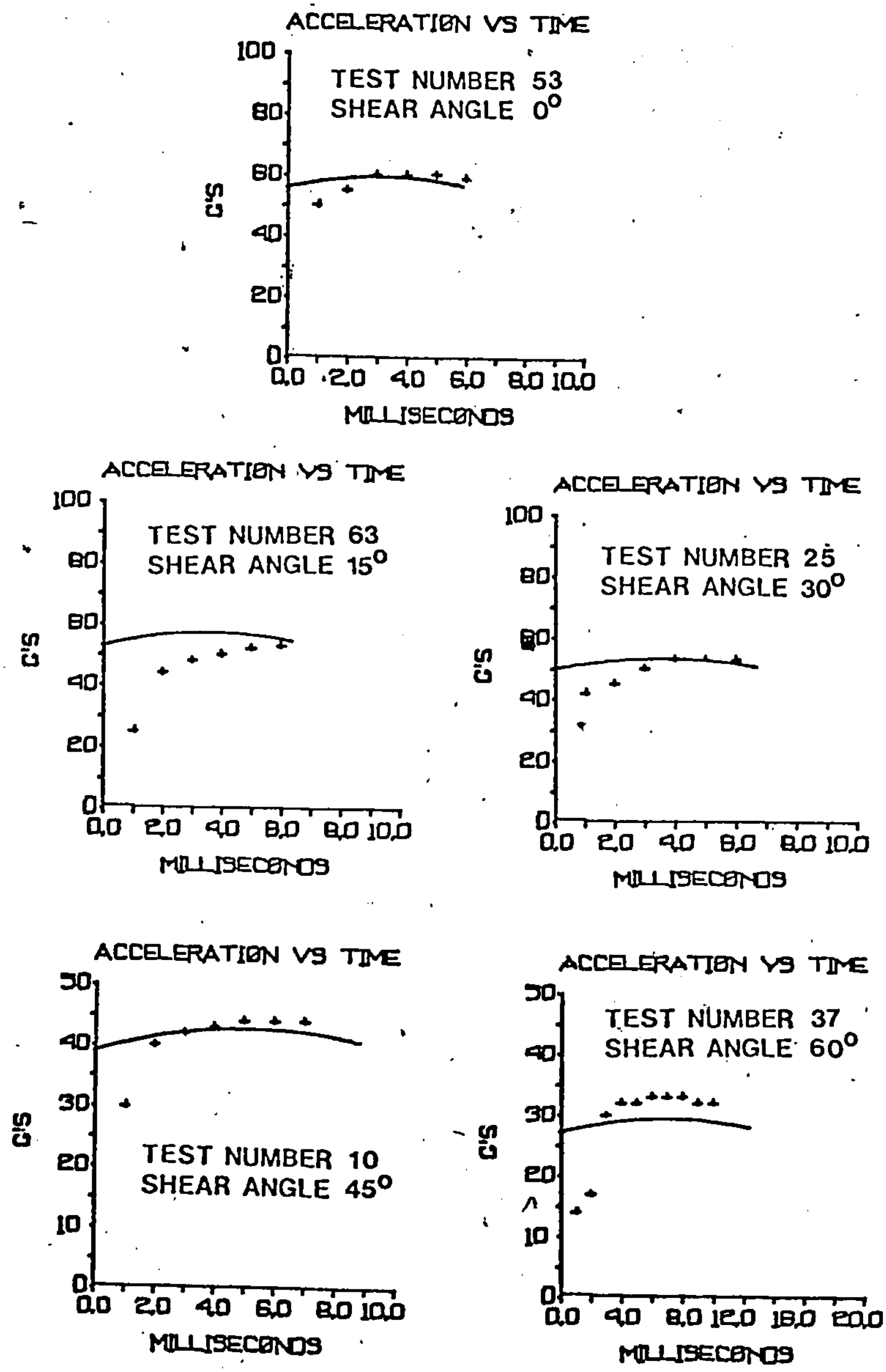
ACCELERATION VS TIME
TEST NUMBER 53
SHEAR ANGLE 0°
G'S
MILLISECONDS
ACCELERATION VS TIME
TEST NUMBER 63
SHEAR ANGLE 15°
G'S
MILLISECONDS
ACCELERATION VS TIME
TEST NUMBER 25
SHEAR ANGLE 30°
G'S
MILLISECONDS
ACCELERATION VS TIME
TEST NUMBER 10
SHEAR ANGLE 45°
G'S
MILLISECONDS
ACCELERATION VS TIME
TEST NUMBER 37
SHEAR ANGLE 60°
G'S
MILLISECONDS

Figure 28

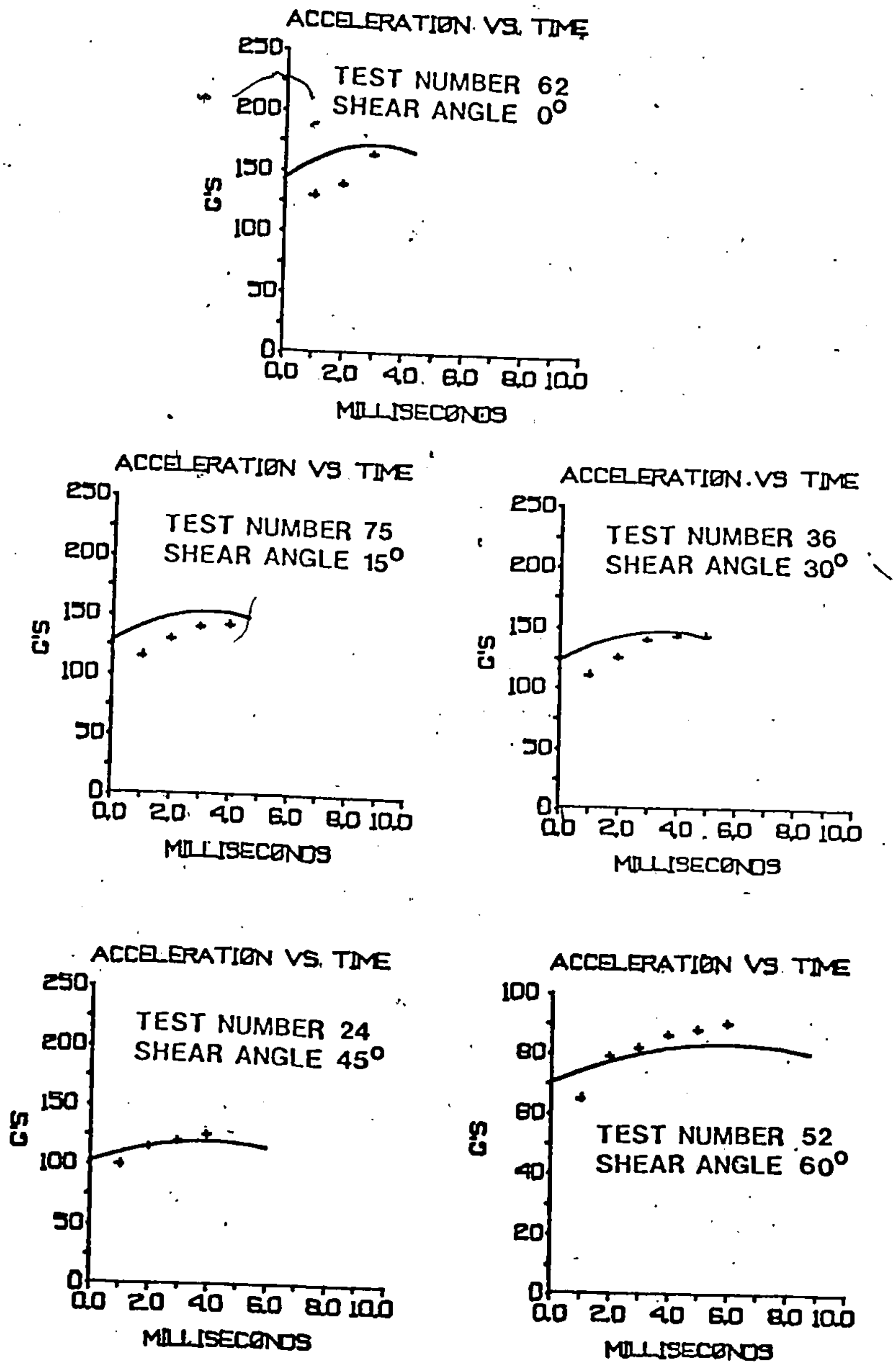
ACCELERATION VS. TIME
TEST NUMBER 62
SHEAR ANGLE 0°
G'S
MILLISECONDS
ACCELERATION VS TIME
TEST NUMBER 75
SHEAR ANGLE 15°
G'S
MILLISECONDS
ACCELERATION VS TIME
TEST NUMBER 36
SHEAR ANGLE 30°
G'S
MILLISECONDS
ACCELERATION VS. TIME
TEST NUMBER 24
SHEAR ANGLE 45°
G'S
MILLISECONDS
ACCELERATION VS TIME
TEST NUMBER 52
SHEAR ANGLE 60°
G'S
MILLISECONDS

Figure 29

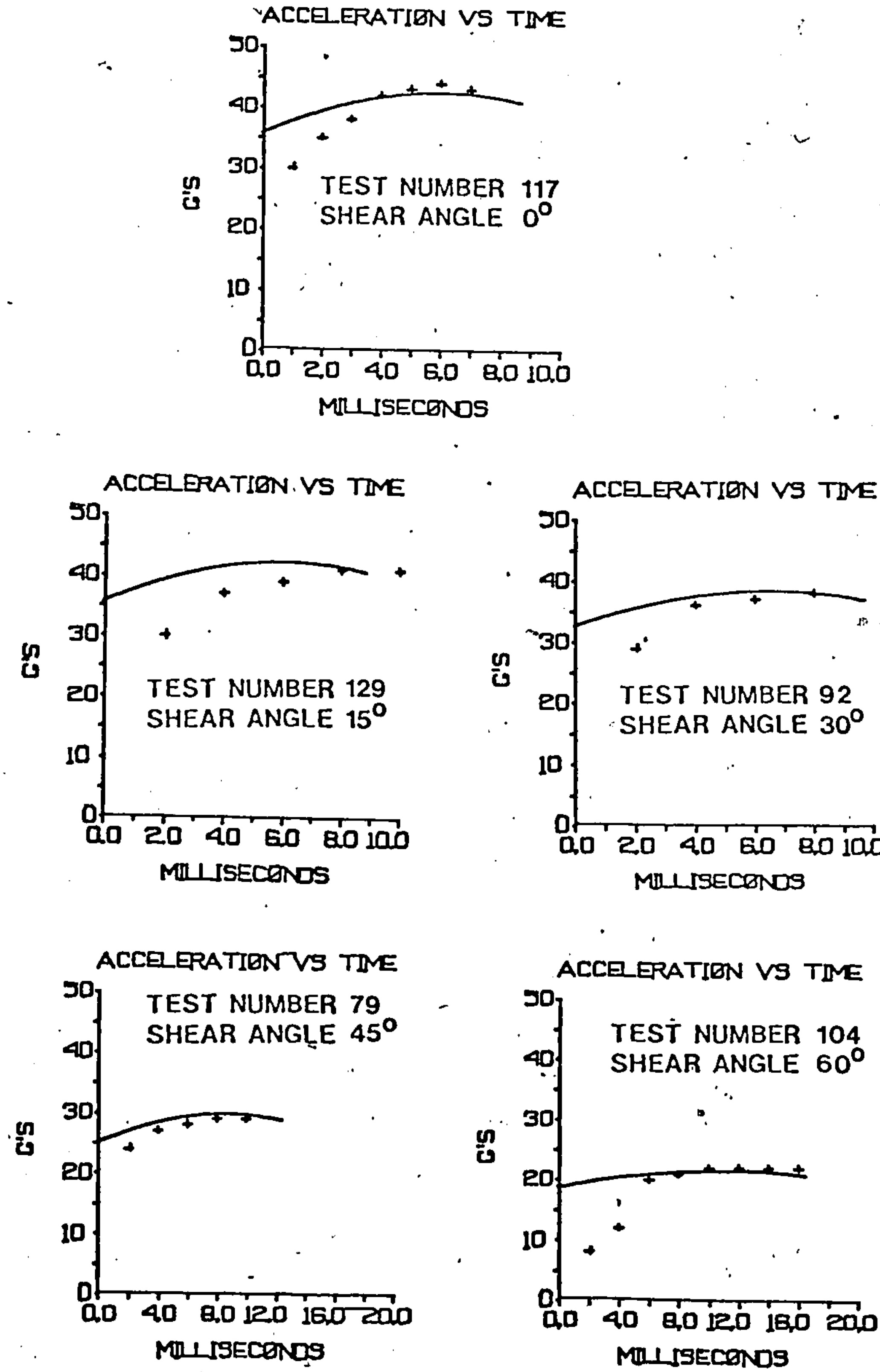
ACCELERATIØN VS TIME
TEST NUMBER 117
SHEAR ANGLE 0°
C'S
MILLISECØNDS
ACCELERATIØN VS TIME
TEST NUMBER 129
SHEAR ANGLE 15°
C'S
MILLISECØNDS
ACCELERATIØN VS TIME
TEST NUMBER 92
SHEAR ANGLE 30°
C'S
MILLISECØNDS
ACCELERATIØN VS TIME
TEST NUMBER 79
SHEAR ANGLE 45°
C'S
MILLISECØNDS
ACCELERATIØN VS TIME
TEST NUMBER 104
SHEAR ANGLE 60°
C'S
MILLISECØNDS

Figure 30

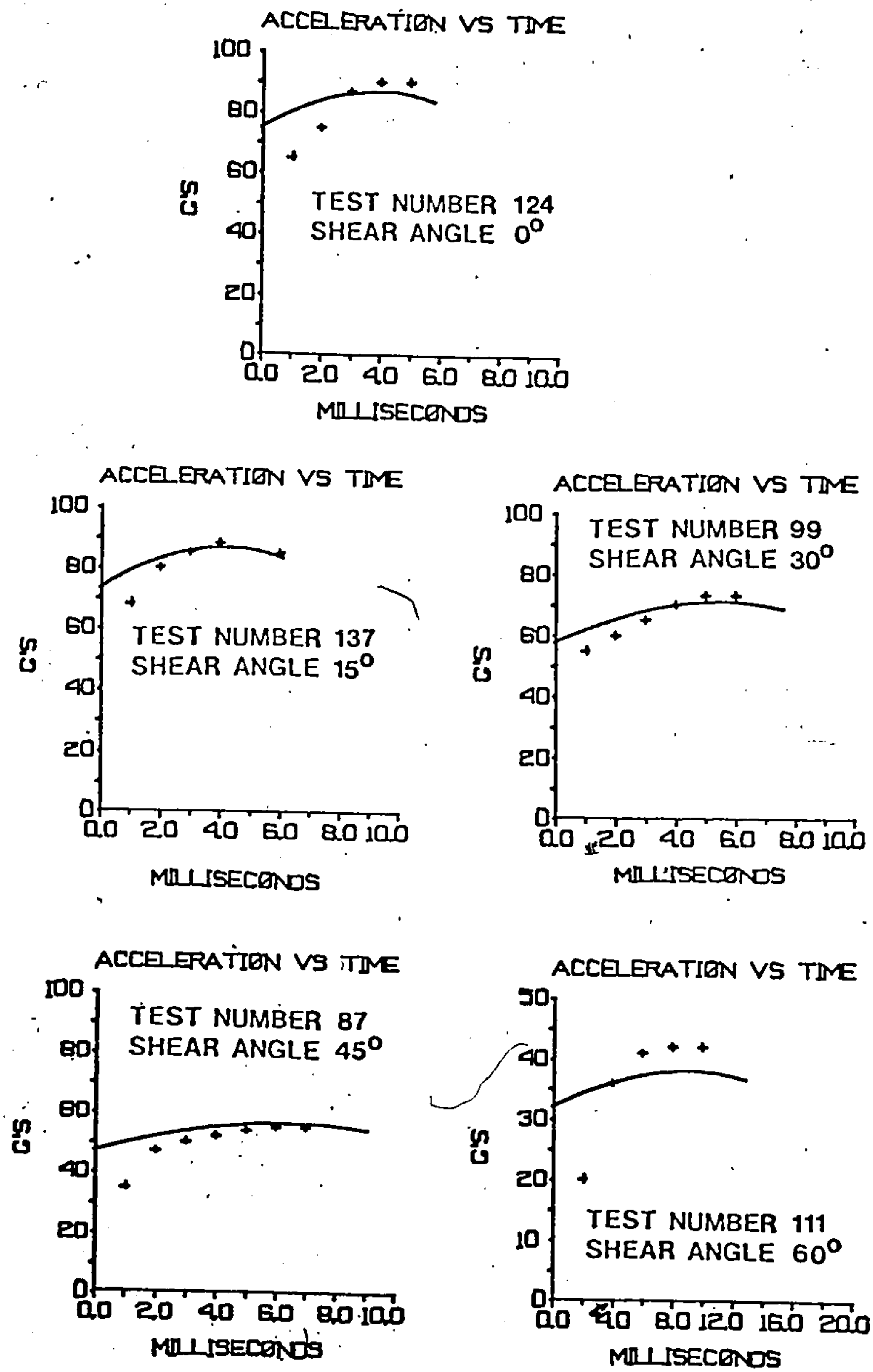
ACCELERATION VS TIME
TEST NUMBER 124
SHEAR ANGLE 0°
G'S
100
80
60
40
20
0
0.0 2.0 4.0 6.0 8.0 10.0
MILLISECONDS
ACCELERATION VS TIME
TEST NUMBER 137
SHEAR ANGLE 15°
G'S
100
80
60
40
20
0
0.0 2.0 4.0 6.0 8.0 10.0
MILLISECONDS
ACCELERATION VS TIME
TEST NUMBER 99
SHEAR ANGLE 30°
G'S
100
80
60
40
20
0
0.0 2.0 4.0 6.0 8.0 10.0
MILLISECONDS
ACCELERATION VS TIME
TEST NUMBER 87
SHEAR ANGLE 45°
G'S
100
80
60
40
20
0
0.0 2.0 4.0 6.0 8.0 10.0
MILLISECONDS
ACCELERATION VS TIME
TEST NUMBER 111
SHEAR ANGLE 60°
G'S
50
40
30
20
10
0
0.0 4.0 8.0 12.0 16.0 20.0
MILLISECONDS

Figure 3

Both of these observations are least accurate for the 60^0 impact situations. This discrepancy is attributed to practical problems stemming from the apparatus and limitations of the test program rather than the behavioral characteristics of the foam. High speed film of the different impact as seen in figure 32 (A-C), revealed that at 60^0, the deformation of the sample during impact was unique. There was evidence of some localized slippage of the sample with respect to the anvil and impact plates. This slippage appeared to be the same even when aluminum plates were glued to the samples. During the 60^0 deformation, the sample ends exhibited a curling action that visually could not be classified as normal or shear strain acting perpendicular to or parallel with the plane of the anvil. This type of combined stress could not be accounted for in this study because it acted in planes other than the two prescribed by the analysis. It is doubtful that these two problems could be overcome by modifying the present apparatus. This suggests that confidence in the result of this testing technique weakens as the increasing impact angle approaches 60^0.

A limitation in the test program may have also attributed to the less than perfect 60^0 impact correlation. The energy levels and impacting masses used for these 60^0 tests were high in relation to the projected area. The projected area of a 60^0 impact sample is only one half of the projected area of a 0^0 impact sample.

Because of this reduction in area, the stress on the 60^0 sample is considerably higher and in many cases the sample was grossly overloaded. This rendered the data useless by diminishing the number of 60^0 impact data available for analysis.

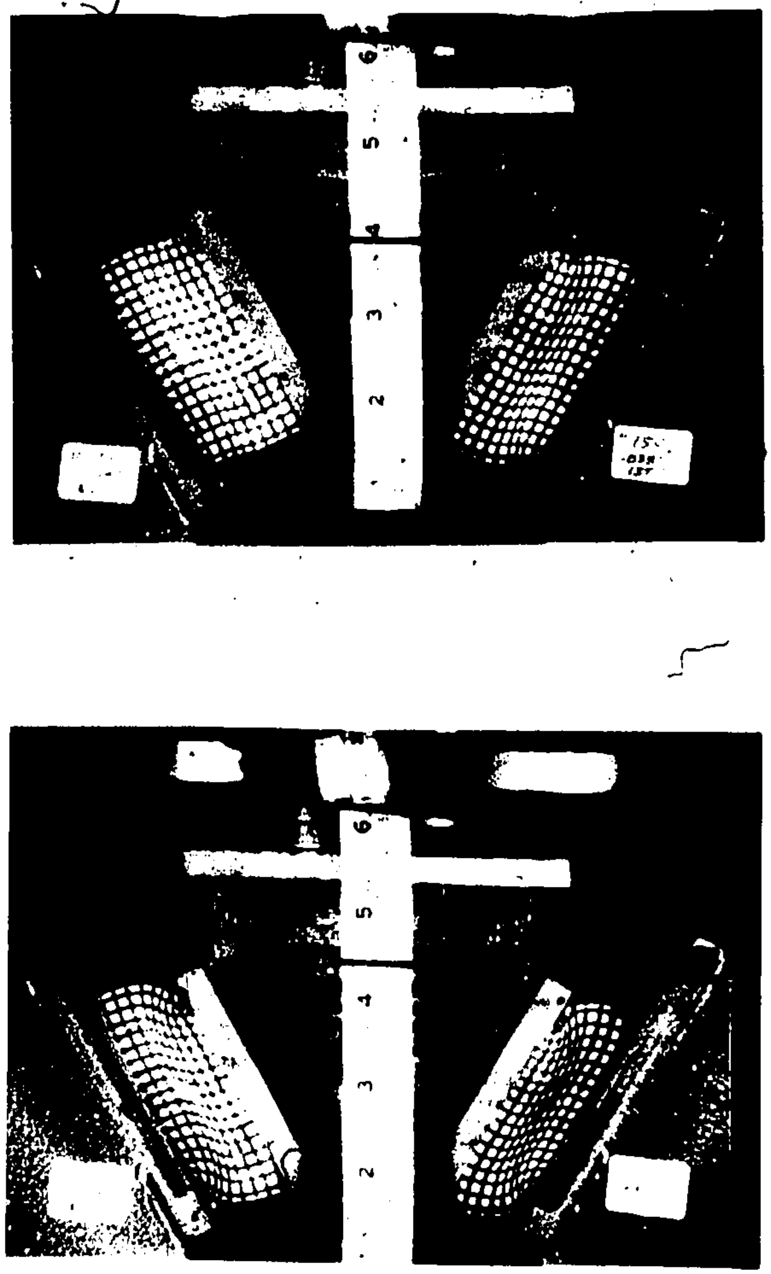

Film Clips of the Deformation Sequence Illustrating the Localized Slippage of the Sample with Respect to the Anvil and Impact Plates.

Figure 32A

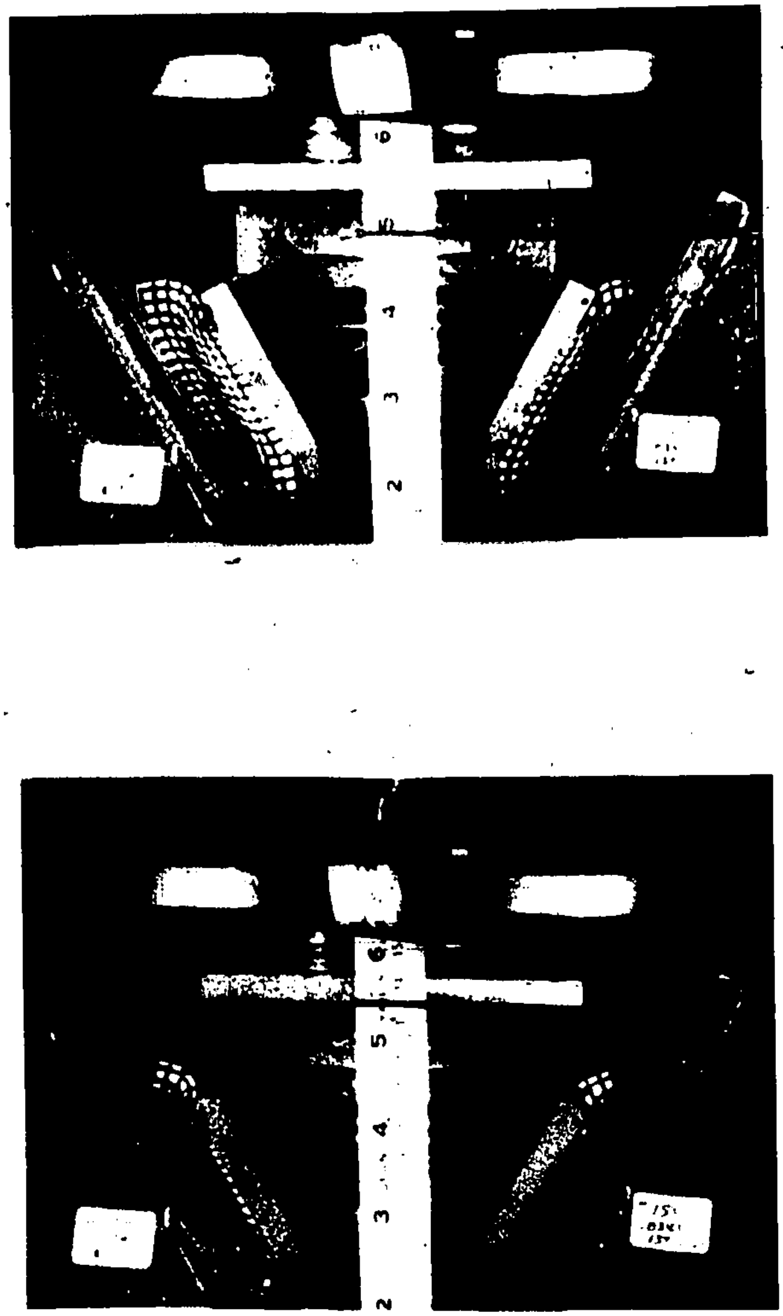

Figure 32B

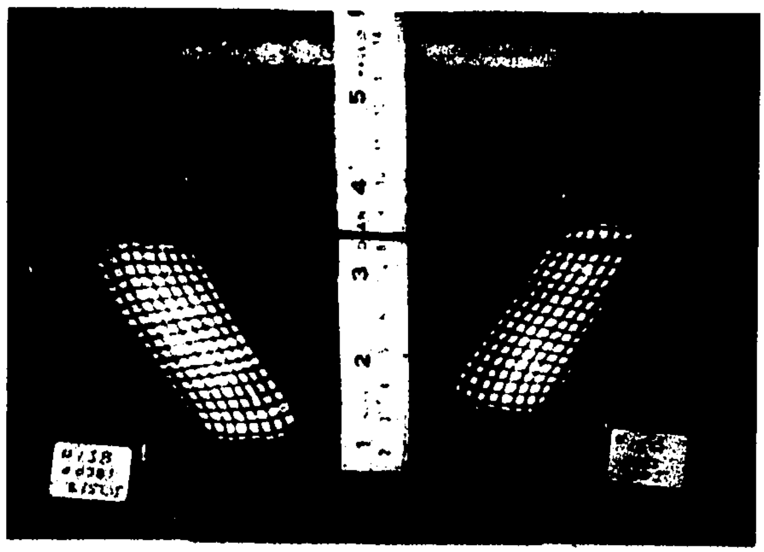

Figure 32C

VII.4 Energy Absorption

Energy absorption is the final property to be discussed. The net energy absorbed by the foam during impact can be determined by an accounting of the kinetic energy as shown by Fan (17).

The maximum kinetic energy of the impactor upon impact can be calculated from the impact velocity. The rebound energy can be acquired through a procedure involving the integration of the acceleration time curve. The difference between these two quantities is the net energy absorbed by the foam.

As seen in Figure 33, with an increase in shear angle there is an increase in energy absorption. Recalling the previous section VI.2 in normalization of the data, it is apparent that a specific conclusion cannot be based on this fact alone. There must be a differentiation made between the quantity of energy absorbed due to sample orientation (i.e. increased effective thickness with increased shear angle), and the quantity of energy absorbed because of the shear component.

Unforturnately equation "A" does not permit this. Equation "A" generates stress strain relationships only to the point of maximum strain. It does not address the unloading portion of the event. Because of this, total theoretical energy absorbed cannot be calculated.

Figure 33, therefore, is an indication that the orientation of the sample will simply result in a change in energy absorption. A distinction cannot be made as to the relative effects that the change in either the thickness or in the shear component have on the energy absorption results.

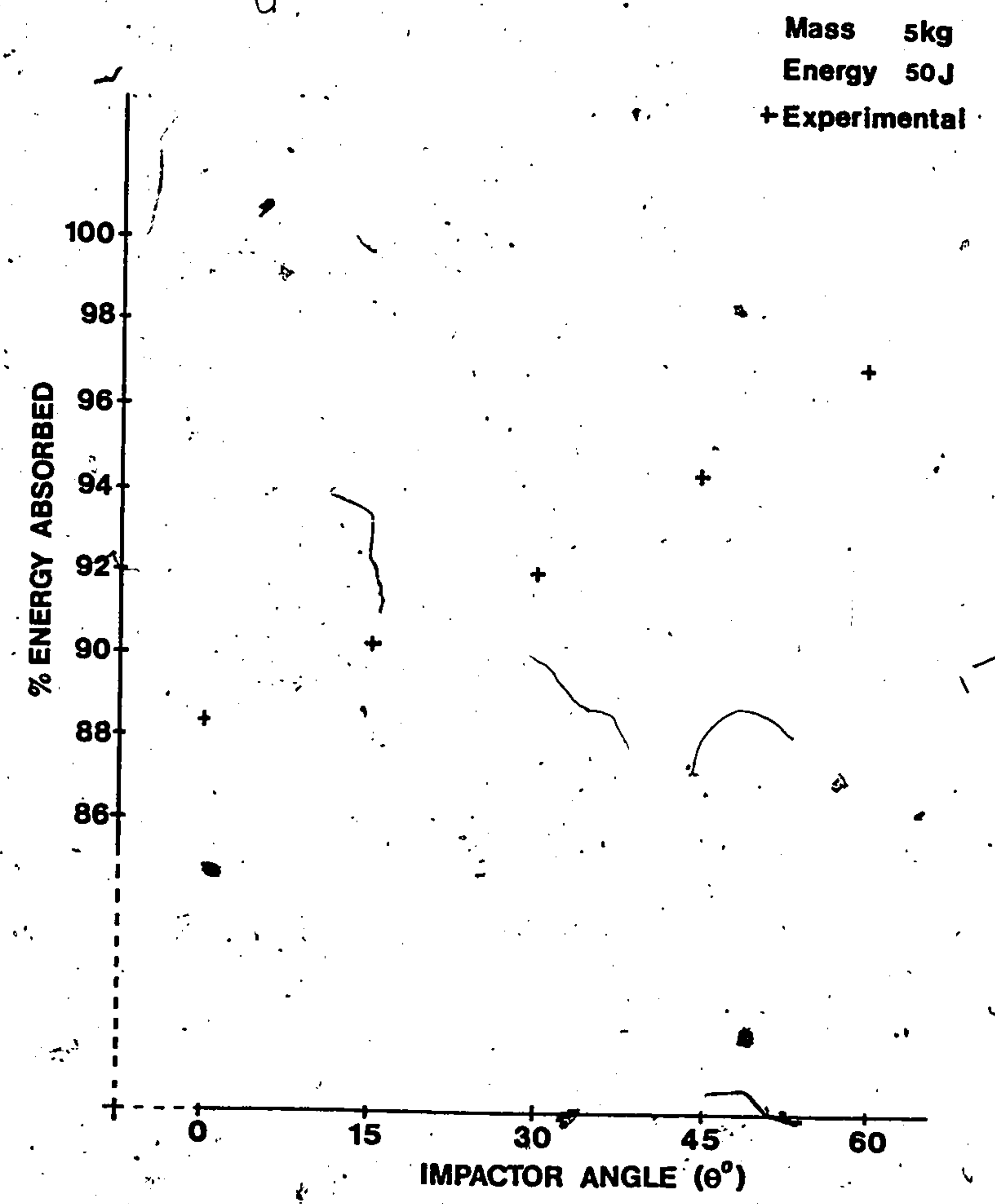

Percent Energy Absorbed
Determined from Experimental Data

Figure 33

Because there is not significant difference between predicted and experimental peak acceleration values, the increase in energy absorption is indicated in the experimental data by increased impact time durations.

VIII CONCLUSIONS

The objectives of this study were to investigate the performance of PSB foam under combined impact loading and to determine if the equation developed by Meunier can be used to predict the behaviour of the foam under such impact conditions.

1. The impact stress-strain characteristic of PSB foam in combined impact loading is similar to that of normal impact loading of PSB foam.
2. A predictive equation developed for normal impact loading of PSB foam can successfully be used to predict the combined loading stress-strain behaviour of PSB foam provided a proper analysis of the impact orientation is conducted. The limitation of this conclusion is, as the angle of shear approaches 60° the accuracy of the prediction may be affected.
3. From the predicted curves, greater confidence can be placed in the peak acceleration values as opposed to other points during the acceleration time history.
4. The trend differences between the predicted curve and experimented points that occur from 0° impact tests carry over to the 15°, 30°, 45° and 60° impacts.

   This indicates that such trend differences are not the result of an increasing shear component but are most likely the result of impact conditions whereby the predictive equation is generally less precise.

6. The grid system printed on the sides of the samples coupled with high speed motion pictures greatly enhances the analysis of the deformation of PSB foam.
7. The deviation of experimental data compared with a predictive value for PSB foam tests cannot be expected to be of similar high precision which is generally found in the testing of more classical material such as steel.

REFERENCES

1. A. Nagy, W.L. Ko, and U.S. Lindholm, "Mechanical Behaviour of Foamed Materials Under Dynamic Compression", J. Cell. Plast., Vol. 10, No. 3, May-June 1974.

2. R.K.S. Chan, W.M. Lee, and M. Nakamura, "Mechanical Properties of Plastic Foams II. The Modulus of Elasticity and Indentation of Bead Type Foams", J. Cell. Plast., Vol. 7, No. 6 Nov./Dec., 1971, PP 302-308.

3. J.W. Melvin and V.L. Roberts, "Compression of Cellular Plastics at High Strain Rates", J. Cell. Plast., Vol. 7, No. 2, March/April, 1971, PP 97-100.

4. A. Nagy, W.L. Ko and U.S. Lindholm, "Mechanical Behaviour of Foamed Material Under Dynamic Compression", J. Cell. Plast., Vol. 10, No. 3, May/June 1974, PP 127-134.

5. F.C. Meunier, "The Determination of a Constitutive Equation For Polystyrene Bead Foam", MA.Sc. Thesis, University of Ottawa 1976.

6. M. Zaslawsky, "Multiaxial - Stress Studies on Rigid Polyurethane Foam", J. of Exp. Mech., Feb. 1973, PP 70-76.

7. R. Patel and Finnie, "The Mechanical Behaviour of Rigid Plastic Foams", Asme, 2nd Inter. American Conf. Mater. Technol. Mexico City, Aug. 24-27, 1970, Pt 1, P 597-615.

8. S. Aspey and K.G. Hoge, "Shear and Compression Properties of Thin Flexible Cellular Silicones", J. Cell. Plast., Vol. 9, No. 1, Jan/Feb. 73, PP 43-49.

9. J.F. Meier and G.E. Rudd, "A Mechanical Shock Absorber Made from Low Density Phenolic Foam. Part 1- Material Section", J. Cell. Plast., Vol. II, No. 1, Jan/Feb. 75, PP 40-44.

10. J.A. Rinde and K.G. Hoge, "Time and Temperature Dependence of the Mechanical Properties of Polystyrene Bead Foam", J. Apl. Poly. Sci., Vol. 15, 1971, PP 1378-1393.

11. M. Patel and I. Finnie, "Structural Features and Mechanical Properties of Rigid Cellular Plastics", J. of Mat. Vol. 5, No. 4, Dec. 1970.

12. ASTM Standard C273, "Shear Test in Flatwise Plane of Flat Sandwich Constructions or Sandwich Cores", ASTM Part 16, July 1970, PP 6-9.

13. G.D. Webster, "A Comparison of the Impact Response of Cadaver Heads and Anthropomorphic Head Forms", MA.Sc Thesis, University of Ottawa 1976.

14. J.A. Rinde, "Poisson's Ratio for Rigid Plastic Foams", J. Appl. Polym. Sci., Vol. 14, 1970, PP 1913-1926.

15. R.K. Traeger and R.D. Hermansen, "Properties of Structural Foams", J. Cell. Plast., Vol. 7, No. 4, July/Aug., 1971.

16. K.C. Rusch, "Impact Energy Absorption by Foamed Polymers', J. Cell. Plast., Vol. 7, No. 2, March/April 1971, PP 78-83.

17. W.R.S. Fan, "A Simulation of the Dynamic Properties of Energy Absorbing Materials", Ford Motor Co. Project S024C, 1970.

APPENDIX A

Illustrations of the Test Apparatus and Support Equipment

And

Details of the Calibration Pad

The calibration pad used during this study is the following;

a 1-inch open Blue Modular Elastomer Programmer, available from M.T.S. Systems Corporation., P.O. Box 24012, Minneapolis, Minnesota, USA 55424.

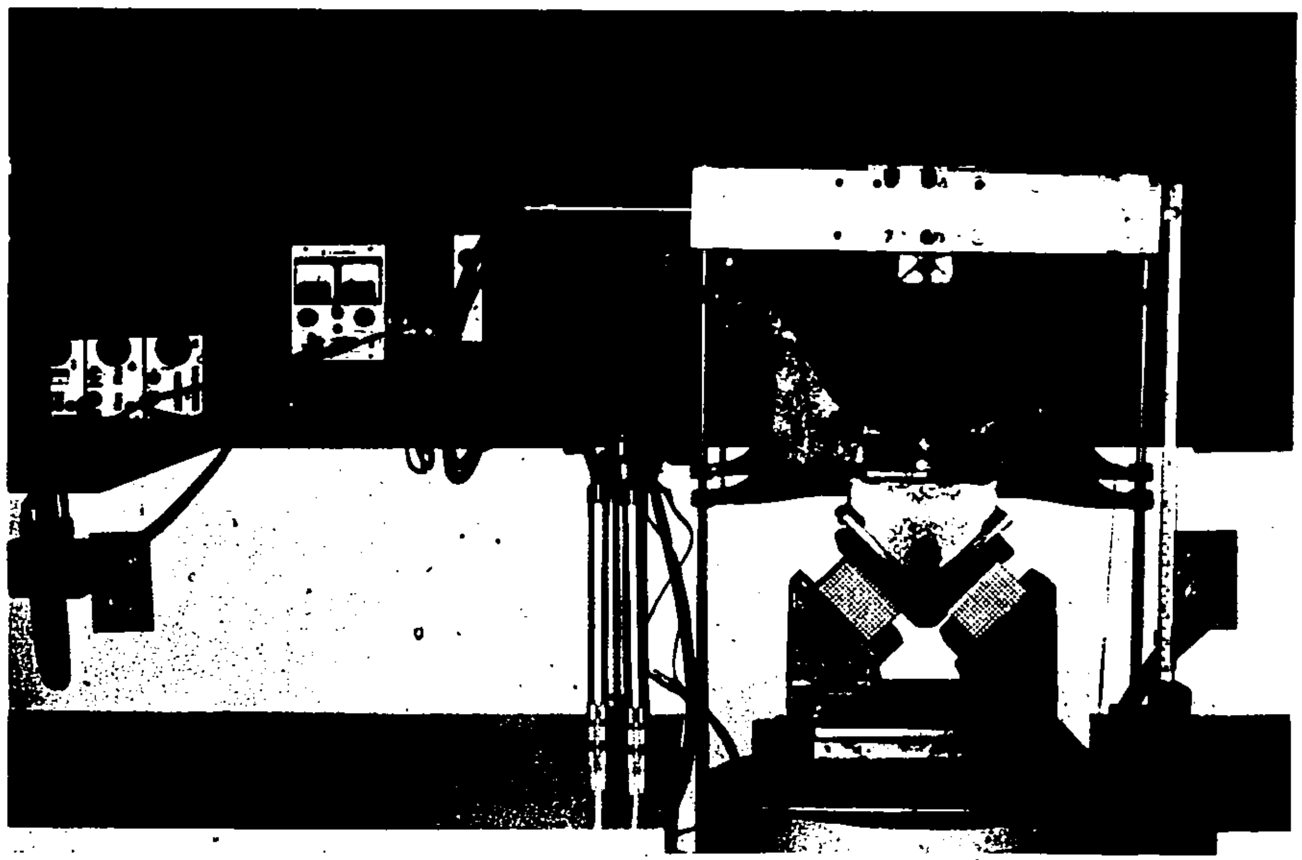

Apparatus and Instrumentation Set Up

Figure A-1

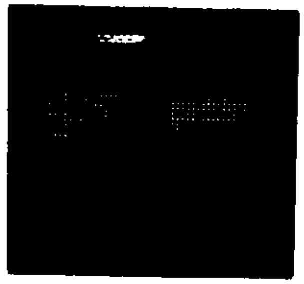

Impactor E-0°

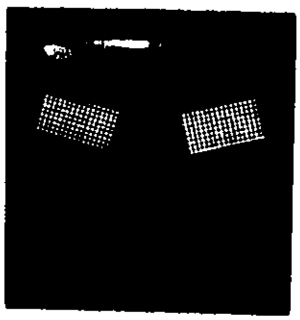

Impactor D-15°

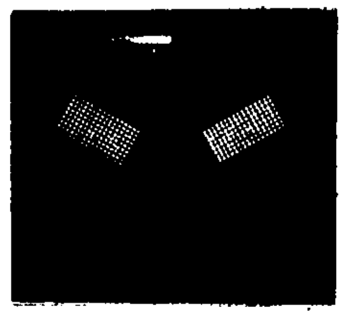

Impactor C-30°

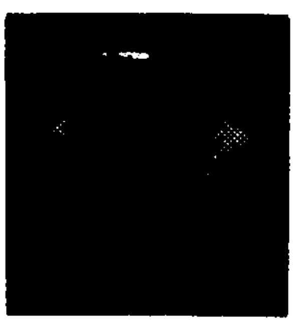

Impactor B-45°

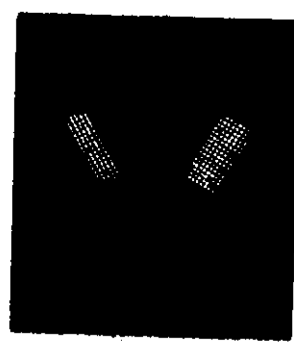

Impactor A-60°

Impactors and Anvils Designed and Constructed
For This Study

Figure A-2

Adjustable Base Plate

Figure A-3

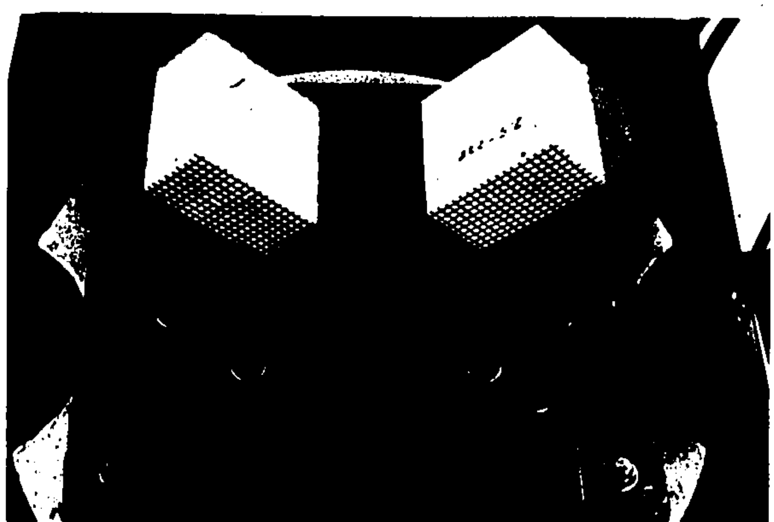

Anvils Mounted on the Adjustable Base Plate

Figure A-4

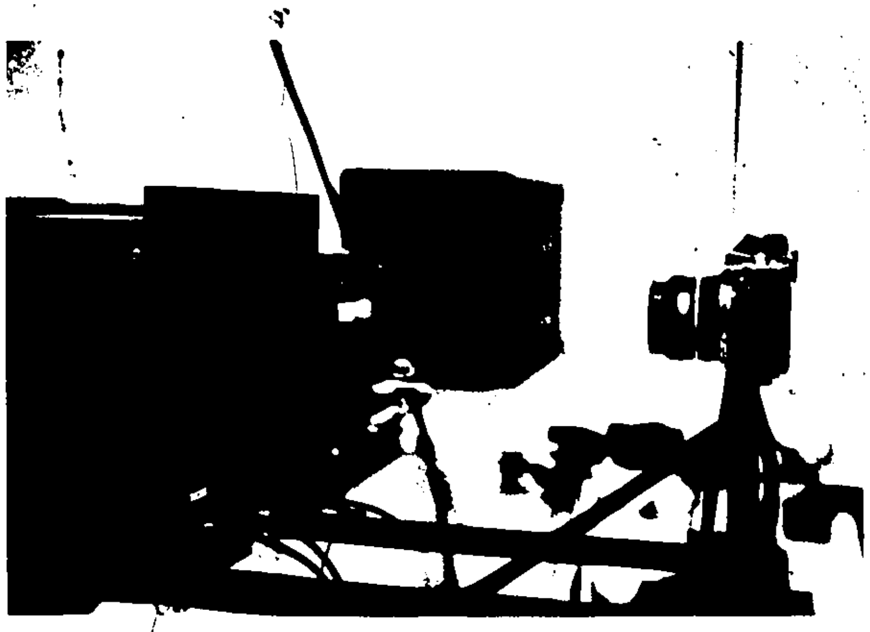

Camera Set Up for Data Recording

Figure A-5

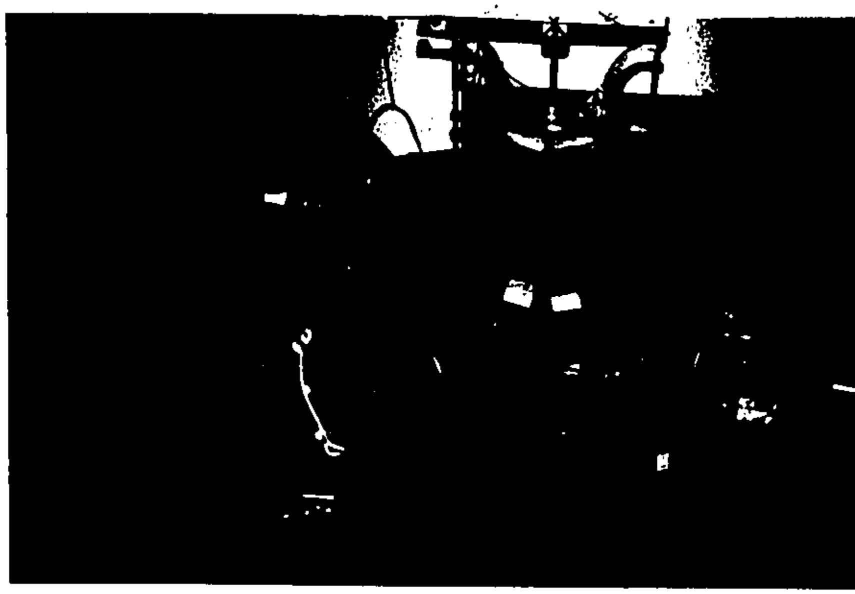

Lighting Arrangement for High Speed Filming

Figure A-6

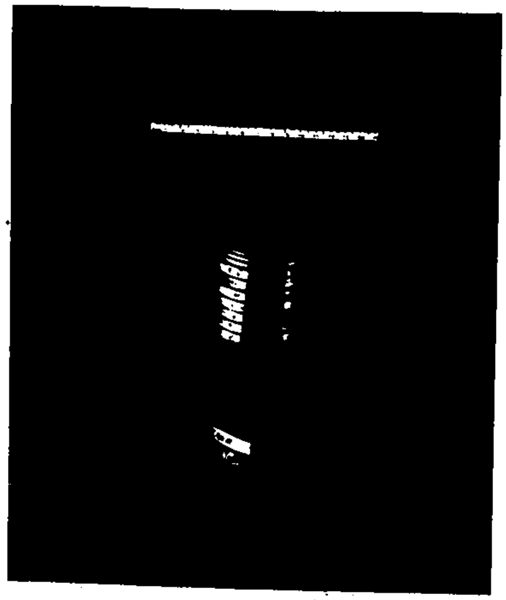

Weights for use on Impactors

Figure A-7

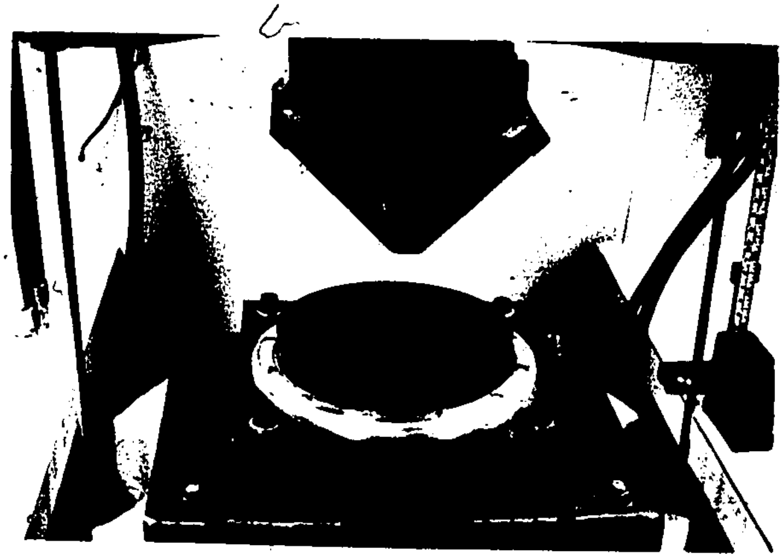

Modular Elastomer Programmer Pad for use in Calibration

Figure A-8

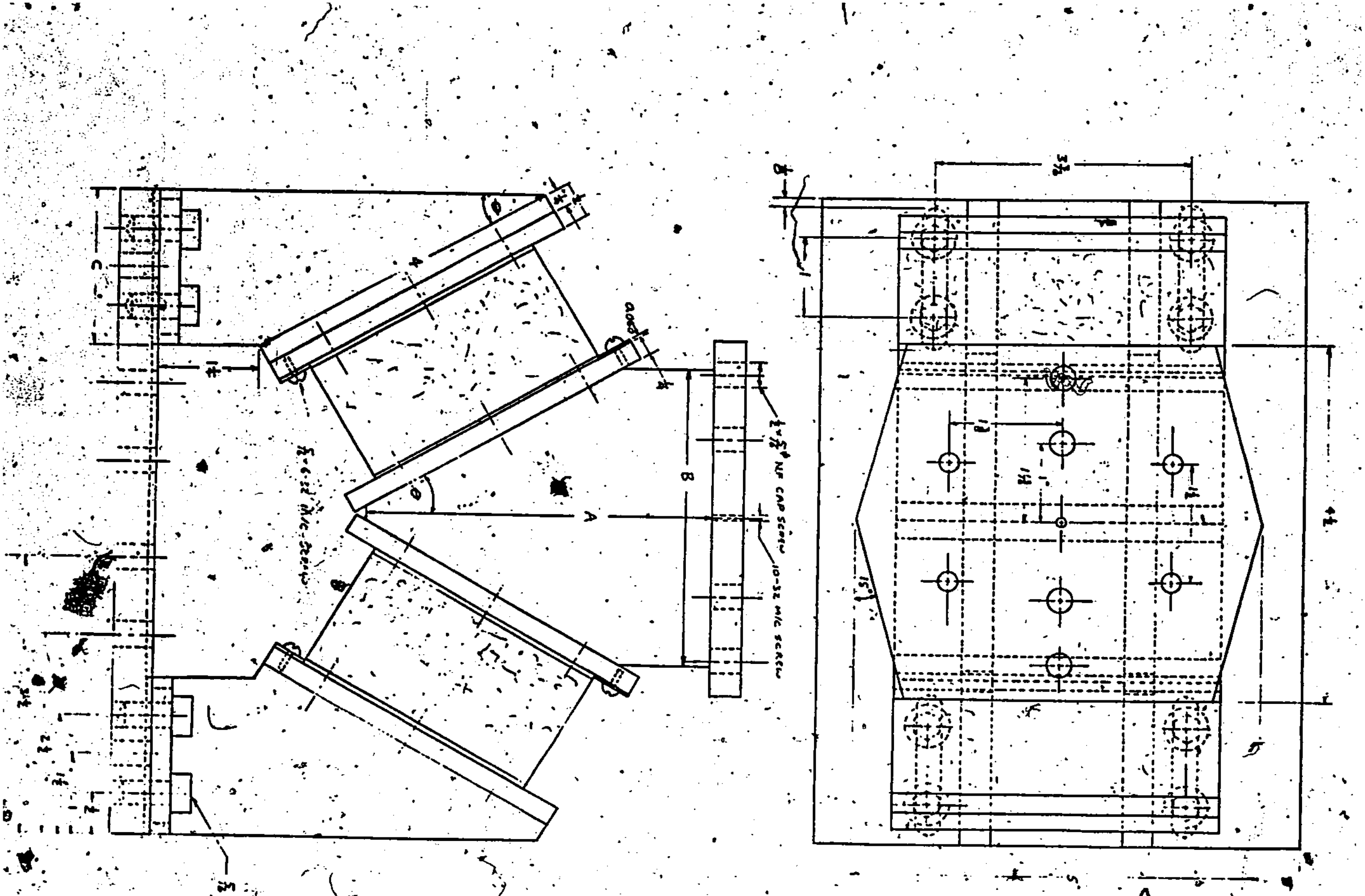

Front and Plan Views of
Apparatus

Figure A-9

Θ	A	B	C
30	4.050	3.750	2.000
45	3.675	5.303	2.828
60	2.930	6.495	3.464
75	2.060	7.244	3.864
90	1.125	7.500	4.000

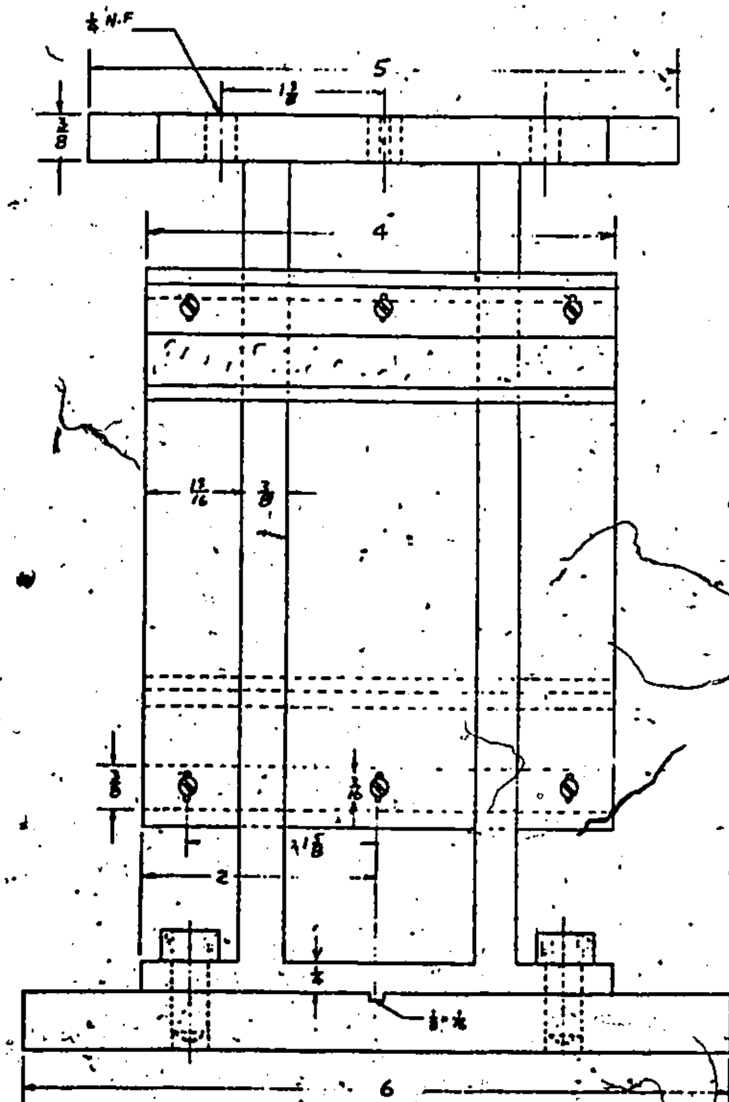

Side View of Test Apparatus

Figure A-10

APPENDIX B

Photographs of Preliminary Test Equipment

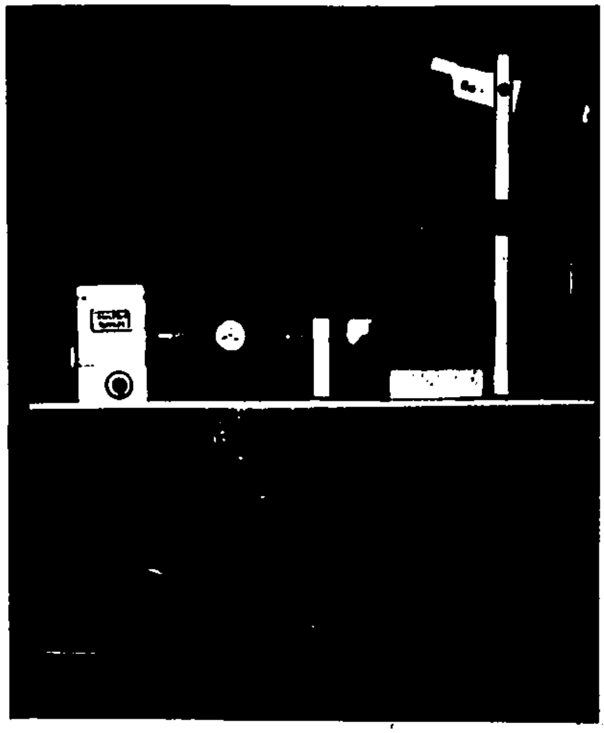

Shear Box Apparatus Commonly Used
for Soil Testing

Figure B-1

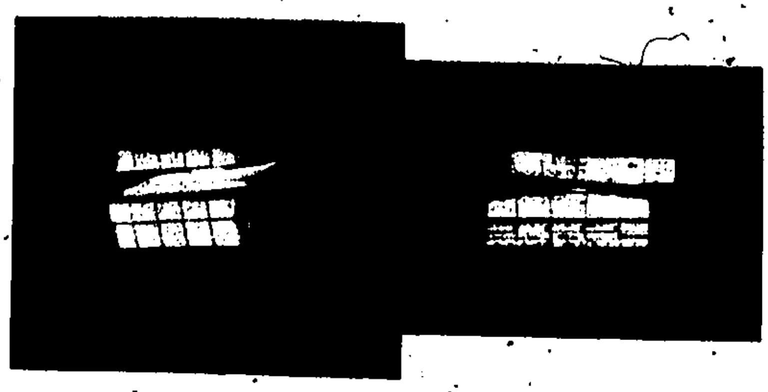

Foam Sample used in Shear Box
(The sample was cut along the shear plane
prior to testing to reduce the stress on the
sample edge.)

Figure B-2

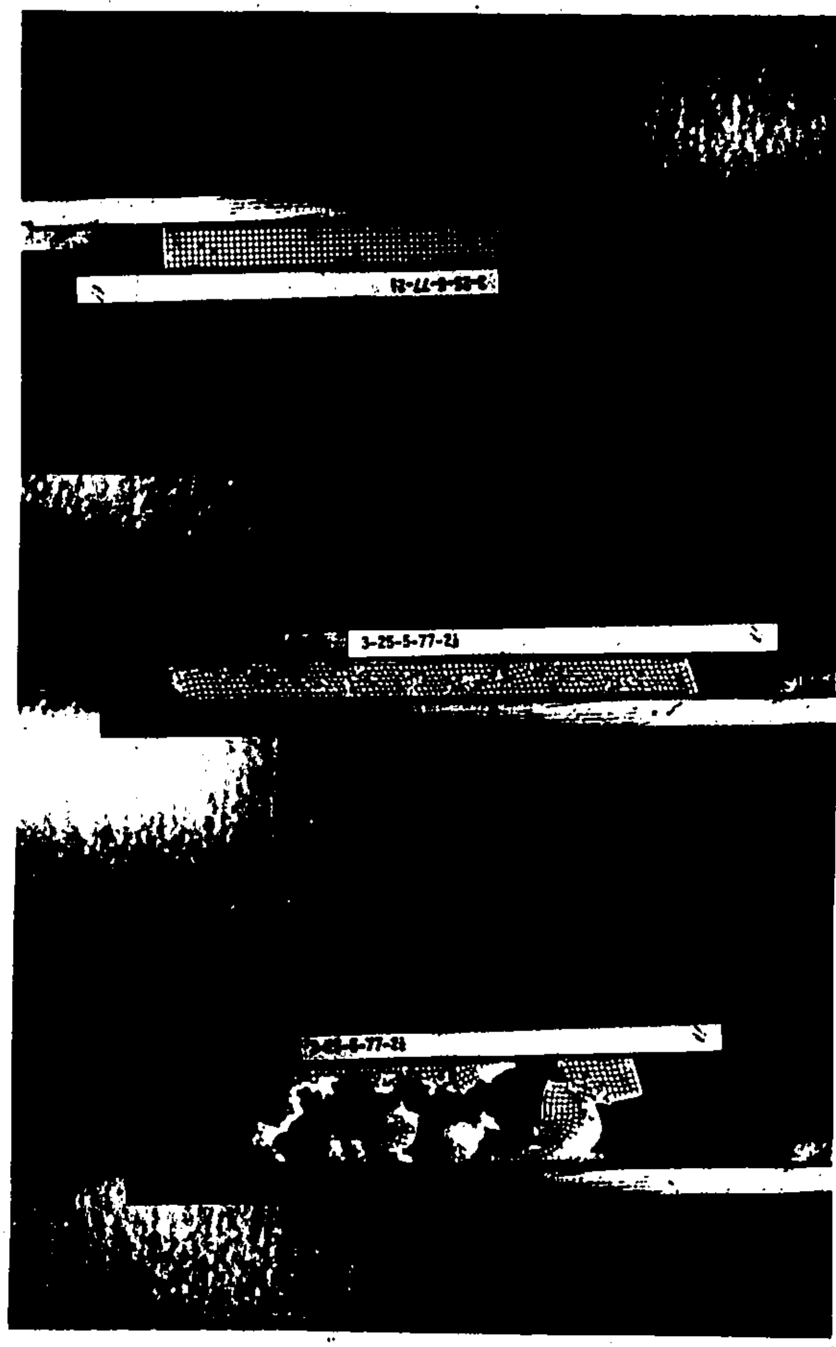

Shear Test Sequency Using
Appartus Prescribed
by ASTM Standard C273

Figure B-3

Fracture Pattern Resulting
from Shear Test

Figure B-4

APPENDIX C

Accelerometer Technical Data

PREVIOUSLY COPYRIGHTED MATERIAL

IN APPENDIX C, Models 2271A, 2275.

NOT MICROFILMED.

MAY BE OBTAINED FROM:

ENDEVCO, Dynamic Instrument Division
801 S. Arroyo Parkway
Pasadena, California
91109

```
//   ,),'J. WCCCROOFFE',MSGLEVEL=(1,1),CLASS=J
//   EXEC FCRTGCLG
//FORT.SYSIN DD *
      DIMENSICN A(800,3),REJECT(50,8),D(5),AVG(7),SUM(7)
      LOGICAL SKIP
      REAL*4 L,M
      SKIP=.FALSE.
      IREJEC=1
      I=0
      JJJ=0
      DO 210 J=1,7
      AVG(J)=0.0
      SUM(J)=0.0
  210 CONTINUE
C
C  +/- DEL IS THE LIMIT ON THE NCMINAL DENSITIES 2.0,2.5,3.0,3.5,4.0
      DEL=.25
C
C  +/-   DELTA IS THE ALLCWABLE RANGE CF DENSITY VARIATICN FCR ANY TWO
C     SAMPLES TO BE SIMULTANECUSLY TESTED
      DELTA=.06
C
    1 I=I+1
      IACT=I-IREJEC
      READ(5,10,END=4)NUMBER,M,L,W,H
   10 FORMAT(I5,F10.4,3F10.2)
      IF(((I-1) /50)*50.EQ.I-1)WRITE(6,30)
   30 FORMAT('1',T2,'SAMPLE',T12,'MASS ',T22,'LENGTH',T32,'WIDTH',
     .T42,'HEIGHT',T50,'VOLUME',T65,'DENSITY'
     ./T54,'3',T66,'2',T76,'2',
     ./' ',T13,'GM',T24,'CM',T34,'CM',T44,'CM',T53,'CM'
     .   ,T62,'G/CM ',T71,'LB/FT ',/'+',75('_')/)
      VOL=L*W*H
      DENSM=M/VOL
      DENSB=DENSM*LI
      DENSB=DENSM*62.3719
      A(I,1)=NUMBER
      A(I,2)=DENSB
      A(I,3)=H
      REJECT(IREJEC,8)=0
      IF(ABS(DENSB-2.0).GT.DEL.AND. ABS(DENSB-2.5).GT.DEL.AND.ABS(DENSE-
     .3.0).GT.DEL.AND.ABS(DENSB-3.5).GT.DEL.AND.ABS(DENSB-4.0).GT.DEL.
     .AND.ABS(DENSE-4.5).GT.DEL)
     .   .REJECT(IREJEC,8)=1
      IF(REJECT(IREJEC,8).EQ.0)GO TO 2
      REJECT(IREJEC,1)=NUMBER
      REJECT(IREJEC,2)=L
      REJECT(IREJEC,3)=W
      REJECT(IREJEC,4)=H
      REJECT(IREJEC,5)=M
      REJECT(IREJEC,6)=DENSM
      REJECT(IREJEC,7)=DENSB
      IREJEC=IREJEC+1
      I=I-1
    2 WRITE(6,20)NUMBER,M,L,W,H,VOL,DENSM,DENSB
   20 FORMAT(' ',I5,F10.4,4F10.2,2F10.4)
      JJJ=JJJ+1
      SUM(1)=M+SUM(1)
      SUM(2)=L+SUM(2)
```

```
      SUM(3)=W+SUM(3)
      SUM(4)=H+SUM(4)
      SUM(5)=VOL+SUM(5)
      SUM(6)=DENSM+SUM(6)
      SUM(7)=DENSB+SUM(7)
      GO TO 1
C
C SORT BY DENSITY--------------------------------------------------------
C
    4 CONTINUE
      WRITE(6,40)
   40 FORMAT('1')
      I=I-1
      IREJEC=IREJEC-1
      DO 6 J=1,I
      IF(A(J,2).EQ.0)GO TO 6
      POINT=A(J,2)
      WRITE (6,100) POINT,DELTA
  100 FORMAT('C'///' ','THE FOLLOWING SPECIMENS HAVE A DENSITY OF ',
     .F10.2,2X,'+/-',F5.2,/
     .          '+',T51,'______','/'0',T10,'NUMBER',T24,'DENSITY',/'+',T10
     .,'______',T24,'_______'/)
      DO 5 JJ=J,I
      IF(ABS(POINT-A(JJ,2)).GT.DELTA) GO TO 5
      WRITE(6,110)(A(JJ,N),N=1,3)
  110 FORMAT(' ',T10,F5.0,T20,F10.4,T30,F16.2)
      A(JJ,2)=0
    5 CONTINUE
    6 CONTINUE
      IF(IREJEC.EQ.0)GO TO 9
      WRITE(6,80)
   80 FORMAT('1',T20,'THE FOLLOWING SPECIMENS HAVE BEEN REJECTED FOR
     . REASONS OF INCORRECT DENSITY')
      DO 9 J=1,IREJEC
      WRITE(6,90)(REJECT(J,JJ),JJ=1,7)
   90 FORMAT(' ',F5.0,4F10.2,2F10.4)
    9 CONTINUE
      WRITE (6,35)
   35 FORMAT('1',T2,'COUNTER',T12,'MASS',T22,'LENGTH',T32,'WIDTH',
     .T42,'HEIGHT',T50,'VOLUME',T65,'DENSITY',T80,
     .'****AVERAGED VALUES****'
     ./T54,'3',T66,'2',T76,'2',
     ./' ',T13,'GM',T24,'CM',T34,'CM',T44,'CM',T52,'CM'
     .     ,T62,'G/CM',T71,'LB/FT ',/'+',75('_')/)
      DO 200 I=1,7
      AVG(I)=SUM(I)/JJJ
  200 CONTINUE
      WRITE (6,30) JJJ,(AVG(I),I=1,7)
      STOP
      END
//GO.SYSIN DD *
```

400	5.6955	6.99	7.02	3.76
401	5.755	7.	7.	3.76
402	5.6195	6.99	6.97	3.74
403	5.8237	6.99	6.98	3.74
404	5.8737	7.	6.99	3.74
405	5.6295	6.97	7.	3.75
406	5.7231	6.99	6.96	3.74
407	5.6293	7.	7.	3.76
408	5.6167	6.98	6.97	3.76
409	5.7418	7.01	6.96	3.74
410	5.4902	6.97	6.99	3.75
411	5.6245	7.	6.99	3.74
412	5.5857	7.	6.99	3.75
413	5.8274	6.99	7.	3.74
414	5.7658	6.97	7.	3.74
415	5.67	6.96	7.	3.75
416	5.75	6.97	6.98	3.74
417	5.7897	6.99	6.99	3.74
418	5.6067	6.98	6.98	3.74
419	5.55	6.99	6.98	3.76
420	5.629	6.99	6.99	3.74
421	5.7230	6.98	6.99	3.75
422	5.7823	7.	6.97	3.75
423	5.73	6.99	7.	3.73
424	5.5267	6.96	6.99	3.74
425	5.7408	6.99	6.98	3.74
426	5.7471	6.97	6.96	3.75
427	5.8039	6.98	6.98	3.74
428	5.5805	6.99	6.98	3.77
429	5.8365	6.98	6.99	3.74
430	5.757	6.98	7.	3.75
431	5.7565	6.99	7.	3.75
432	5.7137	7.	7.	3.74
433	5.6954	7.01	6.98	3.76
434	5.8029	7.02	7.01	3.74
435	5.8084	6.98	6.98	3.75
436	5.7112	6.99	6.98	3.74
437	5.7359	6.98	7.	3.74
438	5.6395	7.	7.	3.75
439	5.6206	6.98	6.98	3.74
440	5.6014	6.98	6.98	3.74
441	5.7049	6.96	6.96	3.75
442	5.8417	6.97	7.01	3.75
443	5.8928	6.98	6.98	3.76
444	5.7864	6.99	6.99	3.76
445	5.9193	6.99	7.	3.74
446	5.7771	6.98	6.98	3.75
447	5.6339	6.95	7.	3.75
448	5.5881	6.99	6.96	3.76
449	5.5999	6.98	7.	3.74
450	5.714	7.	6.99	3.74
451	5.6179	7.	7.	3.76
452	5.8680	6.99	7.01	3.75
453	5.5916	7.	7.	3.74
454	5.7705	7.	7.	3.74
455	5.7382	6.98	6.98	3.74
456	5.7407	6.97	6.98	3.74
457	5.6330	6.98	6.98	3.75
458	5.5739	6.97	6.98	3.74
459	5.7454	7.01	6.95	3.75
460	5.7994	6.96	6.99	3.74
461	5.8034	6.99	7.	3.75
462	5.6758	6.97	7.	3.74
463	5.7798	6.98	7.	3.74
464	5.7229	6.98	6.98	3.74
465	5.6100	6.95	6.99	3.77
466	5.6258	6.98	6.96	3.75

467	5.7277	7.	7.01	3.76
468	5.6622	6.98	7.	3.74
469	5.5763	6.98	6.96	3.75
470	5.7742	6.99	7.01	3.74
471	5.6434	6.97	6.98	3.74
472	5.5581	6.97	6.98	3.74
473	5.5400	7.	6.96	3.74
474	5.6248	6.96	6.98	3.74
475	5.6811	6.96	7.	3.74
476	5.7755	6.98	6.99	3.74
477	5.6287	6.98	6.96	3.74
478	5.6678	6.99	6.99	3.75
479	5.6881	6.97	7.	3.74
480	6.9414	7.	7.01	3.75
481	6.6564	6.99	6.97	3.75
482	6.7752	7.01	6.99	3.76
483	6.8426	6.95	6.99	3.75
484	6.9778	6.98	7.	3.75
485	6.9212	6.99	6.99	3.74
486	6.9541	6.99	7.	3.74
487	6.79	6.98	7.01	3.76
488	6.81	7.	7.01	3.74
489	6.6908	7.02	6.99	3.74
490	6.862	7.	6.99	3.75
491	6.6538	7.	6.99	3.75
492	6.9415	7.01	7.	3.75
493	6.7755	6.98	6.95	3.75
494	6.8009	6.98	7.02	3.75
495	6.8440	6.96	7.	3.76
496	6.624	6.99	7.	3.76
497	6.628	7.02	6.98	3.76
498	6.8144	7.	6.98	3.76
499	6.6988	7.	7.01	3.76
500	6.8144	7.	7.	3.76
501	6.5508	6.98	6.99	3.75
502	6.6594	6.98	6.98	3.75
503	6.9053	6.96	6.99	3.75
504	6.8217	6.98	7.01	3.78
505	6.7106	6.98	6.98	3.76
506	6.7645	6.96	7.01	3.76
507	6.77	6.98	6.98	3.74
508	6.836	7.03	6.98	3.77
509	6.6960	6.98	7.	3.76
510	6.6983	7.01	6.97	3.76
511	6.7777	6.96	7.02	3.75
512	6.6779	6.98	6.98	3.76
513	6.6547	6.98	6.98	3.75
514	6.8814	7.	7.	3.75
515	6.6003	7.	6.98	3.75
516	6.8039	6.99	7.	3.75
517	7.0324	6.98	7.	3.76
518	6.849	7.	7.	3.74
519	6.6885	6.98	6.99	3.75
520	6.8904	6.99	7.	3.74
521	6.8241	7.	6.96	3.75
522	6.9817	6.98	6.99	3.75
523	6.934	6.98	7.02	3.75
524	7.0424	7.	7.	3.75
525	6.9224	7.	6.98	3.74

526	6.6851	6.98	6.98	3.74
527	6.92	7.	7.	3.75
528	7.0083	6.99	7.02	3.75
529	6.8176	6.98	6.98	3.76
530	6.73	6.[illegible]	7.01	3.75
531	7.0975	6.99	7.	3.75
532	7.0051	7.	7.	3.77
533	6.8234	6.98	7.01	3.75
534	6.8347	6.96	7.	3.74
535	6.9	6.99	7.02	3.75
536	6.91	6.98	6.99	3.75
537	6.73	6.98	7.	3.76
538	6.8713	7.01	6.98	3.74
539	6.7813	6.99	7.01	3.75
540	7.0348	6.97	7.01	3.75
541	6.6683	6.98	7.	3.75
542	6.7025	7.	7.	3.75
543	6.6853	6.98	7.	3.75
544	6.6457	7.	6.98	3.75
545	6.8767	7.02	6.99	3.75
546	6.9305	6.98	6.99	3.75
547	7.036	7.01	7.02	3.75
548	6.699	7.	7.02	3.75
549	6.9346	6.99	7.03	3.74
550	8.0238	7.	7.	3.75
551	8.3629	7.	7.02	3.76
552	8.232	7.	7.02	3.76
553	8.2404	7.01	7.01	3.75
554	8.4083	7.	7.03	3.75
555	8.3355	7.01	7.01	3.75
556	8.1023	7.	7.01	3.76
557	8.3118	7.02	7.03	3.76
558	8.0302	7.01	7.01	3.77
559	7.89	7.	7.01	3.76
560	8.0069	7.02	6.98	3.75
561	8.353	7.02	7.	3.77
562	8.6691	7.02	7.03	3.76
563	8.3868	7.	7.02	3.76
564	8.1456	7.	7.	3.75
565	8.1408	7.02	6.97	3.75
566	8.3408	7.01	7.02	3.75
567	7.976	6.98	7.02	3.74
568	8.1371	6.97	7.	3.76
569	8.2402	6.98	7.	3.76
570	8.1866	7.	6.98	3.75
571	8.5759	7.02	7.02	3.74
572	8.3237	7.	6.99	3.77
573	8.3023	6.98	7.03	3.75
574	8.3733	7.02	6.98	3.75
575	7.8596	7.02	6.98	3.75
576	8.	7.01	7.	3.75
577	8.6962	7.02	7.	3.77
578	8.6398	7.02	7.01	3.75
579	8.2484	7.	6.99	3.74
580	8.2619	7.04	7.	3.74
581	8.42	6.99	7.	3.74
582	8.2022	7.	7.01	3.75
583	8.1575	7.02	6.99	3.74
584	8.3566	7.	7.	3.76

585	7.9244	6.98	7.02	3.75
586	8.0144	7.	7.	3.74
587	8.0410	7.01	7.02	3.75
588	8.2633	6.99	6.98	3.75
589	8.3728	6.98	7.01	3.75
590	8.1156	7.	7.02	3.74
591	8.5313	7.	7.01	3.76
592	8.0205	7.02	7.	3.75
593	8.2376	7.01	6.99	3.74
594	8.0175	7.	7.02	3.75
595	8.4726	7.01	7.02	3.76
596	8.2552	7.	7.02	3.75
597	8.5636	7.	6.96	3.75
598	8.1074	7.	7.	3.74
599	8.4171	7.	7.01	3.75
600	8.4395	7.	7.02	3.75
601	8.4564	7.02	7.	3.75
602	8.4167	7.	7.01	3.76
603	8.2167	7.	6.99	3.76
604	8.219	6.98	7.01	3.75
605	6.319	7.01	7.02	3.76
606	8.0011	6.97	7.02	3.76
607	8.336	6.98	6.99	3.75
608	8.5710	7.01	7.03	3.75
609	8.2974	7.02	6.99	3.75
610	8.0756	7.04	7.02	3.75
611	8.0446	6.98	7.01	3.75
612	8.5304	6.99	7.	3.75
613	8.0578	7.	6.96	3.75
614	8.6278	7.05	7.02	3.75
615	8.3046	6.98	7.02	3.75
616	8.5722	6.97	7.	3.74
617	8.0567	7.	7.04	3.75
618	8.3739	7.	7.01	3.75
619	8.3066	7.	6.99	3.75
620	8.166	7.	7.	3.75
621	8.2886	6.98	7.03	3.75
622	8.3439	6.98	7.	3.74
623	8.3041	7.	7.02	3.74
624	8.4479	7.01	6.99	3.75
625	8.3281	7.01	7.	3.75
626	8.3299	7.	7.03	3.75
627	8.2021	7.01	7.02	3.76
628	8.614	6.99	7.	3.75
629	7.89	7.	7.	3.75
630	10.3587	7.	7.02	3.74
631	9.2857	7.	7.02	3.75
632	9.672	7.04	7.01	3.75
633	10.2447	7.02	7.	3.74
634	9.0946	7.02	7.	3.74
635	9.5946	7.	7.03	3.74
636	9.4171	7.04	6.98	3.75
637	10.4616	7.	7.01	3.74
638	9.4437	7.02	7.	3.74
639	9.5116	7.01	7.	3.74
640	10.268	7.01	7.03	3.74
641	10.6661	7.01	7.02	3.74
642	10.4893	7.05	7.02	3.76
643	10.1593	7.03	7.	3.76

526	6.6851	6.98	6.98	3.74
527	6.92	7.	7.	3.75
528	7.0083	6.99	7.02	3.75
529	6.8176	6.98	6.98	3.76
530	6.73	6.97	7.01	3.75
531	7.0975	6.99	7.	3.75
532	7.0051	7.	7.	3.77
533	6.8234	6.98	7.01	3.75
534	6.8347	6.96	7.	3.74
535	6.9	6.99	7.02	3.75
536	6.91	6.98	6.99	3.75
537	6.73	6.98	7.	3.76
538	6.8713	7.01	6.98	3.74
539	6.7813	6.99	7.01	3.75
540	7.0343	6.97	7.01	3.75
541	6.6653	6.98	7.	3.75
542	6.7025	7.	7.	3.75
543	6.6853	6.98	7.	3.75
544	6.6457	7.	6.98	3.75
545	6.8767	7.02	6.99	3.75
546	6.9305	6.98	6.99	3.75
547	7.036	7.01	7.02	3.75
548	6.699	7.	7.02	3.75
549	6.9846	6.99	7.03	3.74
550	8.0239	7.	7.	3.75
551	8.3629	7.	7.02	3.76
552	8.232	7.	7.02	3.76
553	8.2404	7.01	7.01	3.75
554	8.4083	7.	7.03	3.75
555	8.3355	7.01	7.01	3.75
556	8.1023	7.	7.01	3.76
557	8.3119	7.02	7.03	3.76
558	8.0302	7.01	7.01	3.77
559	7.89	7.	7.01	3.76
560	8.0063	7.02	6.98	3.75
561	8.353	7.02	7.	3.77
562	8.6691	7.02	7.03	3.76
563	8.3869	7.	7.02	3.76
564	8.1456	7.	7.	3.75
565	8.1409	7.02	6.97	3.75
566	8.3408	7.01	7.02	3.75
567	7.976	6.98	7.02	3.74
568	8.1371	6.97	7.	3.76
569	8.2402	6.98	7.	3.76
570	8.1866	7.	6.98	3.75
571	8.5759	7.02	7.02	3.74
572	8.3237	7.	6.99	3.77
573	8.3023	6.98	7.03	3.75
574	8.3733	7.02	6.98	3.75
575	7.8596	7.02	6.98	3.75
576	8.	7.01	7.	3.75
577	8.6962	7.02	7.	3.77
578	8.6398	7.02	7.01	3.75
579	8.2484	7.	6.99	3.74
580	8.2619	7.04	7.	3.74
581	8.42	6.99	7.	3.74
582	8.2022	7.	7.01	3.75
583	8.1575	7.02	6.99	3.74
584	8.3566	7.	7.	3.76

585	7.9244	6.98	7.02	3.75
586	8.0144	7.	7.	3.74
587	8.0410	7.01	7.02	3.75
588	8.2633	6.99	6.98	3.75
589	8.3728	6.98	7.01	3.75
590	9.1156	7.	7.02	3.74
591	8.5313	7.	7.01	3.76
592	8.0205	7.02	7.	3.75
593	8.2376	7.01	6.99	3.74
594	8.0175	7.	7.02	3.75
595	8.4726	7.01	7.02	3.76
596	8.2952	7.	7.02	3.75
597	8.5636	7.	6.96	3.75
598	9.1074	7.	7.	3.74
599	8.4171	7.	7.01	3.75
600	8.4395	7.	7.02	3.75
601	8.4964	7.02	7.	3.75
602	8.4167	7.	7.01	3.76
603	8.2167	7.	6.99	3.76
604	8.219	6.98	7.01	3.75
605	6.219	7.01	7.02	3.76
606	8.0011	6.97	7.02	3.76
607	8.336	6.98	6.99	3.75
608	8.5710	7.01	7.03	3.75
609	8.2974	7.02	6.99	3.75
610	8.0756	7.04	7.02	3.75
611	8.0446	6.98	7.01	3.75
612	8.5304	6.99	7.	3.75
613	8.0579	7.	6.96	3.75
614	8.6278	7.05	7.02	3.75
615	8.3046	6.98	7.02	3.75
616	8.5722	6.97	7.	3.74
617	8.0567	7.	7.04	3.75
618	8.3739	7.	7.01	3.75
619	8.3066	7.	6.99	3.75
620	8.166	7.	7.	3.75
621	8.2886	6.98	7.03	3.75
622	8.3439	6.98	7.	3.74
623	8.3041	7.	7.02	3.74
624	8.4479	7.01	6.99	3.75
625	8.3281	7.01	7.	3.75
626	8.3299	7.	7.03	3.75
627	8.2021	7.01	7.02	3.76
628	8.614	6.99	7.	3.75
629	7.89	7.	7.	3.75
630	10.3597	7.	7.02	3.74
631	9.2857	7.	7.02	3.75
632	9.672	7.04	7.01	3.75
633	10.2447	7.02	7.	3.74
634	9.0946	7.02	7.	3.74
635	9.5946	7.	7.03	3.74
636	9.4171	7.04	6.98	3.75
637	10.4616	7.	7.01	3.74
638	9.4437	7.02	7.	3.74
639	9.5116	7.01	7.	3.74
640	10.208	7.01	7.03	3.74
641	10.6661	7.01	7.02	3.74
642	10.4893	7.05	7.02	3.76
643	10.1593	7.03	7.	3.76

644	10.3809	7.	7.03	3.74
645	10.0834	7.	7.03	3.74
646	10.65	7.02	7.05	3.76
647	9.5546	6.99	7.02	3.75
648	10.1672	7.01	7.02	3.75
649	10.0986	7.01	7.	3.74
650	9.4343	7.01	7.01	3.75
651	10.262	7.	7.05	3.75
652	9.8686	7.	6.99	3.74
653	10.1201	7.01	7.02	3.75
654	10.2768	7.04	7.02	3.76
655	9.8987	7.04	7.02	3.76
656	9.6009	7.05	7.04	3.75
657	10.5467	7.	7.01	3.75
658	10.2343	6.99	7.01	3.75
659	9.7333	7.04	7.02	3.76
660	10.2730	7.01	7.01	3.75
661	10.0133	7.01	7.04	3.76
662	10.54	7.	7.02	3.75
663	10.5816	7.05	7.	3.75
664	9.6816	7.	7.	3.75
665	9.9865	7.02	7.06	3.76
666	10.3565	7.02	7.01	3.75
667	10.4565	7.	6.98	3.75
668	10.0608	7.03	7.04	3.75
669	10.4446	7.04	7.05	3.76
670	9.7092	6.99	7.01	3.75
671	10.1525	7.	7.02	3.75
672	10.3963	7.03	7.04	3.74
673	10.2158	7.02	7.	3.74
674	10.6472	7.02	7.01	3.76
675	10.0034	7.02	7.03	3.74
676	10.2933	7.	7.03	3.74
677	10.2717	7.	7.01	3.75
678	9.5717	6.98	7.04	3.75
679	9.5210	7.02	7.02	3.76
680	9.6441	7.01	7.	3.76
681	10.2572	7.01	7.04	3.7 4
682	10.3388	7.02	6.98	3.76
683	10.3464	7.	7.02	3.74
684	10.4159	7.	7.01	3.75
685	9.5241	7.02	7.02	3.74
686	10.0941	7.02	7.04	3.74
687	10.2528	7.02	7.04	3.75
688	10.	7.02	7.	3.75
689	10.5182	7.	7.03	3.75
690	10.35	7.06	7.05	3.75
691	9.8052	7.02	7.02	3.76
692	9.2974	6.99	7.01	3.76
693	9.4584	7.	7.	3.75
694	3.8083	7.03	7.05	3.76
695	10.2545	7.04	7.04	3.74
696	9.2445	7.	6.99	3.76
697	10.4515	7.04	7.05	3.76
698	10.8479	7.03	7.06	3.76
699	9.9933	7.02	7.	3.74
700	10.4333	7.03	6.99	3.75
701	10.335	7.01	7.02	3.76
702	10.0650	6.99	7.05	3.75

703	10.2546	7.03	7.05	3.75
704	10.2388	7.02	7.04	3.76
705	10.4126	7.	7.01	3.75
706	10.9548	7.03	7.	3.74
707	10.1993	7.02	7.	3.76
708	10.5022	7.02	7.05	3.75
709	9.5717	7.02	7.01	3.75
710	10.9526	7.02	7.04	3.76
711	11.533	7.02	7.04	3.75
712	11.443	7.	7.02	3.97
713	10.6969	7.02	7.03	3.75
714	11.5379	7.01	7.02	3.74
715	11.037	7.01	7.02	3.76
716	10.3676	6.99	7.04	3.75
717	11.0415	7.	7.05	3.74
718	11.5546	7.	7.	3.96
719	11.5583	7.05	7.04	3.75
720	10.6457	7.02	7.09	3.75
721	11.027	7.	7.03	3.86
722	11.187	6.99	7.02	3.81
723	10.4747	7.	7.04	3.75
724	10.3808	7.	7.01	3.97
725	10.8652	7.01	7.07	3.91
726	11.3221	7.05	7.03	3.78
727	11.5257	7.04	7.05	3.9
728	11.4337	7.01	7.02	3.75
729	11.8447	7.	7.04	3.9
730	11.8162	7.04	7.05	3.76
731	[illegible]	7.02	7.03	3.75
732	10.9729	6.99	7.02	3.75
733	11.278	7.02	7.05	3.76
734	10.8879	7.06	7.06	3.75
735	10.673	7.01	7.	3.75
736	11.1988	7.04	7.05	3.74
737	10.1233	7.01	7.02	3.75
738	10.9244	7.03	7.04	3.76
739	11.4944	7.03	7.04	3.75
740	11.648	7.01	7.09	3.76
741	11.2247	7.03	7.04	3.75
742	10.7954	7.01	7.04	3.76
743	11.1811	7.	7.04	3.76
744	11.3757	7.03	7.04	3.76
745	11.0928	7.01	7.02	3.75
746	10.7015	6.97	7.01	3.75
747	11.3336	7.02	7.04	3.74
748	10.6008	7.	7.06	3.75
749	11.0854	6.98	7.02	3.93
750	10.9178	7.02	7.04	3.74
751	10.974	7.02	7.03	3.76
752	10.5345	6.99	7.02	3.77
753	11.5854	7.02	7.05	3.76
754	10.4536	7.02	7.02	3.92
755	11.49	[illegible]	6.98	3.76
756	10.5274	7.	7.02	3.76
757	11.0282	7.03	7.	3.76
758	11.3542	7.	7.02	3.74
759	11.1614	7.06	6.99	3.76
760	11.61	7.02	7.02	3.95
761	10.1	7.02	7.05	3.75

762	11.287	6.94	6.95	3.76
763	10.767	7.04	7.02	3.76
764	10.8932	7.02	7.02	3.74
765	10.6382	7.03	7.03	3.74
766	10.8398	7.02	7.05	3.76
767	11.1712	7.01	7.07	3.74
768	10.2208	7.02	7.04	3.84
769	11.8548	7.02	7.02	3.75
770	11.0528	6.99	7.03	3.77
771	10.4168	7.02	7.06	3.77
772	11.1014	7.04	7.	3.88
773	11.7478	7.04	7.04	3.76
774	11.8735	7.05	7.05	3.76
775	11.7949	7.02	7.04	3.77
776	11.6524	7.	7.04	3.75
777	11.0259	7.03	7.03	3.75
778	11.7072	7.	7.04	3.76
779	11.0339	[illegible]	7.05	3.74
780	11.11	7.05	7.05	3.77
781	11.49	7.	7.01	3.74
782	10.9556	7.02	7.02	3.76
783	11.7467	7.03	7.03	3.76
784	11.4319	7.	7.01	3.75
785	11.4164	7.04	7.04	3.75
786	10.9048	7.02	7.05	3.79
787	11.9185	7.02	7.03	3.76
788	11.5159	7.04	7.03	3.75
789	11.4418	7.04	7.04	3.93
790	6.937	7.01	7.	3.75
791	6.917	7.02	6.99	3.75
792	6.7345	7.	6.98	3.77
793	7.2188	7.	7.03	3.76
794	6.8442	7.	6.99	3.74
795	6.92	7.	7.	3.74
796	7.1385	7.01	6.99	3.75
797	6.9254	7.	6.99	3.74
798	6.9221	7.01	6.99	3.75
799	6.9148	6.99	7.02	3.74
65	12.2927	7.00	6.99	3.79
66	12.3701	6.94	6.99	3.77
67	12.8128	7.00	6.98	3.80
68	11.8350	6.93	7.00	3.86
70	11.9858	7.02	6.93	3.76
73	11.0966	6.94	6.99	3.87
77	10.4223	6.92	6.95	3.77
79	10.3528	6.95	6.96	3.79
83	12.8629	6.95	6.93	3.80
86	12.3789	6.91	6.94	3.76
87	12.0680	6.91	6.94	3.76
88	12.2897	6.96	6.92	3.75
89	10.5370	6.93	6.91	3.83
90	10.4214	6.91	6.96	3.81
91	11.1111	6.95	6.93	3.87
92	11.1872	6.94	6.90	3.91
93	11.0000	6.94	6.93	3.88
94	10.4458	6.93	6.95	3.81
96	10.4917	6.92	6.94	3.80
100	7.6343	6.905	6.935	3.95
101	7.1825	6.93	6.93	3.85

108	9.0678	6.94	6.93	3.99
110	8.2446	6.92	6.92	3.94
117	8.8312	6.94	6.94	3.95
118	8.5212	6.92	6.94	4.03
119	7.7798	6.92	6.91	3.89
120	7.5776	6.91	6.92	3.95
122	6.4932	6.94	6.92	3.72
123	6.5103	6.92	6.92	3.7
124	6.6724	6.92	6.92	3.7
125	6.6625	6.84	6.9	3.71
126	6.4244	6.72	6.94	3.7
129	6.5	6.89	6.9	3.73
130	6.5642	6.91	6.86	3.71
131	6.4174	6.91	6.9	3.72
132	6.4022	6.9	6.32	3.72
133	6.4926	6.88	6.92	3.72
134	6.5320	6.91	6.90	3.7
138	6.5371	6.84	6.84	3.65
139	6.4376	6.8	6.83	3.73
142	6.3041	6.83	6.84	3.69
143	6.3946	6.84	6.84	3.64
144	6.5603	6.83	6.83	3.65
145	6.2977	6.83	6.84	3.65
146	6.2934	6.79	6.82	3.66
147	6.3934	6.84	6.84	3.71
148	6.4221	6.84	6.82	3.64
150	6.5401	6.85	6.83	3.65
151	6.5823	6.84	6.82	3.67
152	6.48	6.83	6.84	3.66
153	6.4003	6.84	6.85	3.72
154	6.4788	6.84	6.84	3.68
155	6.295	6.82	6.85	3.72
156	6.3337	6.8	6.86	3.68
157	6.4358	6.84	6.86	3.7
158	6.4522	6.83	6.84	3.68
161	6.611	6.82	6.84	3.66
162	6.5797	6.82	6.86	3.68
163	6.4677	6.8	6.85	3.73
166	6.4833	6.84	6.84	3.69
167	6.6292	6.84	6.86	3.72
171	6.5098	6.86	6.88	3.72
172	6.4520	6.85	6.97	3.72
173	6.4891	6.89	6.87	3.75
174	6.5387	6.87	6.87	3.72
175	6.8033	6.86	6.86	3.71
177	6.5887	6.86	6.84	3.70
178	6.6903	6.86	6.86	3.72
181	6.6213	6.87	6.85	3.72
182	6.7227	6.86	6.84	3.7
191	7.5336	6.84	6.88	3.96
193	7.4916	6.88	6.88	3.99
194	7.5172	6.88	6.85	3.92
195	7.2772	6.89	6.91	3.80
196	7.1311	6.85	6.89	3.82
198	7.3227	6.89	6.84	3.8
199	7.5641	6.86	6.86	4.04
200	7.4613	6.84	6.87	4.06
201	7.3069	6.90	6.86	3.90
202	7.664	6.86	6.87	3.98

203	7.2370	6.89	6.93	3.84
207	7.3945	6.88	6.89	3.96
208	7.275	6.89	6.89	4.
209	7.4296	6.92	6.92	3.93
210	7.662	6.9	6.9	3.99
211	7.3212	6.89	6.89	3.93
212	7.3016	6.98	6.85	3.97
213	7.2283	6.86	6.87	3.96
215	7.4975	6.99	6.98	3.94
216	7.3839	6.99	7.	3.96
217	7.7105	6.97	6.98	3.96
218	7.4539	6.87	6.98	3.99
219	7.3862	6.95	7.03	3.93
220	7.4152	6.99	6.96	3.86
223	7.4048	6.97	7.01	3.8
224	7.4307	6.99	7.	3.8
225	7.2572	6.99	6.98	3.88
227	7.5435	7.02	7.	3.96
228	7.4989	6.99	7.01	3.91
230	7.4073	7.	6.98	3.92
231	7.2693	6.98	6.96	3.88
232	7.4517	6.99	6.97	3.81
233	7.3982	6.99	7.01	3.83
234	7.4782	6.98	7.02	3.76
235	7.429	7.	6.96	3.78
237	7.6389	6.92	7.	3.96
243	9.4312	6.97	6.98	4.08
245	9.1301	6.98	6.99	4.13
246	9.	6.94	6.96	4.08
248	9.1789	6.97	6.93	4.09
259	9.2831	6.98	6.99	4.04
263	9.2841	6.94	7.00	4.03
265	9.0969	6.98	6.98	4.10
266	9.5002	7.00	7.00	4.08
272	9.4547	7.00	7.00	4.10
277	8.9344	6.96	6.98	4.03
280	10.3363	6.99	7.00	3.81
281	10.2354	7.00	7.02	3.75
282	10.7281	6.98	7.00	3.78
283	10.6681	6.99	6.98	3.76
284	10.9713	7.00	7.00	3.81
285	10.7990	7.	7.	3.81
286	10.5017	7.02	7.01	3.84
287	10.3053	7.02	6.99	3.76
288	11.3996	7.00	7.00	3.90
289	10.8049	7.01	7.02	3.85
290	10.8259	7.00	7.01	3.84
291	11.2723	6.99	6.97	3.90
292	10.5046	7.00	7.00	3.78
293	10.7925	7.01	6.99	3.78
294	10.7145	7.01	7.01	3.82
295	10.5073	7.01	7.00	3.77
296	11.4491	7.00	6.99	3.91
297	11.1222	7.00	6.95	3.78
298	10.6338	7.00	7.00	3.78
299	11.1522	6.99	6.99	3.85
300	10.6469	6.99	6.96	3.78
301	10.8754	6.96	6.97	3.79
302	10.6120	6.98	6.95	3.79

303	10.7254	6.99	6.94	3.81
304	10.6565	6.99	6.95	3.84
313	11.0698	6.99	6.99	3.86
314	11.3916	7.	6.99	3.89
316	10.9417	6.98	6.98	3.83
323	10.8517	6.99	7.	3.8
326	10.3047	7.01	6.96	3.91
327	10.4090	6.99	7.	3.79
328	11.2628	7.	6.99	3.89
329	10.8899	6.97	6.99	3.85
332	10.4939	6.98	6.99	3.81
334	10.5061	6.99	7.	3.81
335	10.5599	6.99	6.99	3.79
336	10.2396	6.99	6.98	3.77
338	10.7234	6.99	7.	3.83
340	10.5545	6.99	6.98	3.86
342	10.6177	6.99	6.98	3.79
343	10.4531	6.98	6.99	3.79
346	10.7557	6.99	6.99	3.78
347	10.8172	6.99	6.99	3.79
348	10.8016	6.98	6.98	3.87
350	10.5723	6.99	6.99	3.79
351	11.2172	6.99	6.97	3.88
352	12.0930	6.99	6.98	3.77
353	11.6334	6.97	6.96	3.77
355	12.1596	6.97	6.97	3.75
356	12.9822	6.98	7.	3.78
357	11.9041	7.	6.95	3.76
358	12.7086	6.99	6.98	3.79
359	13.05	6.99	6.96	3.79
360	11.6207	6.99	6.99	3.76
361	11.7589	6.97	7.	3.75
362	11.8616	7.01	7.	3.74
363	12.0301	6.96	6.98	3.76
364	12.5670	6.96	6.98	3.77
365	12.3201	6.97	6.98	3.78
366	11.8156	6.98	7.	3.77
367	11.7377	6.98	7.	3.77
368	11.9790	6.96	7.	3.76
370	11.5690	6.99	6.97	3.77
371	12.0930	6.98	6.98	3.76
372	11.9268	6.98	6.97	3.76
373	12.7775	6.98	6.99	3.78
374	12.4247	6.99	6.97	3.78
375	12.9842	7.	6.98	3.8
376	11.5868	6.92	6.99	3.75
377	11.7660	6.98	6.95	3.76
378	12.2784	6.99	6.98	3.75
379	12.0602	6.97	6.98	3.76
381	12.2332	6.98	6.97	3.78
382	11.8293	6.95	6.99	3.70
383	11.5979	6.96	6.98	3.76
384	12.1824	6.98	6.98	3.76
385	11.9302	6.98	6.93	3.77
386	11.5523	6.93	6.99	3.76
387	12.2257	6.99	7.	3.75
388	12.7501	7.	7.	3.78
389	12.0889	6.98	7.	3.75
390	12.7422	7.	7.	3.78
391	12.2712	6.99	7.	3.79
392	11.4768	6.98	6.98	3.76
393	11.7135	6.99	6.98	3.75
394	12.1778	6.99	6.97	3.75
395	11.8191	6.98	6.97	3.74
396	12.6679	6.98	6.99	3.78
397	11.5689	6.99	6.98	3.75

The following program is based upon Meunier's original PSB foam simulation and plotting routine.

It was used to plot the curves resulting from the predictive equation.

```
****CONTINUOUS SYSTEM MODELING PROGRAM****

***PROBLEM INPUT STATEMENTS***

INCON XIDIC = 41659.,XIIC = 0.0
DYNAMIC
AA = A*AREA/AMASS*(DENSTY**1.5)*(.796+.204*FF)
BB = .03057*ALOG(XX+SQRT((XX**2)+1))
CC =415.72*EXP(.88*DD)+.01343*EXP(13.9*DD)+1.25E-13*EXP(42.*DD)
DD = XI/THICKN
FF = (ABS(XID))/XIDIC
XX = (XIDIC/THICKN)*3.75E13
XIDD = -AA*BB*CC -A
XID = INTGRL(XIDIC,XIDD)
XI = INTGRL(XIIC,XID)
CONST A = 3530532,AREA=84.50,AMASS=5.006,THICKN=4.37, ...
DENSTY=.0316,TESTNO=034,SMPLNO=030
FINISH XID = 0.0
PREPARE  XI,XID,XIDD
PRTPLT XIDD(XI,XID)
TIMER FINTIM=.0004,DELT=.000001,OUTDEL=.000001666
END
STOP
*** CSMP/360 SIMULATION DATA ***

INCON XIDIC = 41659.,XIIC = 0.0

CONST A = 3530532,AREA=84.50,AMASS=5.006,THICKN=4.37, ...

DENSTY=.0316,TESTNO=034,SMPLNO=030

FINISH XID = 0.0

PREPARE  XI,XID,XIDD

PRTPLT XIDD(XI,XID)

TIMER FINTIM=.0004,DELT=.000001,OUTDEL=.000001666

END
      SUBROUTINE UPDATE
      COMMON  ZZ9901(5),IZ9901,ZZ9902,IZ9902,ZZ9903,IZ9903,ZZ9991(54)
      COMMON TIME
     1,DELT   ,DELMIN,FINTIM,PRDEL ,OUTDEL,XID    ,XI     ,XIDD   ,ZZ0003
     1,XIDIC  ,XIIC   ,A      ,AREA   ,AMASS  ,THICKN,DENSTY,TESTNO,SMPLNO
     1,AA     ,BB     ,CC     ,DD     ,FF     ,XX
      COMMON ZZ9992(7975),NALARM,IZ9993,ZZ9994(417),KEEP,ZZ9995(489)
     $,IZ0000,ZZ9996(824),IZ9997,IZ9998,ZZ9999(   68)
      GO TO(39995,39996,39997,39998),IZ0000
C     SYSTEM SEGMENT OF MODEL
39995 CONTINUE
      IZ9993=   26
      IZ9997=    2
      IZ9998=   25
      READ(5,39990)(ZZ9999(IZ9999),IZ9999=1,   68)
39990 FORMAT(18A4)
      IZ9901=    190013
      IZ9902=    250020
      IZ9903=        68
      GO TO 39999
C    INITIAL SEGMENT OF MODEL
39996 CONTINUE
      GO TO 39999
C    DYNAMIC SEGMENT OF MODEL
39997 CONTINUE
      DD=XI/THICKN
      CC=415.72*EXP(.88*DD)+.01343*EXP(13.9*DD)+1.25E-13*EXP(42.*DD)
      XX=(XIDIC/THICKN)*3.75E13
      BB=.03057*ALOG(XX+SQRT((XX**2)+1))
      FF=(ABS(XID))/XIDIC
      AA=A*AREA/AMASS*(DENSTY**1.5)*(.796+.204*FF)
      XIDD=-AA*BB*CC-A
C     XID          =INTGRL       (XIDIC        ,XIDD         )
C     XI           =INTGRL       (XIIC         ,XID          )
      ZZ0003=XID
      GO TO 39999
C   TERMINAL SEGMENT OF MODEL
39998 CONTINUE
39999 CONTINUE
      RETURN
      END
```

```
C     ******************************************************************
C     *                                                                *
C     * 'STEP2' LIT LES VARIABLES MISES SUR DISQUE PAR 'STEP1' (CSMP). LES *
C     *                                                                *
C     * REDUIT A LA BONNE ECHELLE ET EN FAIT LE GRAPHE.  LES TITRES ET LES *
C     *                                                                *
C     * COORDONNEES SONT EGALEMENT PRODUITS PAR 'STEP2'                *
C     *                                                                *
C     ******************************************************************
      DIMENSION ORIX(5),ORIY(5),SPEC1(2),SPEC2(3),SPEC3(11),
     1SPEC4(10),SPEC5(11),SPEC6(7),LINEX(13),LINEY(13),AXISX(68),
     2AXISY(68),NAME(2),TITLE1(5),TITLE2(4),TITLE3(5),
     3TITLE4(5),DUNITS(3),VUNITS(5),AUNITS(1),FUNITS(3),
     4TUNITS(3),AA(6),KB(6),KFNT(6),SEC(6),TIME(200),XI(200),KC(6),
     5XID(200),XIDD(200),XMIN(4),XMAX(4),FF(200),TH(200),V(200),TI(200)
     6,FNT(6),AXX(20),XXX(20),TTT(20),DENS(2),VVV(2),MASS(2),XUNITS(2)
      DIMENSION EXPER(3),SIMU(3)
C     ******************************************************************
C     *                                                                *
C     *  LES 4 PROCHAINES LIGNES COMMENCENT LA PROCEDURE 'MILGO'       *
C     *                                                                *
C     ******************************************************************
      CALL REREAD
      CALL BPLT(4,2)
      CALL PEN(1)
      CALL INCM(0)
      KKKK = 5
C     ******************************************************************
C     *                                                                *
C     *  LES PROCHAINES LIGNES LISENT LES DONNEES ESSENTIELLES A LA    *
C     *                                                                *
C     * PRODUCTION DES AXES, DES COORDONNEES ET DES TITRES             *
C     *                                                                *
C     ******************************************************************
      READ(KKKK,101) (LINEX(I),LINEY(I),I = 1,13)
      READ(KKKK,101)(AXISX(I),AXISY(I),I = 4,68)
      READ(KKKK,101)(ORIX(I),ORIY(I),I = 1,5)
      READ(KKKK,102) SPEC1
      READ(KKKK,103) SPEC2
      READ(KKKK,104)SPEC3
      READ(KKKK,105) SPEC4
      READ(KKKK,106) SPEC5
      READ(KKKK,107)SPEC6
      READ(KKKK,108) TITLE1
      READ(KKKK,109) TITLE2
      READ(KKKK,110) TITLE3
      READ(KKKK,111) TITLE4
      READ(KKKK,112) DUNITS
      READ(KKKK,113) VUNITS
      READ(KKKK,114) AUNITS
      READ(KKKK,115) FUNITS
      READ(KKKK,116) TUNITS
      READ(KKKK,117) NAME
      READ (KKKK,118) NN
      READ(KKKK,119) (AXX(I),XXX(I),TTT(I),I = 1,NN)
      READ(KKKK,120) XUNITS
      READ(KKKK,121) PLUS
      READ(KKKK,122) EXPER
```

```
      READ(KKKK,123) SIMU
  101 FORMAT (F6.2,2X,F6.2)
  102 FORMAT (2(A4))
  103 FORMAT (3(A4))
  104 FORMAT (11(A4))
  105 FORMAT (10(A4))
  106 FORMAT (11(A4))
  107 FORMAT (7(A4))
  108 FORMAT (5(A4))
  109 FORMAT (4(A4))
  110 FORMAT (5(A4))
  111 FORMAT (5(A4))
  112 FORMAT (3(A4))
  113 FORMAT (5(A4))
  114 FORMAT (A4)
  115 FORMAT (3(A4))
  116 FORMAT (3(A4))
  117 FORMAT (2(A4))
  118 FORMAT(I2)
  119 FORMAT (3(F6.2))
  120 FORMAT (2(A4))
  121 FORMAT(A4)
  122 FORMAT (3(A4))
  123 FORMAT(3(A4))
C     ************************************************************************
C     *                                                                      *
C     *  'INIT' EST LA SOUROUTINE QUI LIT LES DONNEES ENREGISTREES SUR DISQUE *
C     *   PAR 'STEP1'.                                                       *
C     *                                                                      *
C     *     'TESTNO' = LE NUMERO DU TEST                                     *
C     *                                                                      *
C     *     'SMPLNO' = LE NUMERO DE L'ECHANTILLON                            *
C     *                                                                      *
C     *     'THICKN' = L'EPAISSEUR ORIGINALE DE L'ECHANTILLON                *
C     *                                                                      *
C     *     'DENSTY' = LA DENSITE ORIGINALE DE L'ECHANTILLON                 *
C     *                                                                      *
C     *     'XIDIC' = LA VELOCITE ORIGINALE DU PROJECTILE                    *
C     *                                                                      *
C     *     'AMASS' = LA MASSE DU PROJECTILE                                 *
C     *                                                                      *
C     ************************************************************************
      CALL INIT(XMIN,XMAX,TESTNO,SMPLNO,DENSTY,THICKN,XIDIC,AMASS,A)
C     ************************************************************************
C     *                                                                      *
C     *  'ICOUNT' EST LE COMPTEUR QUI DETERMINE LE NOMBRE D'ITERATIONS       *
C     *                                                                      *
C     *  NECESSAIRES POUR QUE LA VELOCITE DEVIENNE ZERO.                     *
C     *                                                                      *
C     ************************************************************************
      ICOUNT = 0
      DO 200 I = 1,200
C     ************************************************************************
C     *                                                                      *
C     *  'VALUE' EST LA SOURCUTINE QUI LIT LES VALEURS DES SPECIFICATIONS    *
C     *                                                                      *
C     *  TEL QUE SPECIFIE PAR CSMP.                                          *
C     *                                                                      *
```

```
C     *     'TIME' EST LA VALEUR DU TEMPS ECOULE A CHAQUE ITERATION          *
C     *                                                                      *
C     *     'XI' EST LA DEFORMATION                                          *
C     *                                                                      *
C     *     'XID' EST LA VELOCITE                                            *
C     *                                                                      *
C     *     'XIDD' EST L'ACCELERATION                                        *
C     *                                                                      *
C     'CODE' : LORSQUE CODE = 1.0,LES VALEURS POUR TOUTES LES ITERATIONS ONT *
C     *                                                                      *
C     *         ETE LUES DU DISQUE                                           *
C     *                                                                      *
C     ************************************************************************
      CALL VALUE(TIME(I),XI(I),XID(I),XIDD(I),CODE)
      IF (CODE.EQ.1.) ICOUNT = I-1
      IF(ICOUNT.NE.0) GO TO 205
  200 CONTINUE
  205 CONTINUE
C     ************************************************************************
C     *                                                                      *
C     *  LES PROCHAINES 103 LIGNES DETERMINENT:                              *
C     *                                                                      *
C     *            1)  L'ORDRE DE GRANDEUR DES VARIABLES                     *
C     *                                                                      *
C     *            2)  LES VALEURS A INSCRIRE SUR LES AXES                   *
C     *                                                                      *
C     *            3)  LES FACTEURS PAR LESQUELS LES DONNEES DES VARIABLES   *
C     *                                                                      *
C     *                 SERONT MULTIPLIEES AFIN DE LES REDUIRE A LA BONNE    *
C     *                                                                      *
C     *                 ECHELLE POUR LE GRAPHE.                              *
C     *                                                                      *
C     ************************************************************************
C     ************************************************************************
C     *                                                                      *
C     * LA SECTION QUI SUIT OPERE SUR L'EPAISSEUR.                           *
C     *                                                                      *
C     ************************************************************************
      T = THICKN
      IF (T.GT.7.0) KT = 5
      IF (T.GT.4.0.AND.T.LT.7.0) KT = 4
      IF (T.GT.3.0.AND.T.LT.4.0) KT = 3
      IF (T.GT.2.0.AND.T.LT.3.0) KT = 2
      IF (T.LT.2.0) KT = 1
      AA(1) = 0.
      GO TO (1,2,3,4,5),KT
    1 AINC = .3
      XMULT = 20./3.
      GO TO 6
    2 AINC = .6
      XMULT = 10./3.
      GO TO 6
    3 AINC = 1.0
      XMULT = 2.
      GO TO 6
    4 AINC = 1.5
      XMULT = 10./7.5
      GO TO 6
```

```
      5 AINC = 2.0
        XMULT = 1.
      6 DC 7 I = 1,5
      7 AA(I+1) = AA(I) + AINC
C       ************************************************************************
C       *  ALPHA EST LA SCUROUTINE QUI CONVERTIT LES DCNNEES NUMERIQUES EN     *
C       *  DONNEES ALPHANUMERIQUES; CETTE CPERATICN EST NECESSAIRE PCUR FAIRE  *
C       *  TRACER LES LETTRES PAR 'MILGC'.                                     *
C       ************************************************************************
        CALL ALPHA (AA,KT,6,1)
C       ************************************************************************
C       *                                                                      *
C       *  LA SECTION QUI SUIT OPERE SUR LA VELOCITE                           *
C       *                                                                      *
C       ************************************************************************
        KB(1) = 0
        DC 8 I = 1,5
      8 KB(I+1) = KB(I) + 20.
        CALL ALPHA(AA,KB,6,2)
C       ************************************************************************
C       *                                                                      *
C       *  LA SECTION QUI SUIT OPERE SUR L'ACCELERATION                        *
C       *                                                                      *
C       ************************************************************************
        G = ABS(XMIN(4)/A)
        IF(G.GT.1000) KA=6
        IF(G.LE.1000.AND.G.GT.500) KA=5
        IF (G.LE.500.AND.G.GT.250) KA = 4
        IF (G.LE.250.AND.G.GT.100) KA = 3
        IF(G.LE.100.AND.G.GT.50) KA = 2
        IF (G.LT.50) KA = 1
        KC(1) = 0
        GO TO (13,12,11,10,9,36),KA
     36 KAINC = 250
        AMULT = .008
        GC TO 14
      9 KAINC = 200
        AMULT = .01
        GO TO 14
     10 KAINC = 100
        AMULT = .02
        GC TO 14
     11 KAINC = 50
        AMULT = .04
        GC TO 14
     12 KAINC = 20
        AMULT = .1
        GC TO 14
     13 KAINC = 10
        AMULT = .2
     14 DC 15 I = 1,5
     15 KC(I+1) = KC(I) + KAINC
        CALL ALPHA(AA,KC,6,2)
C       ************************************************************************
C       *                                                                      *
C       *  LA SECTION QUI SUIT CONVERTIT L'ACCELERATION EN FORCE EQUIVALENTE ET *
C       *                                                                      *
C       *  OPERE SUR CETTE FORCE.                                              *
```

```
      F = ABS(XMIN(4)/3.6E7)*AMASS/(THICKN)**2
      IF(F.GT.100) KF=8
      IF(F.GT.50.AND.F.LT.100) KF=5
      IF(F.GT.25.AND.F.LE.50) KF = 4
      IF(F.GT.10.AND.F.LE.25) KF = 3
      IF(F.GT.5.AND.F.LE.10) KF = 2
      IF (F.GT.2.5.AND.F.LE.5) KF = 1
      IF(F.GT.1.AND.F.LE.2.5) KF = 6
      IF(F.LE.1.) KF = 7
      KFNT(1) = 0
      FNT(1) = 0.0
      GC TO (26,19,18,17,16,27,28,37),KF
   37 KFINC = 40.0
      FMULT = .05
      GC TO 20
   16 KFINC = 20.0
      FMULT = .1
      GC TO 20
   17 KFINC = 10.0
      FMULT = .2
      GC TO 20
   18 KFINC = 5
      FMULT = .4
      GO TO 20
   19 KFINC = 2
      FMULT = 1.
      GC TO 20
   26 KFINC = 1
      FMULT = 2.
   20 DC 21 I = 1,5
   21 KFNT(I+1) = KFNT(I) + KFINC
      CALL ALPHA(AA,KFNT,6,2)
      GC TO 35
   27 FINC = .5
      FMULT = 4.
      GO TO 29
   28 FINC = .2
      FMULT = 10.
   29 CCNTINUE
      DC 30 I = 1,5
   30 FNT(I+1) = FNT(I) + FINC
      CALL ALPHA(FNT,KFNT,6,1)
   35 CCNTINUE
C     ***********************************************************************
C     *                                                                     *
C     *  LA SECTION QUI SUIT CPERE SUR LE TEMPS                             *
C     *                                                                     *
C     ***********************************************************************
      TT = XMAX(1)*60000
      IF(TT.GT.10) KTIME = 2
      IF(TT.LE.10) KTIME = 1
      SEC(1) = 0.0
      GC TO (22,23),KTIME
   22 SECINC = 2.0
      TMULT = 1.
      GO TO 24
```

```
   23 SECINC = 4.0
      TMULT = .5
   24 DO 25 I = 1,5
   25 SEC(I+1) = SEC(I) + SECINC
      CALL ALPHA(SEC,KFNT,6,1)
C     ***********************************************************************
C     *                                                                     *
C     *  LA LOUPE QUI SUIT REDUIT LES DONNEES A L'ECHELLE APPROPRIEE        *
C     *                                                                     *
C     *  CALCULEES PLUS HAUT.                                               *
C     *                                                                     *
C     ***********************************************************************
      DO 210 I = 1,ICOUNT
      XI(I) = (XI(I)/THICKN) * 10.
      XID(I) = (XID(I)/XIDIC) * 10.
      FF(I)=((ABS(XIDD(I)/3.6E7)*AMASS)/(THICKN*1.15)**2)*FMULT
      XIDD(I) = ABS(XIDD(I)*AMULT/A)
      TIME(I) = TIME(I)*60000.*TMULT
  210 CONTINUE
      VV = XIDIC/60.
      DO 310 I = 1,NN
      AXX(I) = AXX(I) * AMULT - .2
      XXX(I) = (XXX(I)/THICKN)*10. - .2
      TTT(I) = TTT(I) * TMULT - .2
  310 CONTINUE
C     ***********************************************************************
C     *  BETA EST LA SOUROUTINE QUI CONVERTIT LES VALEURS A ETRE INSCRITES  *
C     *  DANS LES SPECIFICATIONS EN HAUT DU GRAPHE.                         *
C     ***********************************************************************
      CALL BETA (TESTNO,SMPLNO,THICKN,DENSTY,VV,AMASS,TEST,
     1SMPL,THIC,DENS,VVV,MASS)
C     ***********************************************************************
C     *                                                                     *
C     *  GRAPHE EST LA SOUROUTINE QUI REUNIT TOUS LES APPELS NECESSAIRES POUR *
C     *                                                                     *
C     *  FAIRE TRACER LES TITRES,LES AXES,LES COORDONNEES ET LES GRAPHES.   *
C     *                                                                     *
C     ***********************************************************************
      CALL GRAPH(ORIX,ORIY,SPEC1,SPEC2,SPEC3,SPEC4,
     1SPEC5,SPEC6,LINEX,LINEY,AXISX,AXISY,NAME,TITLE1,
     2TITLE2,TITLE3,TITLE4,DUNITS,VUNITS,AUNITS,FUNITS,
     3TUNITS,AA,KB,KC,KFNT,SEC,XI,XID,XIDD,FF,TIME,ICOUNT,TH,V,TI,TO1,
     4TO2,VO1,TEST,SMPL,THIC,DENS,MASS,VVV,FNT,
     5AXX,XXX,TTT,NN,PLUS,XUNITS,EXPER,SIMU)
C     ***********************************************************************
C     *                                                                     *
C     *  LES DEUX PROCHAINES LIGNES TERMINENT LA PROCEDURE DE MILGC.        *
C     *                                                                     *
C     ***********************************************************************
      CALL EPLT
      CALL QUIT
      STOP
      END
```

```
      SUBROUTINE ALPHA(A,K,N,IK)
      DIMENSION A(6),K(6),D(6)
      CALL SETB99(D,24)
      GO TO (50,100),IK
   50 DO 40 I = 1,6
      WRITE(99,51) A(I)
   51 FORMAT(F4.1)
      READ(99,20) A(I)
   20 FORMAT (A4)
   40 CONTINUE
      GO TO 200
  100 DO 60 I = 1,6
      WRITE (99,101) K(I)
  101 FORMAT(I4)
      READ (99,20) K(I)
   60 CONTINUE
  200 CONTINUE
      RETURN
      END
```

```
      SUBROUTINE BETA(TESTNO,SMPLNO,THICKN,DENSTY,XIDIC,AMASS,
     1TEST,SMPL,THIC,DENS,VVV,MASS)
      DIMENSION D(6),DENS(2),VVV(2),MASS(2)
      CALL SETB99(D,24)
      WRITE(99,5) TESTNO
      READ(99,11) TEST
      WRITE(99,6) SMPLNO
      READ(99,11) SMPL
      WRITE(99,7) THICKN
      READ(99,11) THIC
      WRITE(99,8) DENSTY
      READ(99,12) DENS
      WRITE(99,9) XIDIC
      READ(99,12) VVV
      WRITE(99,10) AMASS
      READ(99,12) MASS
    5 FORMAT (F4.0)
    6 FORMAT(F5.0)
    7 FORMAT(F4.2)
    8 FORMAT(F6.4)
    9 FORMAT(F5.1)
   10 FORMAT(F6.3)
   11 FORMAT(A4)
   12 FORMAT (2(A4))
      RETURN
      END
```

```
      SUBROUTINE INIT(XMIN,XMAX,TESTNO,SMPLNO,DENSTY,THICKN,XIDIC,
     1AMASS,A)
      DIMENSION XMIN(4),XMAX(4)
      REWIND 12
      DO 10 LOOP = 1,4
      READ (12)
   10 CONTINUE
      READ (12) XMIN
      READ(12) XMAX
      DO 20 LOOP = 1,3
      READ(12)
   20 CONTINUE
      READ(12) TIME,DELT,DELMIN,FINTIM,PRDEL,OUTDEL,XID,XI,XIDD,ZZ0003,
     1XIDIC,XIIC,A,AREA,AMASS,THICKN,DENSTY,TESTNO,SMPLNO,AA,BB,CC,
     2DD,FF,XX
      READ(12)
      RETURN
      END
```

```
      SUBROUTINE VALUE(TIME,XI,XID,XIDD,CODE)
      READ(12) TIME,XI,XID,XIDD
      IF (TIME.LT.0.0) GO TO 10
      CODE = 0.0
      RETURN
   10 CODE = 1.0
      RETURN
      END

      SUBROUTINE GRAPH(ORIX,ORIY,SPEC1,SPEC2,SPEC3,SPEC4,
     1SPEC5,SPEC6,LINEX,LINEY,AXISX,AXISY,NAME,TITLE1,
     2TITLE2,TITLE3,TITLE4,DUNITS,VUNITS,AUNITS,FUNITS,
     3TUNITS,AA,KB,KC,KFNT,SEC,XI,XID,XIDD,F,TIME,ICCUNT,TH,V,TI,TO1,TO2
     4,VO1,TEST,SMPL,THIC,DENS,MASS,XIDIC,ANT,
     5AXX,XXX,TTT,NN,PLUS,XUNITS,EXPER,SIMU)
      DIMENSION ORIX(5),ORIY(5),SPEC1(2),SPEC2(3),SPEC3(11),
     1SPEC4(10),SPEC5(11),SPEC6(7),LINEX(13),LINEY(13),AXISX(68),
     2AXISY(68),NAME(2),TITLE1(5),TITLE2(4),TITLE3(5),
     3TITLE4(5),DUNITS(3),VUNITS(5),AUNITS(1),FUNITS(3),
     4TUNITS(3),AA(6),KB(6),KC(6),KFNT(6),SEC(6),FNT(6),
     5TIME(200),XI(200),XID(200),XIDD(200),F(200),TH(200),V(200),TI(200)
     6,DENS(2),MASS(2),XIDIC(2),AXX(20),XXX(20),TTT(20),XUNITS(2)
      DIMENSION EXPER(3),SIMU(3)
      CALL CRG(ORIX(1),ORIY(1))
      CALL SPEC(SPEC1,SPEC2,SPEC3,SPEC4,SPEC5,SPEC6)
      CALL LDR(-1.3,3.9,.125,0.0,TEST,3)
      CALL LDR(-1.15,3.65,.125,0.0,SMPL,4)
      CALL LDR(.85,3.4,.125,0.0,DENS,6)
      CALL LDR (1.1,3.15,.125,0.0,THIC,4)
      CALL LDR (1.25,2.9,.125,0.0,XIDIC,5)
      CALL LDR (0.0,2.65,.125,0.0,MASS,6)
      CALL LDR (-2.0,6.0,.2,0.0,NAME,10)
      CALL LDR(1.0,2.2,.1,0.0,EXPER,12)
      CALL LDR(1.0,1.9,.1,0.0,SIMU,9)
      CALL SCL(0.2,0.2)
      CALL LIN(LINEX(1),LINEY(1),7)
      CALL SLEW(0.0,-15.5)
      CALL LIN(LINEX(8),LINEY(8),6)
      CALL LDR(-12.0,7.25,.1,0.0,TITLE1,19)
      CALL CRDNTS(ORIX(2),ORIY(2),AXISX,AXISY)
      CALL LABEL (KB,SEC)
      CALL LDR (2.0,-2.1,.1,0.0,TUNITS,12)
      CALL LDR(-2.2,3.0,.1,1.57,XUNITS,7)
      CALL LIN(TIME(1),XI(1),ICOUNT)
      DO 1 I = 1,NN
      CALL LDR(TTT(I),XXX(I),.08,0.0,PLUS,1)
    1 CONTINUE
      CALL CRG(ORIX(1),ORIY(1))
      CALL LDR(3.0,7.25,.1,0.0,TITLE2,16)
      CALL CRDNTS(ORIX(3),ORIY(3),AXISX,AXISY)
      CALL LABEL(KB,SEC)
      CALL LDR (2.0,-2.1,.1,0.0,TUNITS,12)
      CALL LDR(-2.2,3.0,.1,1.57,XUNITS,7)
      CALL LIN(TIME(1),XID(1),ICOUNT)
      CALL CRG(ORIX(1),ORIY(1))
      CALL SLEW(-14.5,-4.0)
      CALL LDR(-12.0,-8.25,.1,0.0,TITLE3,20)
      CALL CRDNTS(ORIX(4),ORIY(4),AXISX,AXISY)
      CALL LABEL(KC,SEC)
      CALL LDR (2.0,-2.1,.1,0.0,TUNITS,12)
      CALL LDR(-2.2,4.5,.1,1.57,AUNITS,3)
      CALL LIN(TIME(1),XIDD(1),ICOUNT)
      DO 2 I = 1,NN
      CALL LDR(TTT(I),AXX(I),.08,0.0,PLUS,1)
    2 CONTINUE
      CALL CRG(ORIX(1),ORIY(1))
      CALL LDR(3.0,-8.25,.1,0.0,TITLE4,16)
```

```
      CALL CRONTS(ORIX(5),ORIY(5),AXISX,AXISY)
      IF(FNT(1).NE. 0.) GO TO 5
      CALL LABEL(KFNT,KB)
      GO TO 10
    5 CALL LABEL(FNT,KB)
   10 CONTINUE
      CALL LDR(3.0,-2.1,.1,0.0,XUNITS,7)
      CALL LDR(-2.2,2.5,.1,1.57,FUNITS,12)
      CALL LIN(XI(1),F(1),ICOUNT)
      CALL SCL(1.0,1.0)
      CALL ORG(ORIX(1),ORIY(1))
      CALL CUTLIN
      RETURN
      END

      SUBROUTINE CRONTS(X,Y,AXISX,AXISY)
      DIMENSION AXISX(68),AXISY(68)
      CALL ORG(X,Y)
      CALL LIN(AXISX(48),AXISY(48),21)
      DO 10 I = 4,46,2
      IF(I.GT.24) GO TO 5
      XX = 10-((I-4)/2)
      CALL SLEW (XX,0.0)
      GO TO 8
    5 YY = (I-26)/2
      CALL SLEW(0.0,YY)
    8 CONTINUE
      CALL LIN (AXISX(I),AXISY(I),2)
   10 CONTINUE
      RETURN
      END

      SUBROUTINE LABEL(ALABEL,BLABEL)
      DIMENSION ALABEL(6),BLABEL(5)
      DO 10 I = 1,6
      Y = -2.25 + 2*(FLOAT(I))
      CALL LDR(-2.15,Y,.1,0.0,ALABEL(I),4)
   10 CONTINUE
      CALL SLEW(-1.0,-.9)
      DO 20 I = 1,6
      X = -3.0 + 2*(FLOAT(I))
      CALL LDR(X,-.9,.1,0.0,BLABEL(I),4)
   20 CONTINUE
      RETURN
      END

      SUBROUTINE CUTLIN
      DIMENSION X(23),Y(23)
      CALL SLEW(-4.25,5.775)
      DO 10 I = 1,18
      J = I
      Y(I) = 5.525
   10 X(I) = -5.0 + (FLOAT(J))/2.
      CALL LIN(X(1),Y(1),18)
      DO 20 I = 1,23
      J = I
      X(I) = 4.0
   20 Y(I) = 6.025 - (FLOAT(J))/2.
      CALL LIN (X(1),Y(1),23)
      DO 30 I = 1,18
      J = I
      Y(I) = -5.475
   30 X(I) = 4.5 - (FLOAT(J))/2.
      CALL LIN(X(1),Y(1),18)
      DO 40 I = 1,23
      J = I
      X(I) = -4.5
   40 Y(I) = -5.975 + (FLOAT(J))/2.
      CALL LIN (X(1),Y(1),23)
      RETURN
      END
```

APPENDIX E

Record of Data Collected During this Study

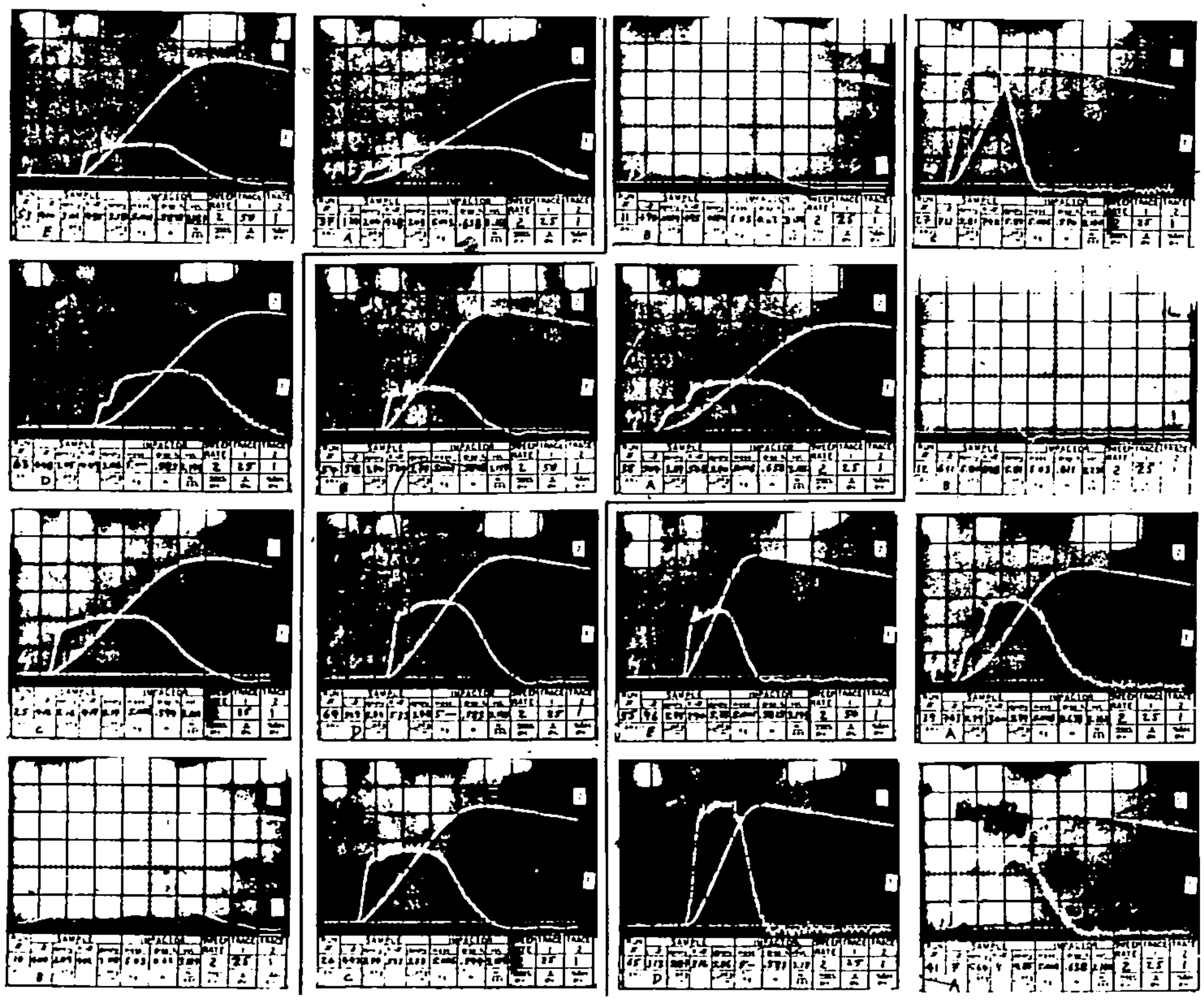

5 kg 25J
$\rho = 0.030 g/cm^3$

5 kg 25J
$\rho = 0.037 g/cm^3$

5 kg 25J
$\rho = 0.058 g/cm^3$

Figure E-1

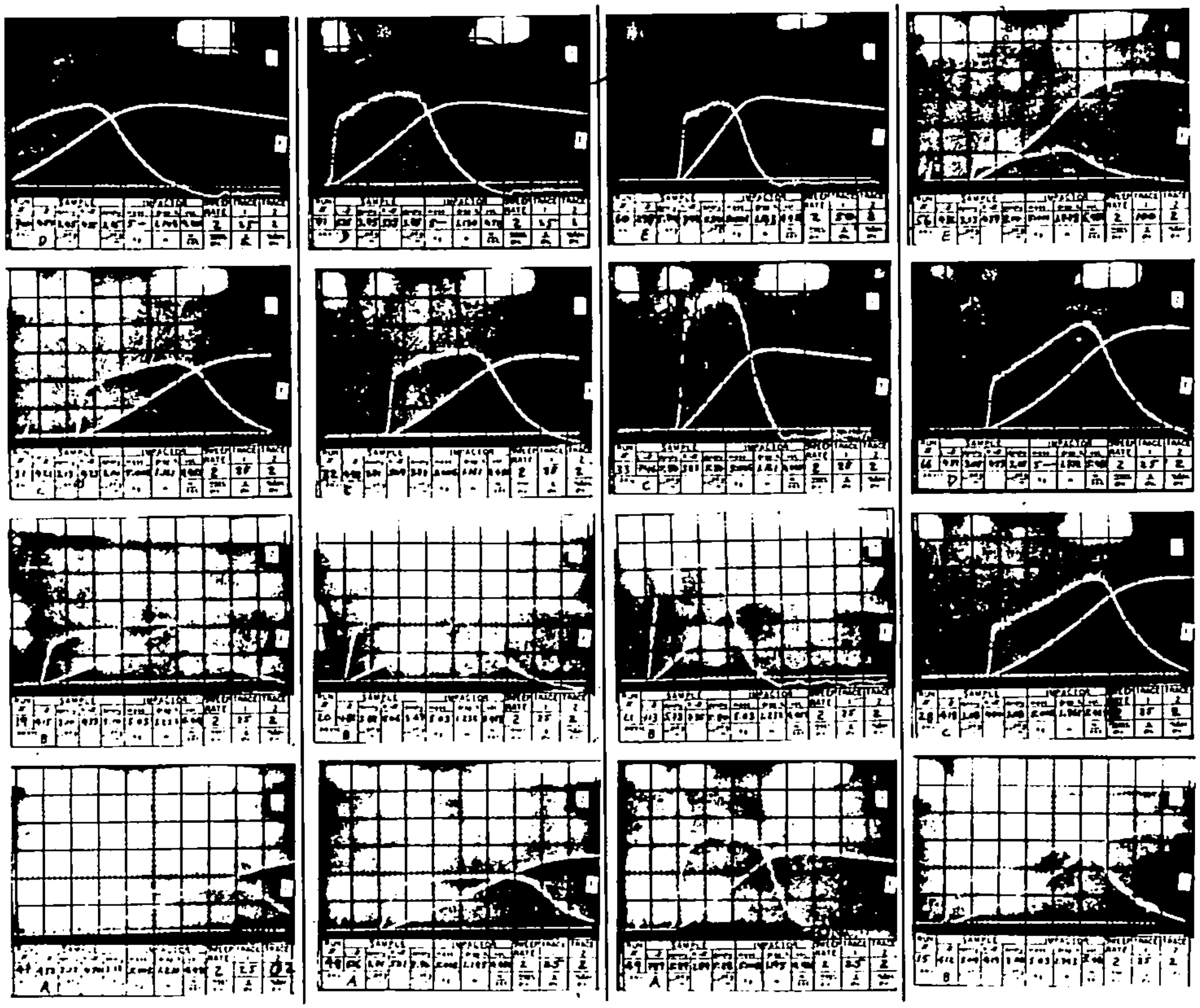

5 kg 50J
$\rho = 0.031\ g/cm^3$

5 kg 50J
$\rho = 0.037\ g/cm^3$

5 kg 50J
$\rho = 0.059\ g/cm^3$

5 kg 50J
$\rho = 0.031\ g/cm^3$

Figure E-2

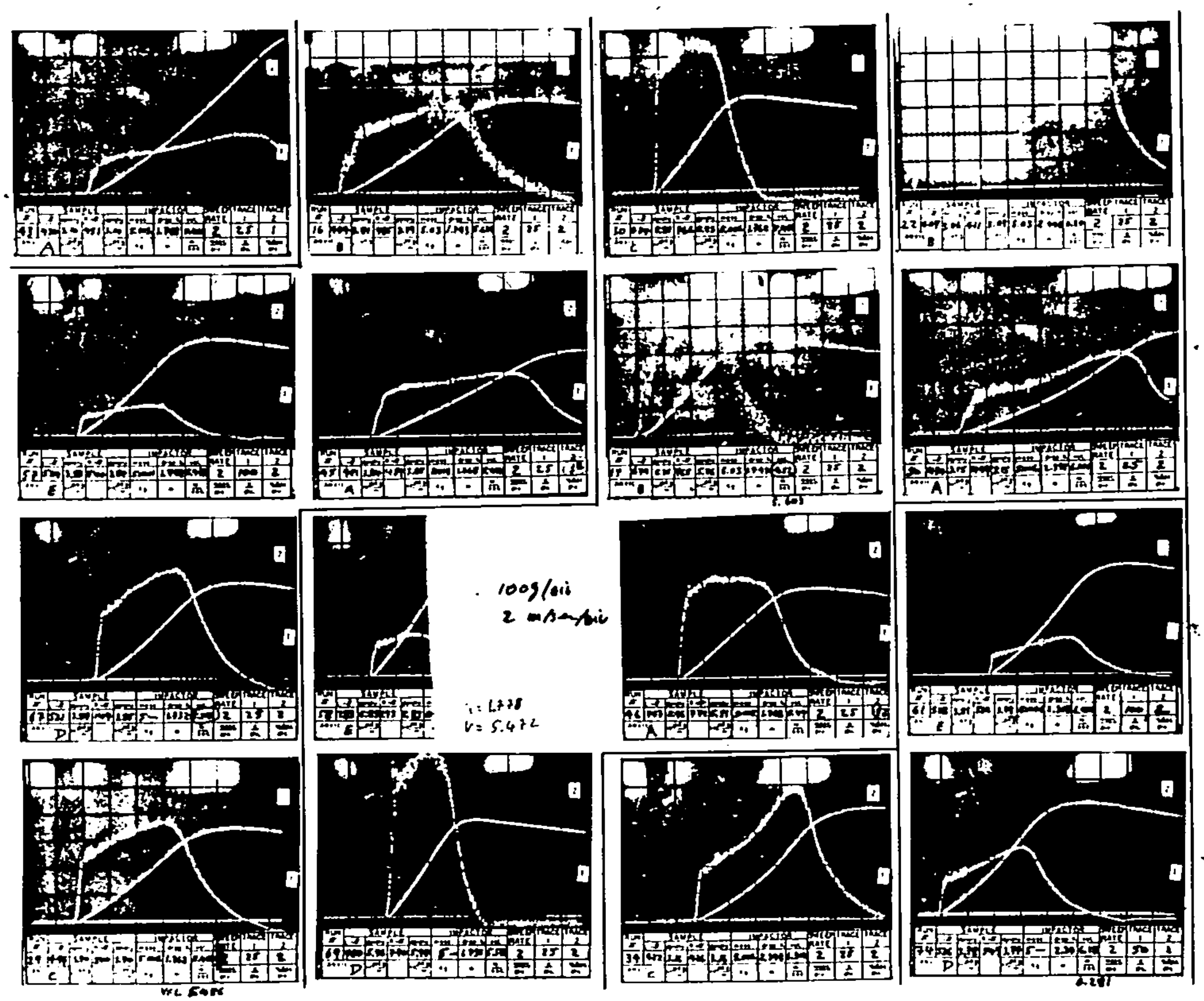

5 kg 75J
$\rho = 0.038\ g/cm^3$

5 kg 75J
$\rho = 0.059\ g/cm^3$

5 kg 75J
$\rho = .0.032\ g/cm^3$

5 kg 75J
$\rho = 0.038\ g/cm^3$

Figure E-3

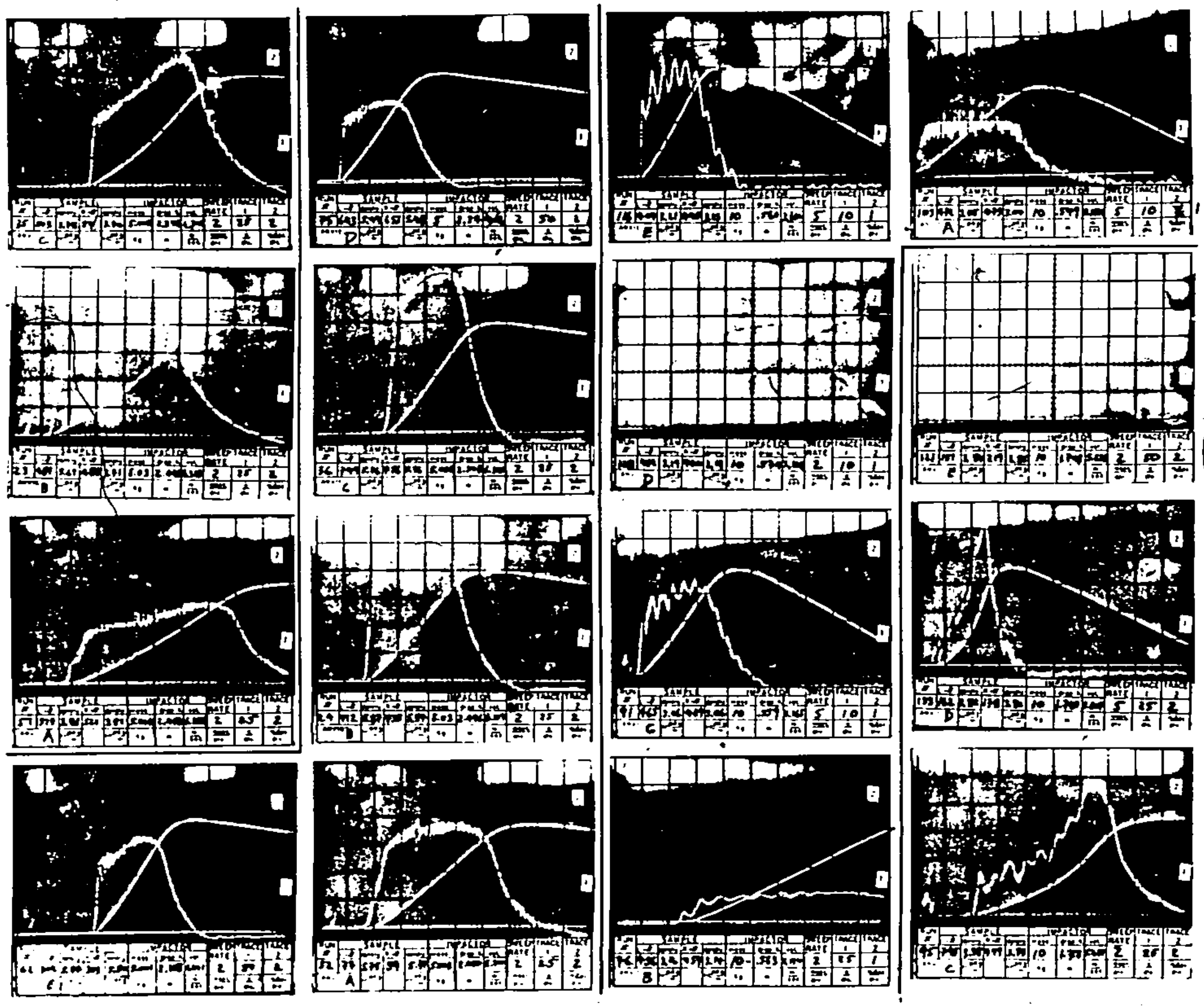

5 kg 100J
ρ= 0.052 g/cm^3

10 kg 50J
ρ= 0.032 g/cm^3

10 kg 50J
ρ= 0.037 g/cm^3

Figure E-4

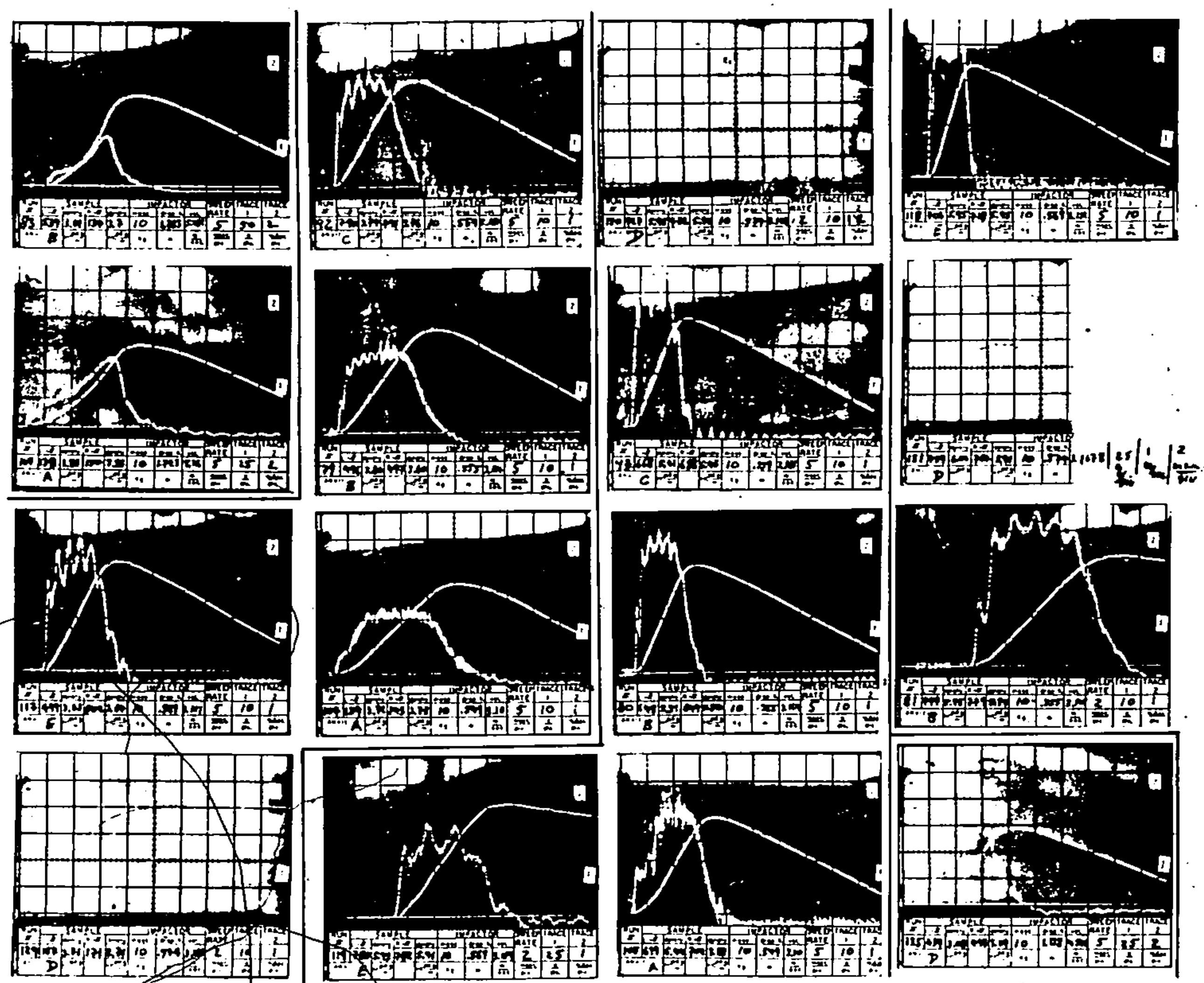

10 kg 50J
$\rho = 0.037\ g/cm^3$

10 kg 50J
$\rho = 0.054\ g/cm^3$

10 kg 100J
$\rho = 0.031\ g/cm^3$

Figure E-5

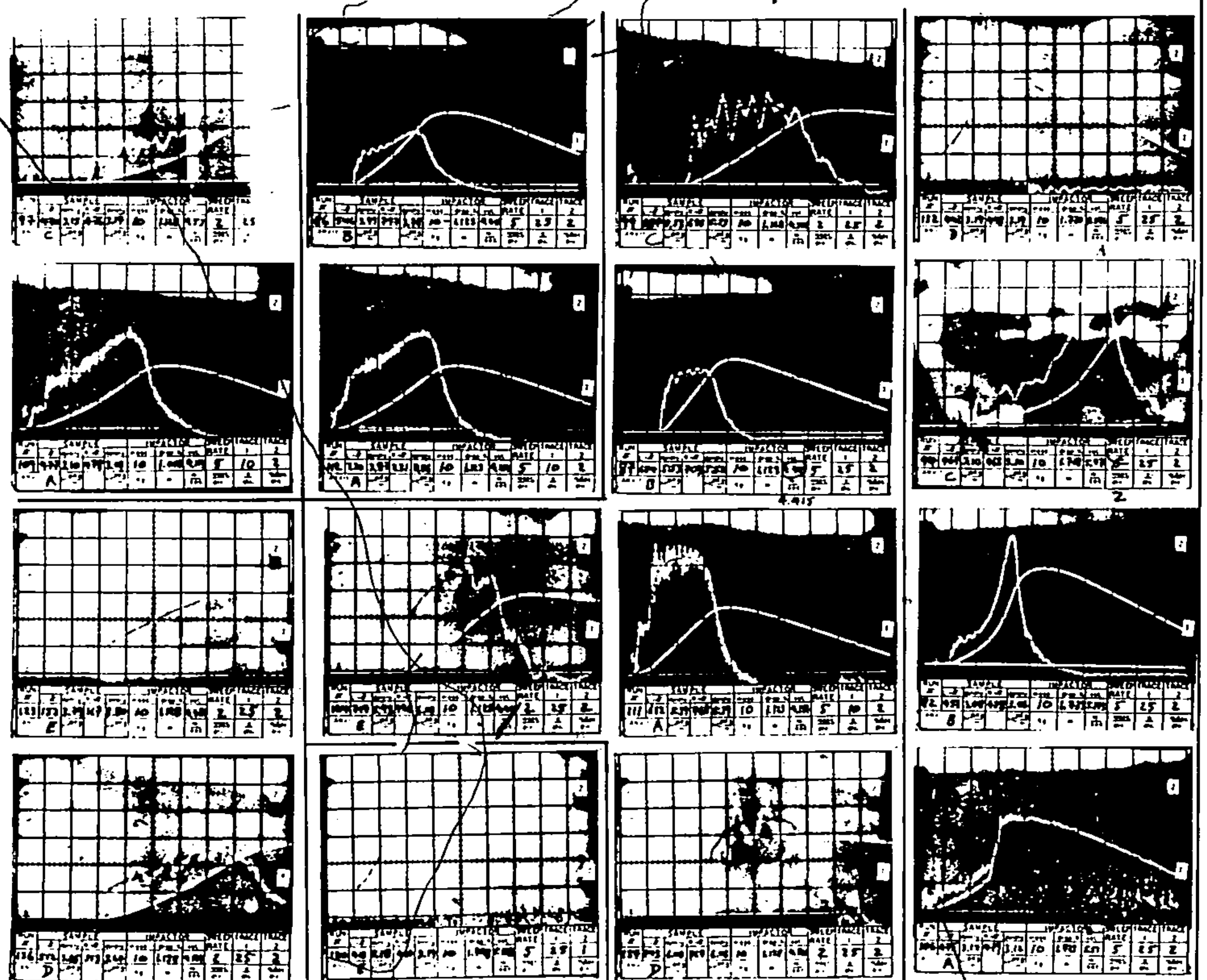

10 kg 100J
$\rho =$ 0.038 g/cm^3

10 kg 100J
$\rho =$ 0.031 g/cm^3

10 kg 100J
$\rho =$ 0.058 g/cm^3

10 kg 100J
$\rho =$ 0.031 g/cm^3

Figure E-6

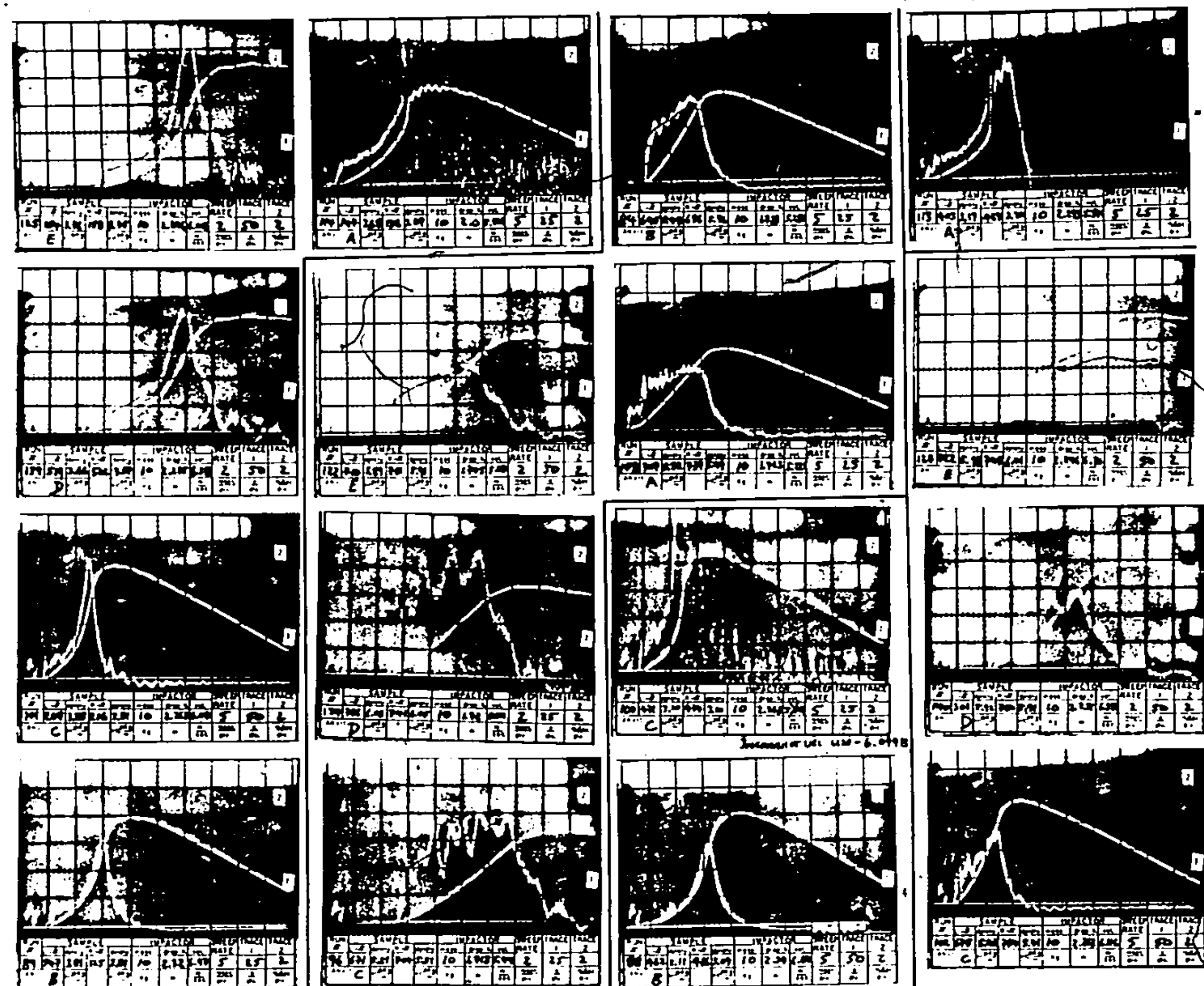

10 kg 150J $\rho = 0.0368\ g/cm^3$ | 10 kg 150J $\rho = 0.055\ g/cm^3$ | 10 kg 200J $\rho = 0.032\ g/cm^3$ | 10 kg 200J $\rho = 0.059\ g/cm^3$

Figure E-7

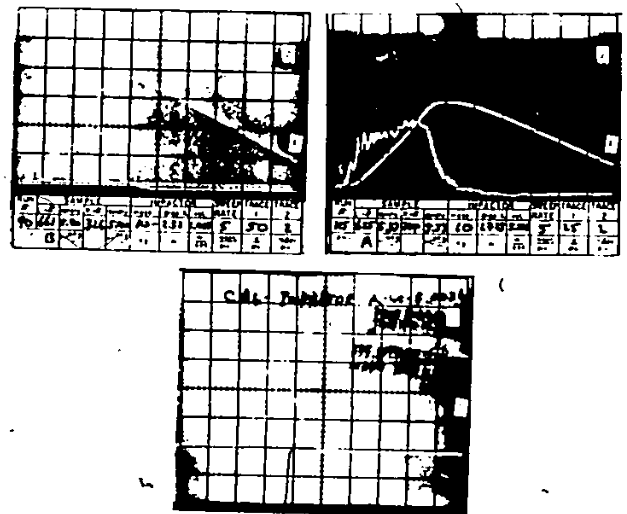

10 kg 200J
$\rho = 0.059\ g/cm^3$

Figure E-8